



# Analyzing the predictive performance of LiDAR-derived metrics in modeling fine-scale resource selection by deer

Henriette Tripke

Master thesis (Student ID 3106709)  
submitted to  
the Faculty of Environment & Natural Resources  
at the University of Freiburg

Supervisor: Dr. Simone Ciuti, Chair of Biometry and Environmental System Analysis  
Co-supervisor: Prof. Dr. Gernot Segelbacher, Chair of Wildlife Ecology and Management

External supervisor: Dr. Marco Heurich, Department of Conservation and Research, Bavarian Forest National Park

Freiburg, 1st of April 2016



# Contents

<b>1</b>	<b>Introduction</b>	<b>2</b>
1.1	Background . . . . .	2
1.2	Objectives . . . . .	4
<b>2</b>	<b>Methods</b>	<b>5</b>
2.1	Study area . . . . .	5
2.2	Species . . . . .	5
2.3	Telemetry data . . . . .	6
2.3.1	Quality of telemetry data . . . . .	7
2.3.2	Resource selection function . . . . .	7
2.3.3	Calculation of available locations . . . . .	8
2.3.4	Sensitivity analysis . . . . .	9
2.4	Environmental metrics . . . . .	10
2.4.1	Preparation of LiDAR data . . . . .	10
2.5	Model fitting . . . . .	13
<b>3</b>	<b>Results</b>	<b>15</b>
3.1	Sensitivity analysis . . . . .	15
3.2	Model comparison . . . . .	15
3.3	Identification of important predictors . . . . .	19
3.4	Predictions of resource selection . . . . .	21
<b>4</b>	<b>Discussion</b>	<b>24</b>
4.1	Predictive power of commonly used environmental metrics . . . . .	25
4.2	Application of LiDAR-based Principle Components . . . . .	29
4.3	Limitations . . . . .	29
4.4	Study design . . . . .	30
4.5	Future implementation . . . . .	30
4.6	Conclusions . . . . .	31
	<b>Acknowledgements</b>	<b>32</b>
<b>A</b>	<b>Results from a Principle Component Analysis of a LiDAR point cloud</b>	<b>38</b>
A.1	Principle Components of LiDAR point cloud at 5 m resolution . . . . .	39
A.2	Principle Components of LiDAR point cloud at 10 m resolution . . . . .	39
<b>B</b>	<b>Sensitivity analysis to estimate random availability</b>	<b>40</b>
<b>C</b>	<b>Model summaries</b>	<b>47</b>
C.1	Red deer telemetry data - 15 minute fix rate . . . . .	48
C.2	Red deer telemetry data - 1 hour fix rate . . . . .	53
C.3	Roe deer telemetry data - 1 hour fix rate . . . . .	58

C.4	Roe deer telemetry data - 4 hour fix rate . . . . .	63
<b>D</b>	<b>Predictions for resource selection in deer</b>	<b>68</b>
D.1	Predictions from five different models for red deer . . . . .	69
D.2	Predictions from five different models for roe deer . . . . .	70

# List of Tables

2.1	Selection of satellite telemetry data from the Bavarian Forest National Park for a resource selection function. . . . .	7
2.2	Environmental variables to analyze resource selection in roe and red deer in the Bavarian Forest National Park (NPBW). Described layers explain the terrain, climatic conditions, daily and seasonal patterns such as human influence and were therefore potential confounding factors for the generalized linear mixed models. After checking for correlation only variables marked in bold were used. . . . .	11
2.3	Abbreviation and description of available remote sensing data to explain resource selection in roe and red deer in the Bavarian Forest National Park (NPBW). Variables have either been calculated from satellite or aerial images or were derived from light detection and ranging (LiDAR) point clouds. . . . .	12
2.4	Model design for comparing different environmental metrics by using generalized linear mixed models with nested random effects. Environmental metrics were exchanged for comparison while the other predictors were included into every model. . . . .	14
3.1	Comparison of generalized linear mixed models explaining the resource selection of red and roe deer based on Aikaike's Information Criterion (AIC). Deer data were tested at different resolutions (GPS-fix rates). Models were fitted using predictors either derived from satellite images, aerial photography or LiDAR data. The name of the model corresponds to the environmental metric(s) used to describe vegetative structures or land cover classes. Model 1 incorporates only individuals and stratum as nested random effects, model 2 additionally includes predictors explaining terrain, human disturbance, and daily patterns but has no predictor for vegetation, whereas models 3 - 10 incorporate the design of model 2 and include one or several additional predictors describing vegetative structures or land cover classes. Next to the $\Delta\text{AIC}$ values the ranking of each model among one data set is provided for a better overview. Detailed summaries of all models can be found in Appendix C. . . . .	16
3.2	Covariate estimate $\beta$ and corresponding standard error SE of four generalized linear mixed models. All predictors were standardized $((x - \bar{x})/\sigma)$ when fitting the models. . . . .	18

# List of Figures

2.1	Study area and its location in Germany. The study area included the Bavarian Forest National Park (boundaries are outlined in black) and a 500 m buffer around it. Red deer (black dots) and roe deer (grey dots) were monitored with GPS-GSM collars (VECTRONIC Aerospace, Berlin, Germany) from 2010 to 2012. Displayed GPS-fixes were measured at a fix rate of 1 hour. . . . .	6
2.2	Movement path of an animal through the landscape (black) and corresponding availability (grey) for a resource selection function. Used locations are truly captured GPS-fixes whereas available locations are randomly calculated starting at a used location of time $i$ with random step length into any direction. The stratum is then defined by all available locations and the used location of time $i + 1$ . . . . .	8
2.3	Predicted step length depending on the time of the day for a) roe deer and b) red deer. Underlying is a gamma distribution. Step length were calculated from GPS-fixes with different time intervals ranging from 15 minutes to 4 hours between fixes. . . . .	9
3.1	Understanding the importance of single predictors: The higher the predicted RSF values $w(x)$ get the more influence this predictor has in the model. Subfigures represent the four data sets a) red deer at 15 minute, b) red deer at 1 hour, c) roe deer at 1 hour and d) roe deer at 4 hour fix rate. The x-axis values are not relevant for highlighting differences in the $w(x)$ values but generally range from "low" to "high". All PC-variables are products of a Principle Component Analysis run on three-dimensional LiDAR point cloud data at 10 m resolution. . . . .	20
3.2	Relative probability of selection $w(x)$ for red and roe deer (telemetry data of 1 hour fix rate) from the best models. Variables were interacted with the time of the day (twilight, night, day). . . . .	21
3.3	Relative probability of selection $w(x)$ of red and roe deer from the best models. Variables were interacted with the time of the day (twilight, night, day). Principle Component (PC) values are derived from a Principle Component Analysis of LiDAR point cloud data at 10 m resolution. They are describe the difference in vegetation height. The middle column displays rotation matrices for each PC. . . . .	23
4.1	Predicted values of Principle Components (PCs) in a landscape. The PC values are derived from the results of a Principle Component Analysis on a LiDAR point cloud data set of 99 variables at 10 m resolution. The area shows an extent from the Bavarian Forest National Park in southeastern Germany. Displayed GPS-fixes were measured at a fix-rate of 1 hour. . . . .	28

B.1 Sensitivity analysis to estimate availability (random points) in a resource selection function. Generalized linear mixed models were fitted (30 replicates) always with a different sample size of availability (1-300). Results of a) the relative probability of selection ( $w(x)$ ) from the exponential form and b) the covariate estimates ( $\beta$ ; beta) for the predictor lidar are presented. In b) also predictions of covariate estimates from a generalized additive model are shown. The model design is presented in a). The dashed line indicates stabilizing estimates. Notes: elevation (meters a.s.l.) at 1 m resolution; lidar: understory vegetation cover (0.5 m - 2 m) derived from light detection and ranging (LiDAR) data at 1 m resolution; distance: closest distance to the next hiking trail; landcover: land cover classification map, * indicates interactions of two predictors. . . . .	41
B.2 Variance in predicted relative probability of selection ( $w(x)$ ) in a resource selection function. Generalized linear mixed models were fitted (30 replicates) always with a different sample size of availability (1-300). Two different models where tested including a) interactions (indicated by *) or b) squared terms (indicated by $^2$ ). Notes: elevation (meters a.s.l.) at 1 m resolution; lidar: understory vegetation cover (0.5 m - 2 m) derived from light detection and ranging (LiDAR) data at 1 m resolution; distance: closest distance to the next hiking trail; landcover: land cover classification map. . . . .	42
B.3 Variance in covariate estimates ( $\beta$ ; beta) in a resource selection function. Generalized linear mixed models were fitted (30 replicates) always with a different sample size of availability (1-300). This model included interactions of predictors. Notes: elevation (meters a.s.l.) at 1 m resolution; lidar: understory vegetation cover (0.5 m - 2 m) derived from light detection and ranging (LiDAR) data at 1 m resolution; distance: closest distance to the next hiking trail; landcover: land cover classification map. . . . .	43
B.4 Variance in covariate estimates ( $\beta$ ; beta) in a resource selection function. Generalized linear mixed models were fitted (30 replicates) always with a different sample size of availability (1-300). This model included squared terms of predictors. Notes: elevation (meters a.s.l.) at 1 m resolution; lidar: understory vegetation cover (0.5 m - 2 m) derived from light detection and ranging (LiDAR) data at 1 m resolution; distance: closest distance to the next hiking trail; landcover: land cover classification map. . . . .	44
B.5 Variance in covariate estimates ( $\beta$ ; beta) in a resource selection function. Generalized linear mixed models were fitted (30 replicates) always with a different sample size of availability (1-300). This model included interactions of predictors (indicated by *). Notes: elevation (meters a.s.l.) at 1 m resolution; lidar: understory vegetation cover (0.5 m - 2 m) derived from light detection and ranging (LiDAR) data at 1 m resolution; distance: closest distance to the next hiking trail; landcover: land cover classification map. . . . .	45
B.6 Variance in covariate estimates ( $\beta$ ; beta) in a resource selection function. Generalized linear mixed models were fitted (30 replicates) always with a different sample size of availability (1-300). Here estimates of the squared terms of predictors are shown. Notes: elevation (meters a.s.l.) at 1 m resolution; lidar: understory vegetation cover (0.5 m - 2 m) derived from light detection and ranging (LiDAR) data at 1 m resolution; distance: closest distance to the next hiking trail; landcover: land cover classification map. . . . .	46

D.1	Predicted relative probability of selection $w(x)$ for red deer at 1 hour fix rate. Predictions are from models always incorporating the same confounding factors as well as nested random effects. Only the predictors to describe habitat characteristics were changing among a) normalized difference vegetation index, b) mean vegetation height, c) fractional vegetation cover, d) number of single trees and e) habitat classification map of the Bavarian Forest National Park. Variables were interacted with the time of the day (twilight, night, day). . . .	69
D.2	Predicted relative probability of selection $w(x)$ for roe deer at 1 hour fix rate. Predictions are from models always incorporating the same confounding factors as well as nested random effects. Only the predictors to describe habitat characteristics were changing among a) normalized difference vegetation index, b) mean vegetation height, c) fractional vegetation cover, d) number of single trees and e) habitat classification map of the Bavarian Forest National Park. Variables were interacted with the time of the day (twilight, night, day). . . .	70

## Abstract

To disentangle the complexity of wildlife responses to their environment, animal behavior and their habitat requirements have to be understood on an increasingly fine scale. Remote sensing provides advanced techniques to describe habitat characteristics used by animals. In particular light detection and ranging (LiDAR) is increasingly used to describe three-dimensional vegetation structure, occasionally in extremely high resolution. Due to its successful application in forest inventory LiDAR data have become more and more available to wildlife ecologists and showed already great potential for understanding fine-scale behavioral patterns in animals.

In this study I tested the predictive performance of high resolution LiDAR data in combination with fine-scale telemetry data. I implemented a resource selection function (RSF) for two deer species native to the Bavarian Forest National Park. In a systematic model design using conditional logistic regressions I compared the predictive power of different LiDAR-derived metrics to more commonly used remote sensing data. Moreover, I applied a newly developed LiDAR product, which was expected to capture vegetation structure better than other common LiDAR products. A principle component analysis (PCA) was used to generate new, linearly uncorrelated variables, so-called principle components (PCs), from the total LiDAR point cloud.

I found that models incorporating these new LiDAR-based PCs performed best among all tested models. In general, products derived from LiDAR data showed highest predictive performance relative to products from satellite or aerial images. The  $\Delta AIC$  values from the best performing model incorporating LiDAR-based PCs to the best performing model not including LiDAR products ranged from 55.1 to 231.2.

These results underline the suitability of LiDAR data, in general, for modeling fine-scale wildlife habitat use. In particular, the novel application of LiDAR-derived PCs could comprehensively capture vegetation structure at a very high resolution. Further exploring this method could increase the effectiveness of wildlife conservation and management in the future.

# Chapter 1

## Introduction

### 1.1 Background

Understanding behavioral patterns and resource requirements is fundamental for the management and conservation of wildlife species. Influences such as habitat loss, increasing human disturbance or climate change affect the behavior and distribution of species. Tools to analyze wildlife behavior should be able to disentangle the complexity of environmental impacts and wildlife responses. Therefore, animal behavior and their habitat requirements should be analyzed on a fine spatial and temporal scale. One way to do so is to analyze the resource selection of a species based on animal movement data and environmental metrics. These so-called resource selection functions (RSFs) are commonly used tools to better understand species distribution, habitat selection or human-wildlife interactions (Manly et al. 2002, Boyce 2006, Lele 2009, Godvik et al. 2009, Northrup et al. 2013, Thurfjell et al. 2014). By introducing more and more fine-scale remote sensing data into the RSF framework unprecedented insights in the resource selection of species can be gained. They can enhance our understanding of habitat selection behavior and thus help to implement more effective and efficient conservation and management practices (Vierling et al. 2008).

During the last decades a rapid progress in the quality of remote sensing data occurred. Probably the most innovative advance in terms of animal tracking was the introduction of global positioning systems (GPS) in the mid-1990s to obtain high accuracy data on animal movements (Tomkiewicz et al. 2010, Hebblewhite & Haydon 2010). Locations obtained from satellite telemetry are highly precise data capturing temporal information that represent animal movement paths (Hebblewhite & Haydon 2010, Neumann et al. 2015). The time intervals (fix rates of collected locations) can be programmed to less than 1 minute, only limited by the size of target species as well as battery life and archival memory of the GPS device (Ryan et al. 2004, Tomkiewicz et al. 2010, Hebblewhite & Haydon 2010). Thereby, increasing frequency of positions ensures the reliability of movement paths of the tracked individuals (Cagnacci et al. 2010). However, to make full use of such fine-scale telemetry data accuracy of environmental metrics describing the visited resources must increase as well. Only if both animal movement data and environmental variables reach the same level of detail and reliability, we will be able to understand fine-scale behavioral patterns and improve wildlife management and conservation (Cagnacci et al. 2010, Gaillard et al. 2010, Neumann et al. 2015).

Parallel to the advancements in animal tracking, increasing availability and improving quality of remote sensing data allows the computation of detailed environmental metrics. These can be used for land cover classification or mapping of vegetation (Neumann et al. 2015, Xie et al. 2008). Satellite images of different spatial and temporal resolution are often

freely available (review Neumann et al. 2015). Various indices based on vegetation phenology provide insights in plant productivity and stress detection (for example see Harris 2016). For example, the normalized difference vegetation index (NDVI), calculated with infra-red and red bands of satellite images, has become a widely used tool in wildlife ecology studies (Neumann et al. 2015). However, these remote sensing products are often limited to coarser spatial scales or not meaningful for certain ecological questions. For capturing vegetation structures that particularly affect wildlife resource selection LiDAR data have proven to be more powerful (Farrell et al. 2013, Ackers et al. 2015).

Light detection and ranging (LiDAR) or airborne laser scanning (ALS) is an active remote sensing method. It measures distances, commonly from airplanes or helicopters, to the earth surface by sending light in the form of laser pulses. These pulses reflect on any surface structure (e.g., vegetation, buildings, rocks or bare earth) and return to the aircraft. For every pulse, at the location where it hit the surface, three-dimensional spatial coordinates (latitude, longitude, and height) are calculated and stored. This results in a detailed three-dimensional set of points, the so-called "point cloud" (NOAA 2015).

The common application of these point clouds is to generate geospatial products such as digital elevation models (DEM) or canopy cover models (NOAA 2015). In addition, highly accurate estimates of vegetation height, and cover, as well as more complex attributes of canopy structure and function can be derived (Lefsky et al. 2002).

The biggest advantage of LiDAR data is the information provided on the vertical structure of vegetation which can often be derived on a very fine scale. In contrast to other remote sensing data, which depict only the horizontal distribution, LiDAR data can even capture the presence of single trees, along with attributes like diameter at breast height (DBH) and standing volume (Lefsky et al. 2002, Yao et al. 2012, Latifi et al. 2015). This makes the application of LiDAR data a valuable tool for fine-scale modeling (Hagar et al. 2014, Neumann et al. 2015, Lefsky et al. 2002) and they can fill the gap in traditional land use mapping (Tattoni et al. 2012, Neumann et al. 2015, Vierling et al. 2008).

LiDAR data have been applied in ecology and wildlife studies and it has been shown that they are a precise tool for forest characterization (Latifi 2012, Hyppae et al. 2012). Their usefulness has been demonstrated in forest inventory (Lefsky et al. 2002, Tsui et al. 2013, Latifi et al. 2015) and the more they are applied for such purposes the more they have become available to wildlife researchers (Lone et al. 2014b).

They have been used in species distribution modeling (Farrell et al. 2013, Nijland et al. 2014, Ackers et al. 2015), for predicting wildlife resource selection (Ewald et al. 2014, Lone et al. 2014b) or quantifying habitat suitability (Graf et al. 2009, Garabedian et al. 2014). Thereby, quite a wide range of different LiDAR-derived metrics have been applied. Among others there are height percentiles of all returns (Lone et al. 2014a,b, Melin et al. 2013) canopy cover (Lone et al. 2014b), the mean height of vegetation (Farrell et al. 2013, Lone et al. 2014a, Ackers et al. 2015), the fractional vegetation cover of different height strata (Ewald et al. 2014, Lone et al. 2014a,b), the number of single trees (Flaherty et al. 2014, Ackers et al. 2015) and more complex metrics such as a canopy solar index or a wet area map (Nijland et al. 2014). In some cases products derived from LiDAR point clouds have been applied in combination with other remote sensing (Ackers et al. 2015, Smart et al. 2012) or field data (Garabedian et al. 2014). Farrell et al. (2013) underline the increasing relevance of LiDAR-derived metrics for analyzing wildlife habitat use and the requirements of species on a local scale.

## 1.2 Objectives

Only recently LiDAR data have become widely available through their application in forest inventory. Thus, the full potential of applying LiDAR data in wildlife ecology studies has not been explored yet.

This study improves previous research in several regards. First, I was able to use high resolution LiDAR data covering a large area, namely the Bavarian Forest National Park in Germany. Second, I had access to a large high quality telemetry data set on two different deer species native to the national park. Third and most important, I applied a newly developed tool that captures a bigger part of the structural information contained in the LiDAR point cloud.

I implemented a RSF protocol to analyze the telemetry data and compared the newly developed LiDAR metrics to other remote sensing products commonly used in wildlife ecology. I expected the LiDAR data to perform better in explaining fine-scale resource selection of the two deer species and thus provide new insights in their habitat requirements. Thus, my findings could help to use LiDAR data more efficiently in wildlife research, conservation and management.

# Chapter 2

## Methods

Most of the preparation of the data, calculations and running models was done with the open source software R version 3.2.2 (R Core Team 2015). For heavy calculations I had access to the Windows server (cluster with up to 24 cores and 60 GB of memory) at the Chair of Biometry and Environmental System Analysis, University of Freiburg. For the examination of some of the environmental layers and the preparation of maps I used the open source software QGIS version PISA 2.10 (QGIS Development Team 2015).

### 2.1 Study area

The study was conducted in the Bavarian Forest National Park (NPBW) which is located in south-eastern Germany (Fig. 2.1). The national park covers an area of 240 km<sup>2</sup> and stretches along the border of the Czech Republic. On the Czech side lies, adjacent to the German national park, the Sumava National Park with an area of 640 km<sup>2</sup>. The NPBW comprises three major forest types that can be differentiated by altitude. In the higher elevation above 1100 m there are sub-alpine spruce forests dominated by Norway spruce (*Picea abies*) and some Mountain ash (*Sorbus aucuparia*). On lower slopes between 600 m and 1100 m altitude, mixed mountain forests with Norway spruce, White fir (*Abies alba*), European beech (*Fagus sylvatica*) and Sycamore maple (*Acer pseudoplatanus*) occur. In contrast, in the valley bottoms spruce forests with Norway spruce, Mountain ash and birches (*Betula pendula*, *Betula pubescens*) are the dominating forest types (Blaschke et al. 2004). In total the elevation within the park ranges from 600 up to 1453 m a.s.l and its mean annual temperature ranges from 2 °C to 7.5 °C (Ewald et al. 2014). The study area was defined by the availability of LiDAR data that was the total area of the NPBW including an additional 500 m buffer along the outside of the border.

### 2.2 Species

The effectiveness of remote sensing products, particularly LiDAR-derived metrics, for predicting resource selection was tested for two behavioral slightly different ungulate species: the rather small concentrate selector roe deer (*Capreolus capreolus*) (Hofmann 1989) and the larger but mixed-feeding ruminant red deer (*Cervus elaphus*) (Tixier & Duncan 1996). Due to their size and foraging behavior those species require slightly different habitat characteristics (Bevanda et al. 2015) which makes them excellent target species for testing whether different remote sensing data can capture these differences in a forest-dominated landscape. Roe deer is a small ungulate species, with typically small home ranges (Radeloff et al. 1999). Its diet consists of fresh leaves and grasses such as other highly digestible and protein rich

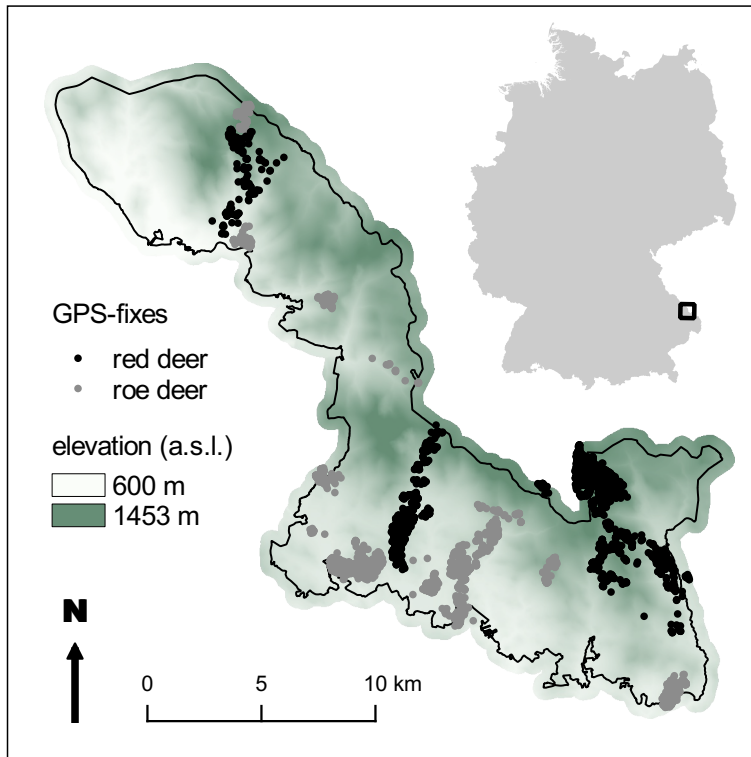


Figure 2.1: Study area and its location in Germany. The study area included the Bavarian Forest National Park (boundaries are outlined in black) and a 500 m buffer around it. Red deer (black dots) and roe deer (grey dots) were monitored with GPS-GSM collars (VECTRONIC Aerospace, Berlin, Germany) from 2010 to 2012. Displayed GPS-fixes were measured at a fix rate of 1 hour.

food items. Therefore, the species is a very selective browser (Demment & Soest 1985). During the summer period roe deer uses the whole area of the national park while in winter the deer moves to lower altitudes with less snow cover (Ewald et al. 2014).

Red deer on the other hand is, a more mobile species with much larger body size. This allows it to cover large distances between feeding and resting grounds. It selects among open habitats for feeding and covered structures for refuge areas (Hebblewhite et al. 2008). The species is classified among intermediate feeders which enables it to choose from a broad spectrum of different food items (Gebert & Verheyden-Tixier 2001). Within the national park red deer ranges freely during the summer period, whereas in winter all individuals are kept in large enclosures at lower elevations as a management measure of the NPBW (Möst et al. 2015). Both species face the Eurasian lynx (*Lynx lynx*) as a natural predator in the national park. For red deer the lynx is most dangerous to young females while lynx prey on roe deer of every age and sex (Weingarth et al. 2012, Stache et al. 2012).

## 2.3 Telemetry data

The telemetry data used for this study are part of multiannual collaring projects in the NPBW. The collars used were GPS-GSM collars from VECTRONIC Aerospace, Berlin, Germany. Because red deer is kept in winter enclosures and the LiDAR data was measured during summer with leaf-on conditions I extracted GPS-fixes within the summer periods from 1st of March until 31st of August for the consecutive years 2010, 2011 and 2012. The two deer species were sampled at different fix rates. This was particularly useful because I could test

Table 2.1: Selection of satellite telemetry data from the Bavarian Forest National Park for a resource selection function.

species	fix rate	used locations <sup>a</sup>	available locations <sup>b</sup>	years	individuals
red deer	15 minutes	11,956	50	2011	10
red deer	1 hour	5,290	50	2011	10
roe deer	1 hour	6,678	50	2010-2012	17
roe deer	4 hours	1,415	50	2010, 2011	15

<sup>a</sup> true GPS-fixes derived from telemetry data

<sup>b</sup> per used location: randomly assigned coordinates in a distance immediately available to the animal at a time (Boyce 2006), for details see Chapters 2.3.3 and 2.3.4

LiDAR data versus non-LiDAR data on four different data sets with varying temporal resolution (Table 2.1). Therefore, I used red deer data at 15 minute fix rate and retained from these GPS-fixes at 1 hour fix rate. Respectively, I used roe deer telemetry data at 1 hour and 4 hour fix rates.

Further preparation of the telemetry data was separated into three steps. First, the selection of GPS-locations with a low spatial error to account for matching resolutions between telemetry data and environmental metrics. Second, the calculation of available locations for the RSF and third, a sensitivity analysis to estimate the right number of available locations.

### 2.3.1 Quality of telemetry data

For successfully applying a resource selection function the temporal and spatial scale of both environmental metrics and GPS-fix rates should match (Cagnacci et al. 2010, Gaillard et al. 2010, Neumann et al. 2015). The resolution of the former ranged from 100 m to <5 m (see Tab. 2.3). For the latter Stache et al. (2012) found that the mean error in the accuracy of GPS-fix acquisition is 13.9 m of GPS locations with the quality label 3D (fixes taken with at least 4 satellites). The accuracy, however, decreases significantly in coniferous stands (own analysis, Stache et al. 2012). By removing GPS locations with a lower quality than 3D a higher share of coniferous forests stands would have been removed from my data and thus affected the results of the RSF. Therefore, I kept all GPS-fixes with a quality label of 3D and 2D (fixes taken with 3 satellites). This compromise led up to an decrease of the mean accuracy of all used GPS-fixes to 14.3 m (in average 2D:3D GPS-fix labels were represented in a ratio of 1:34).

### 2.3.2 Resource selection function

Once the same quality standards for all GPS-fixes was assured for all four data sets, those locations were defined as "used locations" according to the RSF framework. It can be assumed that these locations have been truly visited by the target species.

A RSF is defined as any statistical model designed to estimate the relative probability of an animal using a resource unit versus alternatively available resource units (Manly et al. 2002). It is important to state that here the selection is based on presence/availability data and does not incorporate a presence/absence design. In that case a conditional logistic regression can be used as an estimating function (Boyce et al. 2002) to obtain unbiased estimates of  $\beta$  (from now on called covariate estimates) needed to predict the relative probability of selection  $w(x)$ . Therefore, the exponential form,

$$w(x) = \exp(\beta_1 x_1 + \beta_2 x_2 + \dots + \beta_n x_n) \quad (2.1)$$

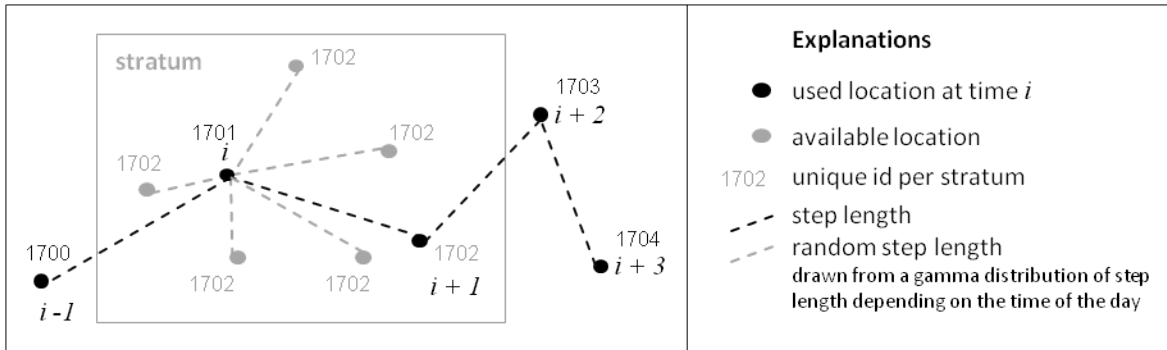


Figure 2.2: Movement path of an animal through the landscape (black) and corresponding availability (grey) for a resource selection function. Used locations are truly captured GPS-fixes whereas available locations are randomly calculated starting at a used location of time  $i$  with random step length into any direction. The stratum is then defined by all available locations and the used location of time  $i + 1$ .

was used with  $x$  being a vector of the length  $n$  for every environmental covariate, with its corresponding vector of coefficients  $\beta$  (Manly et al. 2002, Boyce et al. 2002).

This framework requires (1) animal movement data to define used locations, paired with a set of therefrom generated (2) random points to depict locations immediately available to the animal at a certain time and (3) information on vegetation or habitat structures to explain used and available resource units (Boyce 2006). Each used location with a number of corresponding available locations is defined as a stratum (use and availability at a time, c.f. Fig. 2.2).

Both, the scale of the movement data as well as of the environmental covariates are fundamental when estimating resource selection by animals (Boyce 2006, Kittle et al. 2008, Neumann et al. 2015). They should match the research question but also incorporate already gained knowledge of ecology and behavior of the target species (Thurfjell et al. 2014). However, it is possible to add covariates with different scales to the model design (Boyce 2006).

### 2.3.3 Calculation of available locations

For every used location, as defined above, the RSF framework requires random points in a distance immediately available to the animal (Boyce 2006). According to the different fix rates of each data set, I assigned available locations to a location at time  $i$  in a distance immediately available to the animal within 15 minutes, 1 hour or 4 hours respectively. The stratum was then defined by the calculated available locations and the used location of time  $i + 1$ . Each location within the stratum was assigned the same id unique to any other stratum (Fig. 2.2).

From the species' ecology it is known that activity patterns are higher during civil twilight (Godvik et al. 2009, Stache et al. 2013, Ensing et al. 2014). To capture this daily differences in step length I also accounted for the time of the day when calculating the available locations. Therefore, I fitted a gamma distribution of calculated step length from all used locations depending on the time of the day for each of the four fix rates. Their daily distribution is plotted in Figure 2.3.

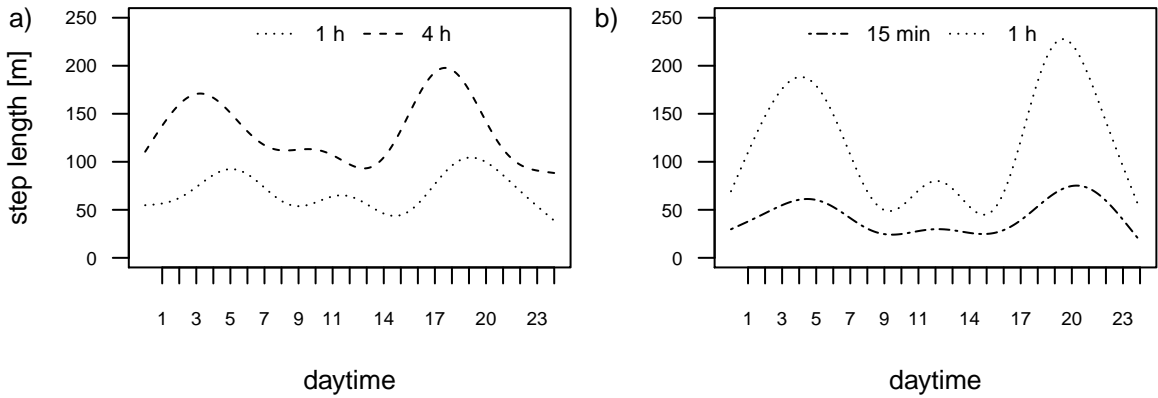


Figure 2.3: Predicted step length depending on the time of the day for a) roe deer and b) red deer. Underlying is a gamma distribution. Step length were calculated from GPS-fixes with different time intervals ranging from 15 minutes to 4 hours between fixes.

### 2.3.4 Sensitivity analysis

The number of available locations, which is needed to get stable covariate estimates (see Chapter 2.3.2) is crucial for implementing a RSF. The number depends on the resolution of variables representing the environment as well as on the heterogeneity of the environment itself. If high heterogeneity is given, more available locations are needed to describe appropriate availability. However, this selection can be limited by computational ability, forcing to reduce number of available location despite the development of covariate estimates (Northrup et al. 2015).

At first Northrup et al. (2013) provide guidance for choosing the availability sample for studies implementing RSF. Considering this, I explored the stability of covariate estimates for my models. For this purpose I fitted models with varying sample size (from 1 to 300) of available locations per used location. Each model was fitted 30 times at each sample size always assigned with new available locations drawn from a set of 4,000 available locations per used location.

To reduce running time of the models I used a subset of the data set with the finest scale (roe deer with 1 hour fix rate). I selected GPS-fixes from every individual for one week of each month of the year 2011 ( $n = 1,219$ ). The model was fitted with covariates ranging from 1 m to 10 m resolution. I expected the estimates for covariates of 1 m resolution (highest) to stabilize last because they contained most environmental heterogeneity. To increase complexity, I tested two model designs, one including interactions and the other including squared terms.

## 2.4 Environmental metrics

All data sets were transformed to the coordinate reference system DHDN/Gauss-Krüger zone 4 (EPSG: 31468). For all used and available locations of the four deer data sets the values of each environmental variable were extracted. For this purpose, I used the R-package *raster* (Hijmans 2015).

### Selection of confounding factors

For building the models I selected variables that describe the terrain, climatic conditions, daily and seasonal patterns such as human influence (see Table 2.2). I used these variables consistently throughout all models referring to them as "confounding factors". Thus, I could for example take into account daily patterns in the behavior of the two deer species (Godvik et al. 2009).

### Commonly used remote sensing products

Next, I prepared those environmental metrics that I wanted to compare to each other in terms of their predictive power in modeling resource selection of deer. I chose them from remote sensing products, which are commonly used in wildlife ecology studies to represent habitat and vegetation structures. Besides the confounding factors they would significantly improve the predictive power of my resource selection models, however, I only tested one environmental metric against the others without combining them. All of these metrics are summarized in Table 2.3 including their resolution and a description of their processing.

I regarded land cover maps as an often used product from satellite images or aerial photographs and used two maps differing in granularity and resolution. Hereby, the map based on corine satellite interpretation is freely available and represents a conventional land cover map. In contrast, the habitat map commissioned by the NPBW is based on manual interpretation of aerial photographs and therefore classified in much more detail; for example taking into account the differences of mature, medium and young forest stands. Furthermore, I calculated monthly NDVI from landsat images from 2010 to 2012. This metric provides continuous data of the spatial distribution of green (productive) vegetation. Against the predictive power of these commonly used remote sensing products I compared LiDAR-derived metrics for predicting resource selection in deer.

#### 2.4.1 Preparation of LiDAR data

The LiDAR data were available for the whole area of the NPBW and an additional buffer of 500 m outside the park boundaries. The flights were conducted by Milan Flug GmbH during three days in June 2012 under leaf-on condition. The used laser scanner was a Riegl 680i with 350 KHz, a nominal point density of 30–40 points per square meter within the altitude of 650 m (for more information see Latifi et al. 2015). From these data all further LiDAR metrics were derived at 1 m resolution. Resolution was lowered to 5 m or 10 m using the function *aggregate* of the package *raster* in R.

Table 2.2: Environmental variables to analyze resource selection in roe and red deer in the Bavarian Forest National Park (NPBW). Described layers explain the terrain, climatic conditions, daily and seasonal patterns such as human influence and were therefore potential confounding factors for the generalized linear mixed models. After checking for correlation only variables marked in bold were used.

Abbreviation	Resolution	Description
elev	1 m	Digital elevation model (DEM) raster layer provided by the NPBW.
aspect	1 m	Derived from DEM using R-function terrain in R (8 neighbors).
slope	1 m	Derived from DEM using R-function terrain in R (8 neighbors).
<b>rugged_10</b>	10 m	Derived from DEM using R-function terrain in R (8 neighbors and Terrain Ruggedness Index (TRI) as option).
<b>dist_trails</b>	cm	Distance to closest hiking trail. For efficiency calculated with a C++ script written by Philipp Jund.
dist_roads	cm	Distance to closest road. For efficiency calculated with a C++ script written by Philipp Jund.
humi	100 m	Mean annual humidity, ESRI shape file provided by the NPBW.
preci	100 m	Mean annual precipitation, ESRI shape file provided by the NPBW.
<b>sol_rad</b>	100 m	Mean monthly solar radiation, ESRI shape file provided by the NPBW, derived from slope and aspect. Source: <a href="http://pro.arcgis.com/de/pro-app/tool-reference/spatial-analyst/an-overview-of-the-solar-radiation-tools.htm">http://pro.arcgis.com/de/pro-app/tool-reference/spatial-analyst/an-overview-of-the-solar-radiation-tools.htm</a>
wetness	100 m	Mean annual wetness, ESRI shape file provided by the NPBW.
temp		A proxy for air temperature. Device is implemented into the GPS-collar (Vectronic Aerospace, Berlin, Germany) of each individual.
<b>sun_elev</b>		Elevation of the sun during the day calculated for every deer location using the R-function sunPosition. Here used as a proxy for the time of the day accounting for annual differences for sunrise and sunset. Source: <a href="http://stackoverflow.com/questions/8708048/position-of-the-sun-given-time-of-day-latitude-and-longitude">http://stackoverflow.com/questions/8708048/position-of-the-sun-given-time-of-day-latitude-and-longitude</a>

## Common LiDAR products

For the comparison of environmental metrics I tested a set of LiDAR-derived metrics applied in previous studies. Accordingly I used three LiDAR products: the mean height of vegetation (Farrell et al. 2013, Lone et al. 2014a, Ackers et al. 2015) calculated from all returns of the point cloud, the fractional vegetation cover of three different height strata (Ewald et al. 2014, Lone et al. 2014a,b), which describes the proportion of returns within a certain height, and the number of single trees within a pixel, which was only available due to the high resolution of the LiDAR data (Flaherty et al. 2014, Ackers et al. 2015).

Furthermore, I tested the predictive power of a LiDAR product that has not been applied yet. From the LiDAR point cloud a non-specific metric was calculated by the implementation of a Principle Component Analysis (PCA) on 99 horizontal layers of a certain height above ground (Antkowiak, unpublished). Although all environmental variables are briefly described in Table 2.3 this particular data set is explained in more detail due to its novelty.

## Newly developed LiDAR-based PCs

To capture most of the information of vegetation structure stored in the LiDAR point cloud its complexity was re-arranged by performing a PCA. LiDAR data was prepared in horizontal raster layers each representing a height of 0.5 m. In every horizontal layer all vegetation returns captured within that height range were added up. Starting from 0.5 m to 1 m, 1 m to 1.5 until 49.5 m to 50 m a total of 99 horizontal layers were calculated. The vegetation returns below 0.5 m were neglected due to their inaccuracy in distinguishing between vegetation and

Table 2.3: Abbreviation and description of available remote sensing data to explain resource selection in roe and red deer in the Bavarian Forest National Park (NPBW). Variables have either been calculated from satellite or aerial images or were derived from light detection and ranging (LiDAR) point clouds.

Abbreviation	Resolution	Description
Products derived from satellite or aerial images		
corine	ca. 100 m	Coordination of Information on the Environment (CORINE) is a consistent land cover classification for whole Europe. Here, the updated map from 2006 was provided. From 37 land cover classes within Germany the NPBW is differentiated in 14 including a distinction of e.g., deciduous, coniferous and mixed forest types. Source: <a href="http://corine.dfd.dlr.de/">http://corine.dfd.dlr.de/</a>
map2012	<5 m	manually interpreted aerial photography of 2012. The map was commissioned by the NPBW to the photogrammetry company Geoplana and covers only the area within the park boundaries. In total 25 land cover classes are differentiated including fine-scale specifications such as coniferous stand mature, medium and young.
ndvi	30 m	Normalized difference vegetation index (ndvi) which is calculated as one value per month. Values have been derived from Landsat 4-5 and 7 satellite images using the tool Vegetation index (slope based) in QGIS. If missing values occurred they were interpolated with the remaining values and elevation programmed in R. Source: <a href="http://earthexplorer.usgs.gov/">http://earthexplorer.usgs.gov/</a>
Products derived from LiDAR point cloud		
MeanHeight	5 m	Mean vegetation height in meters from all cover returns. Calculated by Ramiro Silveyra González using spdlib. Source: <a href="http://spdlib.org/doku.php">http://spdlib.org/doku.php</a>
UStory	5 m	Fractional vegetation cover of strata 0.5 m - 2 m describing understory vegetation. Calculation was performed following Ewald et al. (2014).
MStory	5 m	Fractional vegetation cover of strata 2 m - 10 m describing midstory vegetation. Calculation was performed following Ewald et al. (2014).
OStory	5 m	Fractional vegetation cover of strata 10 m - 50 m describing overstory vegetation. Calculation was performed following Ewald et al. (2014).
res5_PC1 - PC11 <sup>a</sup>	5 m	first 11 PCs (explaining 85% variance, see App. A) from a Principal Component Analysis of the point cloud. Calculated by Peter Antkowiak using statistical software R.
res10_PC1 - PC9 <sup>a</sup>	10 m	first 9 PCs (explaining 91% variance, see App. A) from a Principal Component Analysis of the point cloud. Calculated by Peter Antkowiak using statistical software R.
st_conif	10 m	Single tree detection capturing the number of coniferous trees per pixel. Raster layer provided by the NPBW.
st_deci	10 m	Single tree detection capturing the number of coniferous trees per pixel. Raster layer provided by the NPBW.
st_dead_all	10 m	Single tree detection capturing the number of coniferous trees per pixel. Raster layer provided by the NPBW.

<sup>a</sup> a detailed description of the data preparation is given in Chapter 2.4.1.

ground returns (Heurich et al. 2008). The maximum height was set 50 m according to the maximum height of the trees in the national park.

In order to compensate for the overlap in the transects flown by the aircraft, all horizontal layers were normalized. This was done by dividing them by the total amount of pulses sent within a raster cell. At that point data was ready to run a PCA of all 99 horizontal layers. A PCA describes differences in a set of more or less correlated variables. By calculating a correlation matrix of the data and performing an eigenvector decomposition on it, a set of linearly uncorrelated variables is generated (Dormann, Carsten 2013). In this case the 99

horizontal layers are the correlated variables explaining vertical and horizontal structure of vegetation. For example a low number of vegetation returns in low height (representing low or no vegetation) is likely to be correlated with a high number of vegetation returns in the higher layers (representing closed canopy cover and high forests). In simple words, high forests with closed canopy cover often have low understory vegetation. However, this comparatively easy assumption is not the only information hidden in the LiDAR point cloud. The PCA turns the most important differences in the data (e.g. high versus low vegetation in one raster cell) into new variables. It results in a number of Principle Components (PCs) that capture this information but are not correlated anymore, which makes them perfect new predictors in a model. These PCs are sorted by importance (explained percentage of variance in the data) starting with PC1, which explains most variance. Additionally, PC2 can only explain differences in the data that were not captured in PC1 and the same is true for PC3, which can only capture differences not explained from PC1 and PC2, and so on. Here, the variables the PCA was run on were all 99 horizontal layers of the LiDAR point cloud.

However, the LiDAR data covered the total area of the NPBW which resulted in a data set of approximately 31,000 x 33,000 data points at 1 m resolution. Running a PCA on such a large data set was computationally not feasible. Instead, random points were assigned within the national park boundaries and values for each raster cell within the horizontal layers were extracted. To ensure consistency among PCA results a cross-validation was performed by running PCAs on different random point samples. The PCA results were proven stable at 1 Million random points. With this new and smaller data set PCAs could easily be conducted at 5 m and 10 m resolution. Resulting PCs of the two data sets and their explained proportion of variance are provided in Appendix A.

The computation was conducted by Antkowiak (unpublished) and I was provided with the final PC values for each data set. I included all PCs that explained more than 1% variance of the data in the models. Thus, I had two new data sets: 11 LiDAR-based PCs at 5 m resolution (85% explained variance) and respectively 9 LiDAR-based PCs at 10 m resolution (91% explained variance, see App. A). From the PCA results, PC values were predicted for each location of the four deer data sets.

## 2.5 Model fitting

Before fitting the models, I tested for correlations among environmental metrics and removed one covariate if it was highly correlated ( $|r| > 0.7$ ) with another covariate.

I used a conditional logistic regression by fitting generalized linear mixed models (GLMMs) in R. The GLMMs were used to obtain covariate estimates for the exponential form described in Equation 2.1 (Boyce et al. 2002, Manly et al. 2002). Hereby, I used the R-package *lme4* (Bates et al. 2015). Using the function *glmer* allowed me to specify fixed effects as well as random effects in a simple way. Per default the function uses the maximum likelihood for fitting the GLMMs. As it is proposed by Boyce et al. (2002) I chose Akaike's Information Criterion (AIC) for comparison of models. The AIC helps to identify the model that explains the most variation with the fewest variables. All covariates were standardized by subtracting the median and dividing by the standard deviation  $((x - \bar{x})/\sigma)$  which could be easily achieved with the *scale* function in R. For enabling a systematic comparison the "confounding factors" as fixed effects as well as nested random effects were included into every model. In contrast, the "environmental metrics" (as fixed effects) were exchanged for every new model as they were the predictors I wanted to compare to each other (Tab. 2.4). As response variable the used locations were assumed to be 1 while the available locations were 0. This required a binomial distribution for fitting the GLMMs. All models fitted with the same data set were also fitted on exactly the same number of observations as presented in Table 2.1.

Table 2.4: Model design for comparing different environmental metrics by using generalized linear mixed models with nested random effects. Environmental metrics were exchanged for comparison while the other predictors were included into every model.

Predictor	
sun_elev	fixed effects
sun_elev <sup>2</sup>	”confounding factors“
rugged_10	
rugged_10 <sup>2</sup>	
dist_trails	
dist_trails <sup>2</sup>	
solrad	
sun_elev:dist_trails	
sun_elev:solrad	
id	nested random effects
loc_id	
environmental metrics	fixed effects
environmental metrics <sup>2</sup>	”predictor for vegetation“
sun_elev:environmental metrics	

# Chapter 3

## Results

In this study I compared the predictive power of LiDAR and more commonly applied remote sensing products in the resource selection of roe and red deer. After checking correlation of variables, sun elevation, ruggedness, distance to trails, and solar radiation were kept as fixed effects in all models. Additionally each model contained one out of eight different environmental metrics, derived from (1) satellite images namely being NDVI, corine land cover classes; (2) aerial photography namely being habitat classification map NPBW; and (3) LiDAR data namely being mean vegetation height, fractional vegetation cover, and number of single trees. Furthermore, I tested newly developed LiDAR-derived PCs at 5 m and 10 m resolution.

### 3.1 Sensitivity analysis

To find a suitable number of available locations I fitted a subset of the roe deer data with differing availability sample size. Covariate estimate from the generalized linear mixed models started to stabilize at 40 available locations (plotted results are provided in Appendix B). No differences among the covariate estimate development for the model fitted with squared terms or with interactions could be found. Therefore, a sample size of 50 random points per used location was assumed to represent available resources well enough for all four data sets.

### 3.2 Model comparison

For comparing different generalized linear mixed models I used the AIC values of each model (Boyce et al. 2002). Table 3.1 provides  $\Delta\text{AIC}$  values for 10 different models fitted with varying environmental metrics.

Overall, models incorporating LiDAR products outperformed models including predictors derived from satellite images. The best model among all tested environmental predictors was the one incorporating the newly developed LiDAR-based PCs at 10 m resolution. Among the non-LiDAR variables only the habitat map of the NPBW had a comparably high predictive power.

The second best model for roe deer data incorporated again the LiDAR-based PCs this at 5 m resolution. For red deer data the second best model incorporated fractional vegetation cover which is a common product derived from LiDAR point cloud data. At 15 min fix rate this model performed almost as good as the best model incorporating LiDAR-based PCs ( $\Delta\text{AIC}$  of 1.3). This indicates high predictive power of both, LiDAR-derived PCs and fractional vegetation cover, on a very fine spatial scale.

Table 3.1: Comparison of generalized linear mixed models explaining the resource selection of red and roe deer based on Akaike's Information Criterion (AIC). Deer data were tested at different resolutions (GPS-fix rates). Models were fitted using predictors either derived from satellite images, aerial photography or LiDAR data. The name of the model corresponds to the environmental metric(s) used to describe vegetative structures or land cover classes. Model 1 incorporates only individuals and stratum as nested random effects, model 2 additionally includes predictors explaining terrain, human disturbance, and daily patterns but has no predictor for vegetation, whereas models 3 - 10 incorporate the design of model 2 and include one or several additional predictors describing vegetative structures or land cover classes. Next to the  $\Delta\text{AIC}$  values the ranking of each model among one data set is provided for a better overview. Detailed summaries of all models can be found in Appendix C.

no.	model name	$\Delta\text{AIC}$					
		red deer 15 minutes	red deer 1 hour	roe deer 1 hour	roe deer 4 hours	examples for the application of LiDAR products	
1	null model	371.4	10	577.9	10	848.4	10
2	no vegetation	354.8	8	507.1	9	792.6	8
3	corine land cover classes <sup>1</sup>	363.6	9	499.6	8	801.3	9
4	normalized difference vegetation index <sup>1</sup>	333.9	7	454.0	7	752.2	7
5	mean vegetation height <sup>2</sup>	287.9	6	393.8	6	300.1	5
6	number of single trees <sup>2</sup>	208.7	4	284.8	5	422.0	6
7	habitat classification map NPBW <sup>3</sup>	229.4	5	231.2	4	169.9	3
8	fractional vegetation cover <sup>2</sup>	1.3	2	45.1	2	179.9	4
9	LiDAR-based PCs (5 m resolution) <sup>2</sup>	40.8	3	74.4	3	71.8	2
10	<b>LiDAR-based PCs (10 m resolution)<sup>2</sup></b>	<b>0</b>	<b>1</b>	<b>0</b>	<b>1</b>	<b>0</b>	<b>1</b>

<sup>1</sup> satellite image product

<sup>2</sup> light detection and ranging (LiDAR) point cloud product

<sup>3</sup> aerial photography product, manually interpreted

NPBW: Bavarian Forest National Park; PC: Principle Component from a Principle Component Analysis

Model 2 "no vegetation", fitted as a generalized linear mixed model, incorporated the following predictors:  
 ruggedness, distance to trails, sun elevation (as squared terms), the categorical variable solar radiation (low, medium, high)  
 and interactions of sun elevation with distance to trails and sun elevation with solar radiation.  
 Individuals and stratum were included as nested random effects.

The model including the habitat map land cover classification of the NPBW achieved rankings between 3, 4 and 5 among the different data sets, while the other two non-LiDAR products performed much worse. Worst among all models incorporating a predictor for vegetation structure was in 3 cases corine and in 1 case NDVI. For red and roe deer at the smaller fix rates the models including corine were even outperformed by the model with no additional predictor for vegetation. This means the corine land cover classes did not add any additional information when fitting the models. Among the LiDAR products least suitable to predict resource selection in deer was the model incorporating mean vegetation height.

Looking at the best performing model (LiDAR-based PCs at 10 m resolution) in more detail one can understand the significance of single predictors in the model. The covariate estimates ( $\beta$ ) and their corresponding standard error (SE) were summarized in Table 3.2 for all four data sets. Significance of a predictor was assumed with a p-value  $< 0.05$ . For all four data sets the confounding factor ruggedness and distance to trails were highly significant. In contrast, solar radiation was almost never significant.

This model incorporated the first 9 PCs from the PCA of the LiDAR data at a 10 m resolution. All of them were included as linear and squared terms as well as interacted with sun elevation to show daily differences among the selection of these predictors. Most notably, PC3 (linear & squared) was highly significant for all four data sets. Second most, PC1 was significant for red deer (squared) and roe deer (linear). The roe deer data sets show significance of PC1 to PC5 if interacted with sun elevation which shows that the deer significantly differs in the selection of those PC during the day. For red deer this pattern is not as expressive.

Table 3.2: Covariate estimate  $\beta$  and corresponding standard error SE of four generalized linear mixed models. All predictors were standardized  $((x - \bar{x})/\sigma)$  when fitting the models.

predictor	red deer				roe deer			
	15 minutes		1 hour		1 hour		4 hours	
	$\beta$	SE	$\beta$	SE	$\beta$	SE	$\beta$	SE
Intercept	-3.841	0.028	***	-3.829	0.044	***	-3.899	0.045
sun_elev	-0.019	0.017		-0.037	0.026		0.088	0.024
sun_elev <sup>2</sup>	-0.052	0.013	***	-0.092	0.020	***	-0.058	0.017
rugged_10	0.014	0.013		-0.015	0.020		0.051	0.023
rugged_10 <sup>2</sup>	-0.019	0.006	**	-0.028	0.010	**	-0.038	0.010
dist_trails	0.004	0.016		-0.020	0.023		0.082	0.024
dist_trails <sup>2</sup>	-0.036	0.014	**	-0.080	0.022	***	-0.029	0.006
solrad_low	0.012	0.023		0.037	0.034		0.002	0.032
solrad_medium	0.014	0.023		0.009	0.034		0.037	0.031
res10_PC1	0.014	0.031		-0.121	0.049	*	-0.249	0.024
res10_PC2	0.045	0.022	*	0.066	0.036		0.050	0.029
res10_PC3	0.075	0.020	***	0.170	0.032	***	0.256	0.021
res10_PC4	0.080	0.026	**	0.106	0.041	*	0.117	0.032
res10_PC5	0.002	0.023		0.006	0.036		0.014	0.021
res10_PC6	0.015	0.017		0.001	0.029		0.019	0.019
res10_PC7	-0.031	0.018		-0.057	0.029		-0.044	0.018
res10_PC8	-0.029	0.017		-0.043	0.027		0.002	0.019
res10_PC9	0.024	0.015		0.024	0.024		-0.027	0.017
res10_PC1 <sup>2</sup>	-0.054	0.013	***	-0.045	0.023	*	-0.046	0.028
res10_PC2 <sup>2</sup>	-0.001	0.012		-0.001	0.019		0.011	0.021
res10_PC3 <sup>2</sup>	0.042	0.010	***	0.069	0.016	***	0.080	0.020
res10_PC4 <sup>2</sup>	0.010	0.011		0.001	0.016		-0.004	0.015
res10_PC5 <sup>2</sup>	-0.016	0.011		-0.019	0.015		-0.040	0.015
res10_PC6 <sup>2</sup>	-0.009	0.008		-0.006	0.013		0.000	0.011
res10_PC7 <sup>2</sup>	-0.004	0.008		-0.016	0.012		-0.001	0.011
res10_PC8 <sup>2</sup>	0.003	0.007		0.010	0.011		0.004	0.010
res10_PC9 <sup>2</sup>	-0.003	0.006		-0.008	0.009		-0.015	0.009
sun_elev:dist_trails	0.035	0.011	**	0.093	0.017	***	0.020	0.014
sun_elev:solrad_low	0.003	0.023		0.011	0.035		-0.067	0.032
sun_elev:solrad_med	-0.001	0.023		-0.013	0.035		-0.040	0.031
sun_elev:res10_PC1	0.010	0.012		0.036	0.021		0.035	0.015
sun_elev:res10_PC2	-0.008	0.013		-0.065	0.022	**	-0.063	0.015
sun_elev:res10_PC3	-0.020	0.013		-0.030	0.022		-0.045	0.015
sun_elev:res10_PC4	0.045	0.016	**	0.104	0.027	***	0.042	0.015
sun_elev:res10_PC5	-0.074	0.018	***	-0.113	0.031	***	-0.117	0.015
sun_elev:res10_PC6	0.023	0.016		0.042	0.028		-0.008	0.015
sun_elev:res10_PC7	0.018	0.016		0.033	0.027		0.012	0.015
sun_elev:res10_PC8	-0.015	0.016		-0.013	0.027		0.014	0.015
sun_elev:res10_PC9	-0.008	0.014		-0.019	0.022		-0.009	0.015

Significance code for  $p < 0.001$  \*\*\*,  $p < 0.01$  \*\* and  $p < 0.05$  \*

### 3.3 Identification of important predictors

In the RSF framework the covariate estimates from the generalized linear mixed model have to be calculated in the exponential form (Eq. 2.1) to retain the relative probability of selection  $w(x)$  for every predictor. For the best model, which was incorporating LiDAR-derived PCs at 10 m resolution, these RSF values are plotted in Figure 3.1. Predictors of high importance for the model can be identified by a high  $w(x)$  value or a distinct shape. Their absolute values can only be compared to other predictors in the same model. Here, in all four models PC3 reached highest RSF values meaning this was the driving predictor for all four models. Besides that, all predictors have a certain impact on the model due to their hump-shape implying a selection for certain values. The x-axis values are negligible at this point because they carry no information on the importance of the predictor in a model but will be considered in the next Chapter.

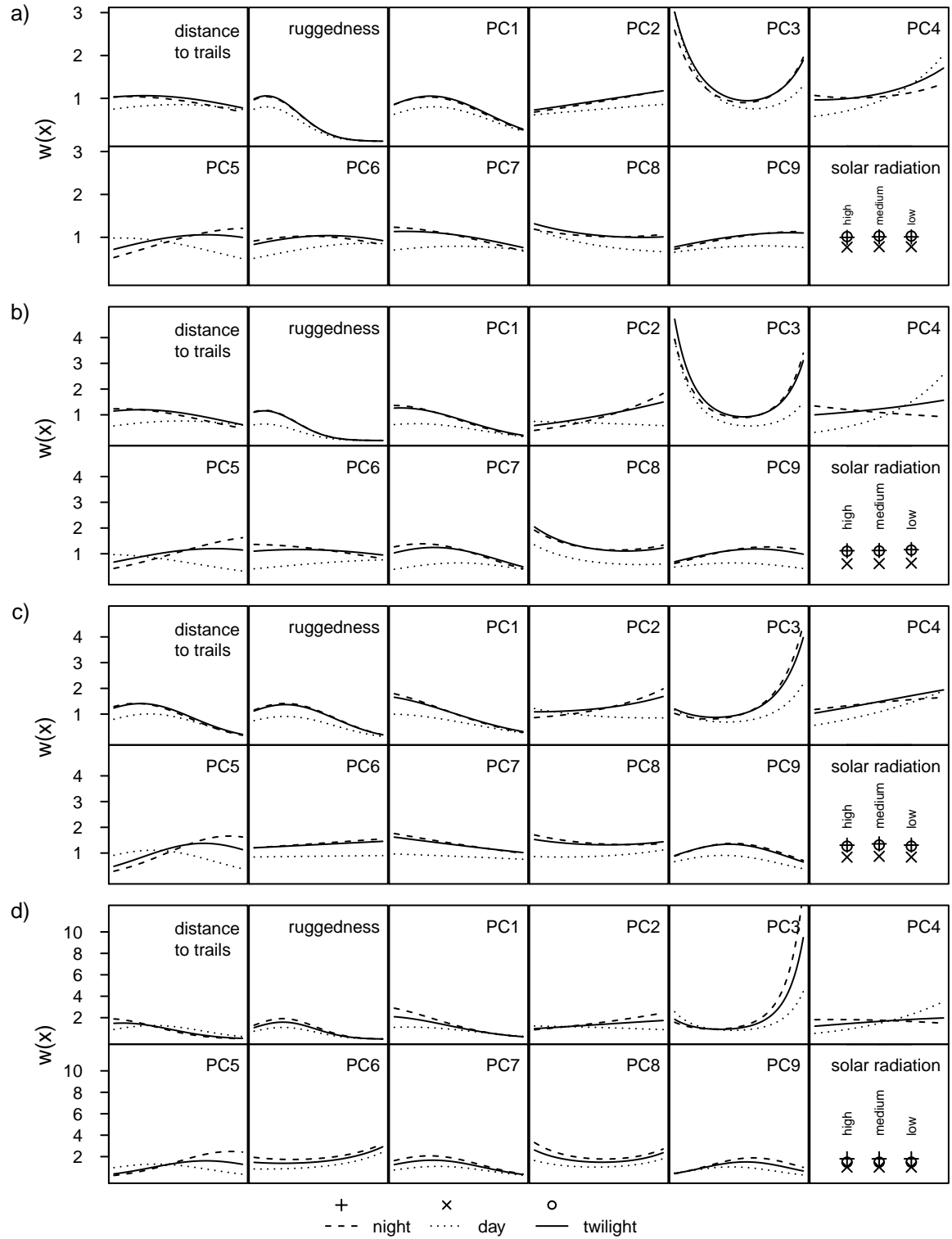


Figure 3.1: Understanding the importance of single predictors: The higher the predicted RSF values  $w(x)$  get the more influence this predictor has in the model. Subfigures represent the four data sets a) red deer at 15 minute, b) red deer at 1 hour, c) roe deer at 1 hour and d) roe deer at 4 hour fix rate. The x-axis values are not relevant for highlighting differences in the  $w(x)$  values but generally range from "low" to "high". All PC-variables are products of a Principle Component Analysis run on three-dimensional LiDAR point cloud data at 10 m resolution.

### 3.4 Predictions of resource selection

#### Confounding factors

I predicted resource selection of the confounding factors for both species at 1 hour fix rate from the best model. Both species show clear patterns in their selection of terrain ruggedness and distance to trails (Fig. 3.2). Red deer clearly select for less rugged terrain although this selection is less important during the day. The selection along trails is opposite from night to day. At daytime red deer stay at longer distances to trails with a preference at 1200 m whereas during twilight they prefer 600 m distance and at night, when they are not threatened by human encounters, they select for trails or areas next to trails.

Roe deer on the other hand also prefer less rugged terrain. Similar to red deer they prefer areas with a terrain ruggedness of 1 or 2, meaning flat terrain. During the day they prefer to stay at distances of 300 m away from trails while during night and at twilight the curve is more distinct with a peak at 200 m. In general they select areas closer to trails.

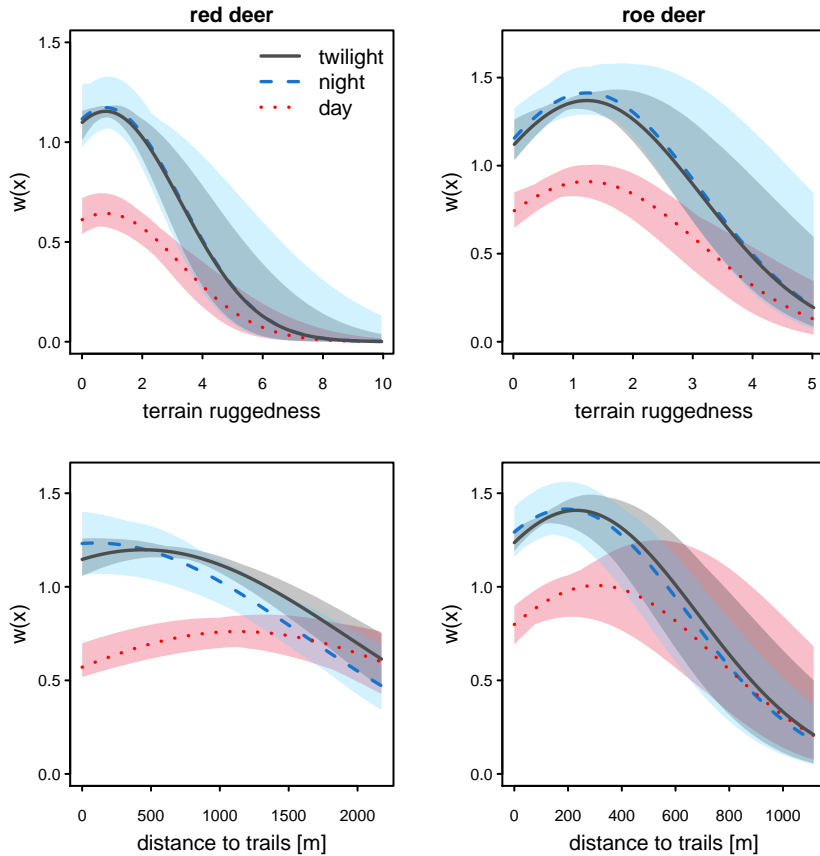


Figure 3.2: Relative probability of selection  $w(x)$  for red and roe deer (telemetry data of 1 hour fix rate) from the best models. Variables were interacted with the time of the day (twilight, night, day).

## **LiDAR-based PCs**

Furthermore, the best model among all tested models incorporated 9 LiDAR-based PCs as predictors. In Figure 3.3 predictions of the first 5 PC variables are presented for both species. The selection of both deer species is very similar to each other for all plotted PCs. A different pattern in resource selection can only be found for PC3, which is also the most important driver in the two models. However, for understanding the selection of vegetative structures from the PCA results it is advisable to start with PC1.

Both deer species select for negative values of PC1, more importantly during civil twilight and night, but always with a clear trend (Fig. 3.3). For better understanding the PC values I plotted the rotation matrix of the PCA next to the predictions of each PC variable. The PCA rotation matrix describes how much each variable loads on each PC. Given that, the preference of negative values for PC1 of both deer species indicates that they select rather for open habitat in absence of trees with a height between 15 m to 30 m.

A single PC can only describe differences in vertical vegetation structure. Thus, predictions of PC2 are limited to information not already contained in PC1. This property of PCs becomes accessible when looking at the rotation matrix plots again: In the altitudes where PC1 reaches high absolute values on the x-axis PC2 changes from negative to positive or vice versa, thereby distinguishing the most important vertical structures that have not been captured by the previous PC. The same pattern appears when comparing the plots for PC2 and PC3, PC3 and PC4, and so on.

Further interpretation of this kind of data and ideas how to draw ecologically meaningful conclusions are provided in the Discussion, Chapter 4.2.

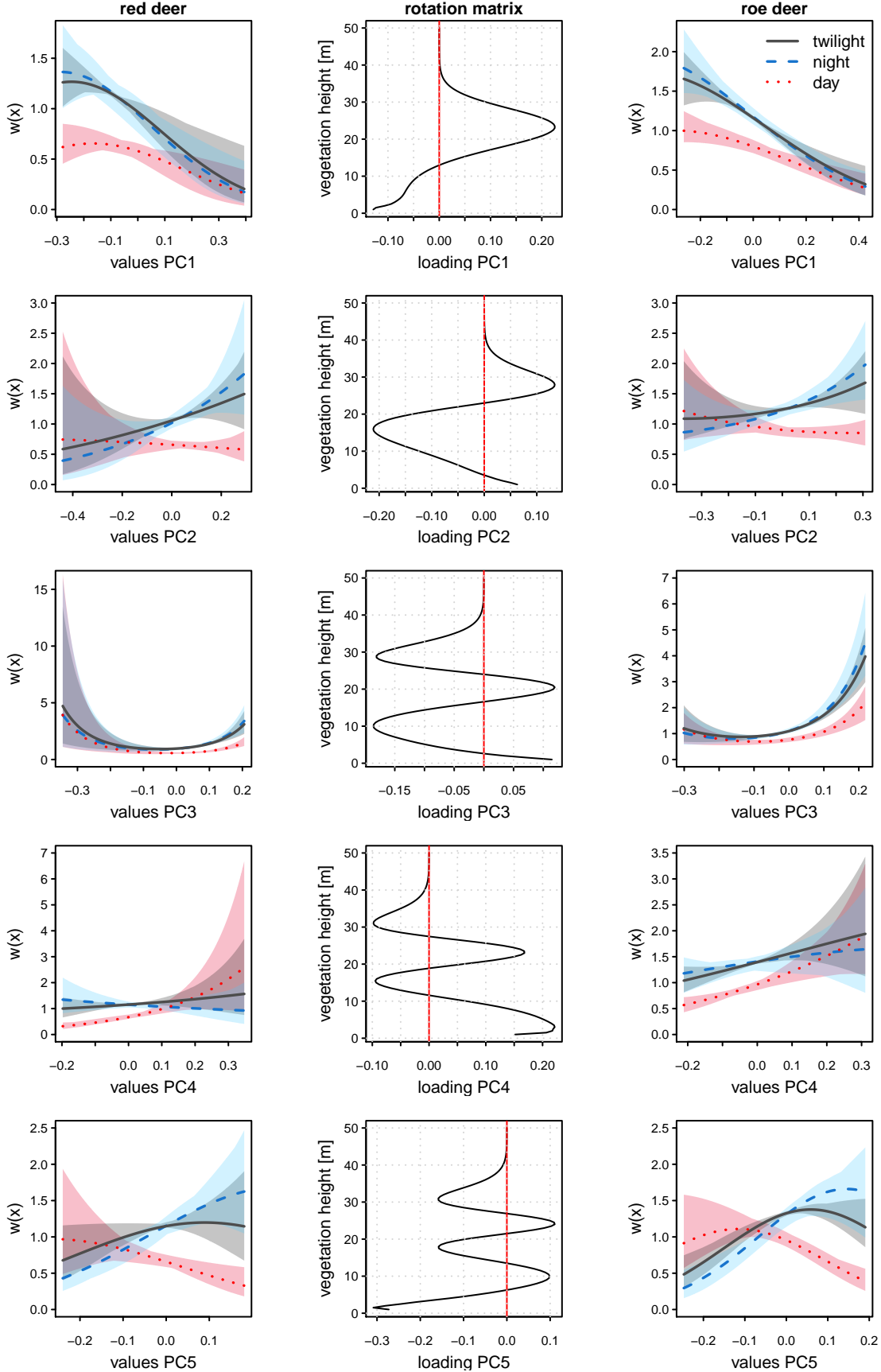


Figure 3.3: Relative probability of selection  $w(x)$  of red and roe deer from the best models. Variables were interacted with the time of the day (twilight, night, day). Principle Component (PC) values are derived from a Principle Component Analysis of LiDAR point cloud data at 10 m resolution. They are describe the difference in vegetation height. The middle column displays rotation matrices for each PC.

# Chapter 4

## Discussion

LiDAR data is an increasingly well understood and established remote sensing technology (Neumann et al. 2015) that can be used to explain wildlife behavior particularly on a fine scale and thus helps us to improve management and conservation measures. The goal of this study was to compare the predictive performance of different remote sensing products with a particular focus on LiDAR-derived metrics. For this purpose, a fine-scale resource selection function for two deer species in the Bavarian Forest National Park was implemented.

The results indicate that the application of LiDAR-derived metrics can provide fine-scale predictions of the resource selection in deer. Their resolution and granularity matches the scale, in which deer make decisions on habitat use, more accurately than coarser remote sensing data tested in this study. It was found that models based on LiDAR-derived metrics performed superior relative to models with more commonly used products of satellite or aerial images. Thereby, the results of this study support the general trend in wildlife ecology studies to use LiDAR-derived vegetation metrics for explaining habitat use on an unprecedented fine scale (e.g., Graf et al. 2009, Farrell et al. 2013, Ackers et al. 2015).

The biggest innovation in this study was using LiDAR-based Principle Components to better capture the variation in the vertical vegetation structures from the LiDAR point cloud. These LiDAR-based PCs were tested comparing 5 m and 10 m resolution. I could show that for both spatial scales LiDAR-based PCs were well suited to predict fine-scale habitat use in deer on a large area.

## 4.1 Predictive power of commonly used environmental metrics

### Habitat Classification Map of the NPBW

Out of all eight tested models those incorporating LiDAR-derived metrics were always among the best six, only with the exception of the models incorporating the habitat classification map provided from the NPBW. The predictive performance of this map is comparatively high due to its manually interpretation of aerial photographs that resulted in fine-scale differentiation of land cover classes. Classes have been designed to explicitly describe ecologically relevant habitat characteristics. This map captures even complex structures such as "dead wood standing" or "dead wood lying" and incorporates structures like "ecotone" that have been found missing in conventional habitat mapping by satellite images (Tattoni et al. 2012). The predictions of habitat selection by both deer species from this map provided insights in different habitat selection of red and roe deer (see App. D). Most important selection of red deer were found during night and thereby particularly for cultivated meadows. Less importantly they selected for ecotones, natural meadows but also residential areas during night. In contrast, roe deer selection captured from this map was mainly important during the day. Hereby, rather dense habitat structures such as young coniferous or deciduous stands were selected while natural and cultivated meadows were selected with a similar proportion throughout the whole day. Additionally, during the day they highly preferred ecotones but avoided residential areas at any time of the day.

These two examples showed how well the habitat classification map of the NPBW can provide insights in the resource selection of deer species. Because the map captures 25 different habitat classes throughout the whole national park it is well suited for further habitat modeling approaches.

### Corine Land Cover Classes

The two products derived from satellite images did not perform very well in relation to the LiDAR-derived metrics. In 2 out of 4 cases, models incorporating the corine land cover classification map performed even worse than the models with no additional predictor of vegetation. This very poor predictive power can be explained due to the coarse resolution of the corine map which did not match the fine-scale RSF that was implemented in this study. The two cases where it performed worse than the model without a predictor for vegetation were the models fitted with the smallest fix rate for both species. This was 1 hour for roe deer and 15 minutes for red deer. According to Figure 2.3 the step length of both species at such fix rates is very similar and at maximum 100 m (during cilvil twilight). When assessing such fine-scale movement patterns, used and available locations are likely to be located in the same category of the corine map. Thus, no additional information was added to the model fit, instead, only extra noise was introduced. For red deer monitored at 1 hour fix rate and thus, the coarsest scale applied in this study (see Fig. 2.3), the corine map was performing better than the model including the NDVI as predictor for vegetation. This result underlines the importance of choosing the right spatial scale also highlighted by authors like Thurfjell et al. (2014) and Neumann et al. (2015).

### Normalized Difference Vegetation Index

Initially, I expected a main advantage of calculating the NDVI because it included changes in time. Here, a NDVI value for every month (May to August) was calculated from the landsat images from 2010 to 2012. However, because of its rather low resolution (30 m) NDVI could

not compete with the other models tested in this study. Moreover, it only represents the productivity of the site and does not necessarily yield information on understory vegetation relevant to deer. Even though landsat satellite images are freely available in continuous time series in this study their predictive power was limited. Considering this, their application seems more reasonable at coarse spatial scales (sensu Neumann et al. 2015).

### Mean Vegetation Height

The mean vegetation height is a useful measure to generate ecologically meaningful quantities on the vertical structure of vegetation. It is calculated from LiDAR returns of all heights and was included as one predictor in my models. In other studies it has been applied in combination with other environmental metrics such as mean canopy cover (Farrell et al. 2013) or standard deviation of canopy height and maximum canopy height (Müller et al. 2009) which resulted in well-performing models for modeling abundance of avian species. In my study, however, its performance was worst of all LiDAR-derived metrics for the red deer and the second worst for roe deer data. Even though this metric is a measure for vegetation accessible by deer and according to Müller et al. (2009) also a strong surrogate for vegetation density, in my case it is apparently missing relevant information to predict resource selection in deer relative to the other LiDAR metrics tested.

### Number of Single Trees

I could also show that the models incorporating the number of single trees per 100 m<sup>2</sup> were performing poorer among models with LiDAR-derived metrics. In contrast, Flaherty et al. (2014) used number of trees derived from LiDAR data to create habitat suitability maps for the conservation management of endangered red squirrels (*Sciurus vulgaris*). The big advantage in their study design was that they combined their raster layer of single trees with other LiDAR-derived metrics such as canopy cover and mean tree height (95th percentile of height). Furthermore, a high predictive potential of LiDAR-derived single trees is expected to lay in more sophisticated calculations to generate species specific information. For example Ackers et al. (2015) created a field validated stem map for computing a density map of large conifers (>76 cm DBH) to predict habitat suitability for northern spotted owls (*Strix occidentalis caurina*). For both species the number of single trees is an explicitly valuable habitat characteristic. Herein lies a great potential for the application of LiDAR metrics based on single tree detection measures. In my case the number of single trees only provides information on the presence and density of a forest, even if distinguishing coniferous, deciduous and dead trees. By calculating single trees the information stored in the LiDAR point cloud about the vertical structures meaning tree height or canopy cover height were lost. A combination with such LiDAR metrics could increase the performance of the resource selection models for deer since their selection is not only based on the presence of trees but rather on their ability to provide shelter or food sources.

### Fractional Vegetation Cover

Among the models incorporating LiDAR-derived variables the fractional vegetation cover performed second best after the PCA-based metrics. This result is in line with the results of Ewald et al. (2014) investigation, who showed that the fractional vegetation cover was well suited to depict relevant forest structures for habitat selection of roe deer in winter. Furthermore, its application could improve predictions of ungulate habitat use (Lone et al. 2014a,b). Here, being calculated at high resolution (5 m) and incorporating three height

strata it compromises ecologically meaningful habitat characteristics that showed high predictive performance particularly for red deer. When predicting resource selection fractional vegetation cover was the only predictor to detect slight differences in the resource selection of roe and red deer. While red deer clearly select for low fractional understory cover at night and civil twilight roe deer select a medium fraction (App. D). It is known that red deer prefers open areas (pastures) for feeding (Hebblewhite et al. 2008, Godvik et al. 2009) whereas roe deer more likely selects for woodland or hedgerows as substitutable woodland habitat (Morellet et al. 2011).

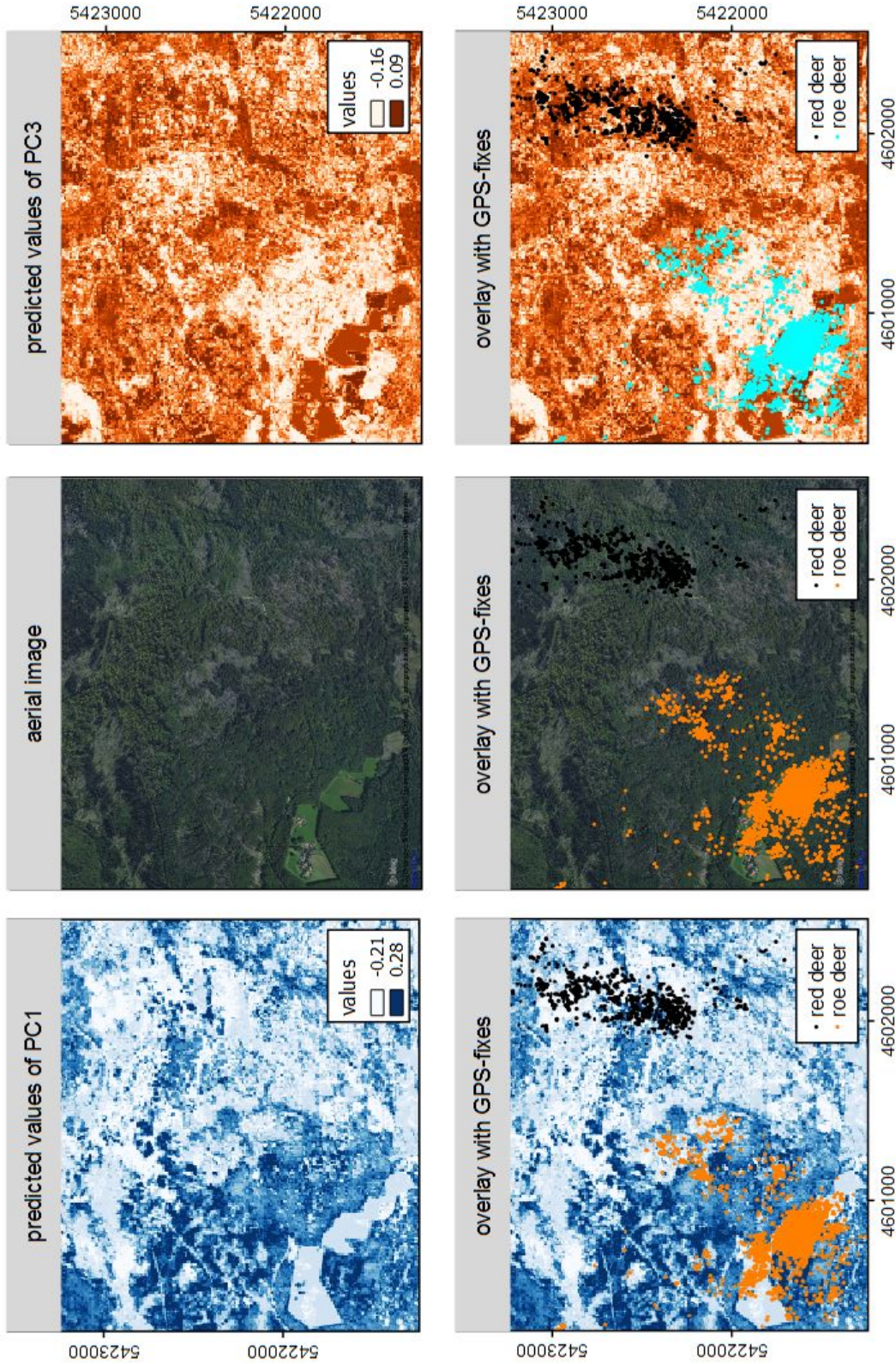


Figure 4.1: Predicted values of Principle Components (PCs) in a landscape. The PC values are derived from the results of a Principle Component Analysis on a LiDAR point cloud data set of 99 variables at 10 m resolution. The area shows an extent from the Bavarian Forest National Park in southeastern Germany. Displayed GPS-fixes were measured at a fix-rate of 1 hour.

## 4.2 Application of LiDAR-based Principle Components

Performing a PCA on LiDAR data in order to represent vertical vegetation structure is novel to this study and finds no comparison in literature. By creating this new metric an ecologically relevant continuous measure could be provided, which is in contrast to land cover classification maps not subjective and does not require pre-interpretation of the data.

I found that by applying a PCA to the LiDAR point cloud vertical and horizontal structures of vegetation were captured best compared to all other tested metrics. At a resolution of 10 m an original set of 99 variables could almost completely be represented by 9 variables explaining 91% of the original variance (at 5 m resolution respectively 85% explained variance with 11 variables, see App. A). These newly created LiDAR-based PCs were expected to predict resource selection of deer at best. I could prove that the predictive power of models incorporating these metrics outperformed others models tested in this study by far.

As already stated in the Results, Chapter 3.4 the predictions of deer selection from these PC variables are not always intuitively understandable. Their interpretation becomes even more complex with increasing number of dimensions. Each PC is per definition created to explain variance in the data which has not been depicted before. Thus, the importance of each PC for explaining the variance in e.g. the 10 m resolution LiDAR point cloud decreases from PC1 (34% explained variance) to PC9 (1% explained variance).

The results of this study show that both deer species prefer low values of PC1. From the rotation matrix in Figure 3.3 we already know that these values are likely to be open habitats with no large trees. Which "true" habitat characteristics are captured by these values can only be understood by predicting them to the landscape. The map provided in Figure 4.1 provides predictions of PC1 and PC3 together with an aerial image and locations visited by red and roe deer. Thus, we can compare PC values to landscape features in the photograph and the distribution of deer.

Looking at the map it is obvious that PC1 differentiates between open areas with no canopy cover (pastures at the bottom left side and gaps in the forest on the right side) and closed forest. In both cases deer locations match with these open areas. In this example roe deer locations accumulate on pastures, however, few locations are also within the gaps of the forest. Whereas PC1 differentiates more the complexity of structures with closed canopy cover, PC3 depicts different structures among the open habitats. Especially, on the right side, where the red deer location are, PC3 displays increasing complexity compared to the same area in PC1. Knowing from PC1 that open habitats are favored by deer this makes PC3 so valuable and a driving predictor in all tested models. It can depict the slight differences within the open habitats and thus also found tiny differences among the selection of the two species (Fig.??). From this map the great potential of LiDAR-derived PCs for habitat suitability modeling becomes clear. Combining the increasing complexity of each PC in one map would provide an extremely fine-scale habitat selection by both deer species. Obviously its usefulness is not only limited to ungulate species and thus could provide a great tool for future wildlife habitat modeling in general.

## 4.3 Limitations

The application of high resolution LiDAR-derived PCs on an area of 240 km<sup>2</sup> provided great opportunities to understand fine-scale habitat selection throughout the whole area of the national park. However, the computation and further handling of LiDAR data at this resolution and extent was limited to computational ability. The calculation of the PCA using the total LiDAR point cloud was not feasible due to the large area covered neither at 1 m nor at 5 m or 10 m resolution. Therefore, the PCA was run on a sub sample of 1 Million random points and PC values were predicted to the used and available locations of each data set. For

creating habitat suitability maps, as I suggested earlier, values of the environmental variables for the whole area of interest are required, hence the national park. Same is true for species distribution models. In this case, I only had the predicted values for my used and available locations. Therefrom, no sufficient suitability map could be created. Computing all required PC layers (e.g., the first 9 PCs from model 11 at a 10 m resolution) exceeded the scope of this study.

Nevertheless, I strongly recommend to make such an effort in computing LiDAR-based PCs. If computational abilities are sufficient these metrics can improve the understanding of resource selection in wildlife drastically by providing an unprecedented accuracy of continuous measures of ecologically relevant habitat structures. Furthermore, these layers are non-species-specific and can therefore be used for any other target species. I suggest to further invest in the creation of these PC layers for the total area of the NPBW. This is not only useful to further analysis of deer resource selection but also other ecological studies in the national park could profit from such a data set.

## 4.4 Study design

To understand the predictive power of LIDAR and non-LiDAR derived environmental metrics I used a systematic modeling approach. I applied a fixed model design that always incorporated confounding factors and exchanged the predictors describing vegetative structures (see Tab. 2.4). In the final Table 3.1 that compares the quality of my models  $\Delta AIC$  values ranged from 1.3 to 801.3 among the models which included a predictor for vegetation. These high  $\Delta AIC$  values underline the comparatively low predictive performance of most of the predictors not based on LiDAR-derived metrics. On the other hand these values could also be explained by the fact that I did not do any model selection. The design of this study was bound to the systematic model design. Model selection would have increased the predictive power of one single model but probably not change the ranking of models outlined in Table 3.1. If the aim was to find the best performing model out of these a model selection should be performed. For presence/availability data as applied in this study model selection can be based on the AIC (Boyce et al. 2002) and could, for example, be implemented by a stepwise forward (Lone et al. 2014a) or backward (Ewald et al. 2014) selection of predictors added to the model. However, with the study design implemented here I could demonstrate the high predictive performance of LiDAR-derived variables to more commonly applied remote sensing data and further understand their utility for exploring deer habitat selection.

## 4.5 Future implementation

The application of LiDAR data in forest inventories has been considered as a cost-effective alternative to conventional forest inventory (Latifi et al. 2015). While for wildlife ecologists alternatives to LiDAR data such as satellite images are freely available researchers or managers can also profit from this progress. Lone et al. (2014b) describe for the Scandinavian countries that using LiDAR data collected for such purposes can be a cheap opportunity to get nearly countrywide data.

With this increasing availability more researchers should evaluate the usefulness of LiDAR data to their research questions. Particularly, finding the right spatial scale at which LiDAR data can be implemented should be of major interest for future research. In this study the effects of scale were not tested systematically. However, the comparison of models predicting resource selection was conducted on two different species with varying fix rates. The results suggest that LiDAR data is capable of depicting resource selection at a very fine scale even at a 15 minute fix rate of red deer.

Even though in my study LiDAR-driven products performed best among all tested variables to describe vegetation structures in the literature there are also other examples. Lone et al. (2014a) showed that the combination of field data and LiDAR data provided the best models for lynx predation risk and hunter predation risk. However, in both cases the models only based on LiDAR data could not outperform the models only based on field data. Therefore, I suggest to combine LiDAR-derived metrics with other remote sensing products or field data. Because the collection of field data is limited to smaller areas their combination particularly with LiDAR data provides great opportunities for fine-scale modeling on larger areas (Müller & Brandl 2009, Garabedian et al. 2014).

In this study the newly developed LiDAR-based PCs were most effective in predicting deer resources selection. Even though their direct ecological interpretation might be limited to a certain degree (see Discussion, Chapter 4.2) their implementation could be particularly useful when extrapolating the model in order to predict habitat selection in a spatial landscape. From these new metrics fine-scale habitat suitability maps could be generated, which then illustrate preferred areas of deer or other wildlife. From the data sets developed in this study it is still challenging to prepare predictions of resource selection to the whole area of the national park but on smaller areas this could be more easily achieved. When used in habitat suitability modeling my findings can contribute to local management purposes as demonstrated by Farrell et al. (2013).

## 4.6 Conclusions

To analyze the predictive performances of LiDAR-derived metrics in wildlife ecology modeling I compared eight different remote sensing products derived from (1) satellite images, (2) aerial photographs and (3) LiDAR point cloud data for predicting resource selection in deer.

The major advantage of this study was the application of fine-scale telemetry data of two deer species paired with high resolution remote sensing products. Hereby, models incorporating LiDAR data performed best among all tested models. My findings are in line with previous studies on the applicability of LiDAR data in wildlife ecology modeling. Beyond that I could demonstrate the high performance in predicting resource selection of LiDAR-derived metrics at an extremely fine spatial and temporal scale.

Another novelty to this study was the application of LiDAR-derived PCs to better capture vegetation structures. These metrics were expected to show high predictive power because of their ability to cover almost all information of vegetation structure represented by the LiDAR point cloud. I found that the LiDAR-derived PCs at both, 5 m and 10 m resolution, were well suited to predict resource selection in deer and moreover provide an extremely complex measure of habitat characteristics. This makes them valuable remote sensing products for ecology and wildlife modeling.

Due to the increasing availability of LiDAR data to wildlife ecologists and researchers the full potential of LiDAR-derived products can be examined and exploited in future. From the results of this study particularly the application of LiDAR-based PCs should be further investigated to provide a useful tool for wildlife ecological research in general. It might be promising to try and use these novel metrics in hierarchical models in order to distinguish different habitat types. Furthermore, they should be applied in combination with for example field data to increase accuracy and precision of modeling.

All in all, high resolution LiDAR data are applicable to a wide range of wildlife research questions and can help to understand animal habitat use in more detail than was previously possible.

# Acknowledgements

This project was conducted in collaboration with Dr. Marco Heurich from the Bavarian Forest National Park. I would like to thank him for providing me with most of the data and his "remote" help throughout the whole time. Also I would like to thank Dr. Simone Ciuti for being my supervisor here in Freiburg, for his valuable input while developing this thesis and all his time he spent brainstorming and discussing with me. Furthermore, I would like to thank my co-supervisor Prof. Dr. Gernot Segelbacher first of all for taking this job but also for all his knowledge he shared with me throughout my studies at the University of Freiburg. Grateful thanks to Ramiro Silveyra González and Peter Antkowiak for making computational things so much easier and for providing me with all those pre-processed remote sensing data. Thanks to Philipp Jund for his fast solution of a time consuming problem.

Furthermore, I would like to thank Prof. Dr. Carsten Dormann for his ideas and fruitful discussions at the beginning of this study.

I also must not forget to say that I had a great time at "the master student's office" and with everyone being part of this. Thank you for providing a productive working atmosphere but more than that for always creating an inspiring and joyful environment.

Finally, I would like to thank my family for their support throughout my whole studies. Liebe Familie, vielen Dank für die Unterstützung während meines Studiums und in letzter Zeit zunehmend in Form von Postkarten und Zeitungsartikeln, mit denen ich mich so schön ablenken konnte!

# Bibliography

- Ackers, S. H., Davis, R. J., Olsen, K. a., & Dugger, K. M. (2015). The evolution of mapping habitat for northern spotted owls (*Strix occidentalis caurina*): A comparison of photo-interpreted, Landsat-based, and lidar-based habitat maps. *Remote Sensing of Environment*, 156, 361–373.
- Bates, D., Mächler, M., Bolker, B., & Walker, S. (2015). Fitting Linear Mixed-Effects Models Using {lme4}. *Journal of Statistical Software*, 67(1), 1–48.
- Bevanda, M., Fronhofer, E. A., Heurich, M., Mueller, J., & Reineking, B. (2015). Landscape configuration is a major determinant of home range size variation. *Ecosphere*, 6(10), 1–12.
- Blaschke, T., Tiede, D., & Heurich, M. (2004). 3D Landscape Metrics To Modelling Forest Structure and Diversity. *International Archives of the Photogrammetry, Remote Sensing and Spatial Information Sciences*, 36(8/W2), 129–132.
- Boyce, M. S. (2006). Scale for resource selection functions. *Diversity and Distributions*, 12(3), 269–276.
- Boyce, M. S., Vernier, P. R., Nielsen, S. E., & Schmiegelow, F. K. (2002). Evaluating resource selection functions. *Ecological Modelling*, 157(2-3), 281–300.
- Cagnacci, F., Boitani, L., Powell, R. a., & Boyce, M. S. (2010). Animal ecology meets GPS-based radiotelemetry: a perfect storm of opportunities and challenges. *Philosophical transactions of the Royal Society of London. Series B, Biological sciences*, 365(1550), 2157–62.
- Demment, M. W. & Soest, P. J. V. (1985). A Nutritional Explanation for Body-Size Patterns of Ruminant and Nonruminant Herbivores. *The American Naturalist*, 125(5), 641.
- Dormann, Carsten, F. (2013). *Parametrische Statistik. Verteilungen, maximum likelihood und GLM in R*. Leipzig, Germany: Springer Spektrum.
- Ensing, E. P., Ciuti, S., de Wijs, F. a. L. M., Lentferink, D. H., ten Hoedt, A., Boyce, M. S., & Hut, R. a. (2014). GPS Based Daily Activity Patterns in European Red Deer and North American Elk (*Cervus elaphus*): Indication for a Weak Circadian Clock in Ungulates. *PLoS ONE*, 9(9), e106997.
- Ewald, M., Dupke, C., Heurich, M., Müller, J., & Reineking, B. (2014). LiDAR remote sensing of forest structure and GPS telemetry data provide insights on winter habitat selection of european roe deer. *Forests*, 5(6), 1374–1390.
- Farrell, S. L., Collier, B. a., Skow, K. L., Long, a. M., Campomizzi, a. J., Morrison, M. L., Hays, K. B., & N, W. R. (2013). Using LiDAR-derived vegetation metrics for high-resolution, species distribution models for conservation planning. *Ecosphere*, 4(March), 1–18.

- Flaherty, S., Lurz, P. W. W., & Patenaude, G. (2014). Use of LiDAR in the conservation management of the endangered red squirrel ( *Sciurus vulgaris* L. ). *Journal of Applied Remote Sensing*, 8(1), 083592.
- Gaillard, J.-M., Hebblewhite, M., Loison, A., Fuller, M., Powell, R., Basille, M., & Van Moorter, B. (2010). Habitat-performance relationships: finding the right metric at a given spatial scale. *Philosophical Transactions of the Royal Society of London. Series B, Biological sciences*, 365(1550), 2255–2265.
- Garabedian, J. E., McGaughey, R. J., Reutebuch, S. E., Parresol, B. R., Kilgo, J. C., Moorman, C. E., & Peterson, M. N. (2014). Quantitative analysis of woodpecker habitat using high-resolution airborne LiDAR estimates of forest structure and composition. *Remote Sensing of Environment*, 145, 68–80.
- Gebert, C. & Verheyden-Tixier, H. (2001). Variations of diet composition of Red Deer (*Cervus elaphus* L.) in Europe. *Mammal Review*, 31(3-4), 189–201.
- Godvik, I. M. R., Loe, L. E., Vik, J. O., Veiberg, V., Langvatn, R., & Mysterud, A. (2009). Temporal scales, trade-offs, and functional responses in red deer habitat selection. *Ecology*, 90(3), 699–710.
- Graf, R. F., Mathys, L., & Bollmann, K. (2009). Habitat assessment for forest dwelling species using LiDAR remote sensing: Capercaillie in the Alps. *Forest Ecology and Management*, 257(1), 160–167.
- Hagar, J. C., Eskelson, B. N. I., Haggerty, P. K., Nelson, S. K., & Vesely, D. G. (2014). Modeling marbled murrelet (*Brachyramphus marmoratus*) habitat using LiDAR-derived canopy data. *Wildlife Society Bulletin*, 38(2), 237–249.
- Harris (2016). Vegetation Indices Background. URL: <http://www.harrisgeospatial.com/docs/BackgroundVegetationIndices.html>, accessed 2016-03-15.
- Hatten, J. R. (2014). Mapping and monitoring Mount Graham red squirrel habitat with Lidar and Landsat imagery. *Ecological Modelling*, 289(June 1987), 106–123.
- Hebblewhite, M. & Haydon, D. T. (2010). Distinguishing technology from biology: a critical review of the use of GPS telemetry data in ecology. *Philosophical Transactions of the Royal Society of London. Series B, Biological sciences*, 365(1550), 2303–2312.
- Hebblewhite, M., Merrill, E., & McDermid, G. (2008). A multi-scale test of the forage maturation hypothesis in a partially migratory ungulate population. *Ecological Monographs*, 78(2), 141–166.
- Heurich, M., Fischer, F., Knoerzer, O., & Krzystek, P. (2008). Assessment of Digital Terrain Models (DTM) from Data gathered with Airborne Laser Scanning in Temperate European Beech (*Fagus sylvatica*) and Norway Spruce (*Picea abies*) Forests. *Photogramm. Fernerkund. Geoinf.*, 6, 473–488.
- Hijmans, R. J. (2015). *raster: Geographic Data Analysis and Modeling*. URL: <http://cran.r-project.org/package=raster>.
- Hofmann, R. R. (1989). Evolutionary steps of ecophysiological adaptation and diversification of ruminants: view of their digestive system. *Oecologia*, 78(4), 443–457.

- Hyyppae, J., Yu, X., Hyyppae, H., Vastaranta, M., Holopainen, M., Kukko, A., Kaartinen, H., Jaakkola, A., Vaaja, M., Koskinen, J., & Alho, P. (2012). Advances in forest inventory using airborne laser scanning. *Remote Sensing*, 4(5), 1190–1207.
- Kittle, A. M., Fryxell, J. M., Desy, G. E., & Hamr, J. (2008). The scale-dependent impact of wolf predation risk on resource selection by three sympatric ungulates. *Oecologia*, 157(1), 163–175.
- Latifi, H. (2012). Characterizing forest structure by means of remote sensing: a review. In B. Escalante (Ed.), *Remote Sensing: Advanced Techniques and Platforms* (pp. 4–28). Zagreb, Croatia: Intech Open Access Publisher.
- Latifi, H., Fassnacht, F. E., Mueller, J., Tharani, A., Dech, S., & Heurich, M. (2015). Forest inventories by LiDAR data: A comparison of single tree segmentation and metric-based methods for inventories of a heterogeneous temperate forest. *International Journal of Applied Earth Observation and Geoinformation*, 42, 162–174.
- Lefsky, M. A., Cohen, W. B., Parker, G. G., & David, J. (2002). Lidar Remote Sensing for Ecosystem Studies. *BioScience*, 52(1), 19–30.
- Lele, S. R. (2009). A New Method for Estimation of Resource Selection Probability Function. *Journal of Wildlife Management*, 73(1), 122–127.
- Lone, K., Loe, L. E., Gobakken, T., Linnell, J. D. C., Odden, J., Remmen, J., & Mysterud, A. (2014a). Living and dying in a multi-predator landscape of fear: Roe deer are squeezed by contrasting pattern of predation risk imposed by lynx and humans. *Oikos*, 123(6), 641–651.
- Lone, K., van Beest, F. M., Mysterud, A., Gobakken, T., Milner, J. M., Ruud, H.-P., & Loe, L. E. (2014b). Improving broad scale forage mapping and habitat selection analyses with airborne laser scanning : the case of moose. *Ecosphere*, 5(11), 1–22.
- Manly, B. F. J., McDonald, L. L., Thomas, D. L., McDonald, T. L., & Erickson, W. P. (2002). *Resource Selection by Animals. Statistical Design and Analysis for Field Studies*. Dordrecht/Boston/London: Kluwer Academic Publishers, 2nd edition.
- Melin, M., Packalén, P., Matala, J., Mehtätalo, L., & Pusenius, J. (2013). Assessing and modeling moose (*alces alces*) habitats with airborne laser scanning data. *International Journal of Applied Earth Observation and Geoinformation*, 23(1), 389–396.
- Morellet, N., van Moorter, B., Cargnelutti, B., Angibault, J. M., Lourtet, B., Merlet, J., Ladet, S., & Hewison, A. J. M. (2011). Landscape composition influences roe deer habitat selection at both home range and landscape scales. *Landscape Ecology*, 26(7), 999–1010.
- Möst, L., Hothorn, T., Müller, J., & Heurich, M. (2015). Creating a landscape of management: Unintended effects on the variation of browsing pressure in a national park. *Forest Ecology and Management*, 338, 46–56.
- Müller, J. & Brandl, R. (2009). Assessing biodiversity by remote sensing in mountainous terrain: The potential of LiDAR to predict forest beetle assemblages. *Journal of Applied Ecology*, 46(4), 897–905.
- Müller, J., Moning, C., Bässler, C., Heurich, M., & Brandl, R. (2009). Using airborne laser scanning to model potential abundance and assemblages of forest passerines. *Basic and Applied Ecology*, 10(7), 671–681.

- Neumann, W., Martinuzzi, S., Estes, A. B., Pidgeon, A. M., Dettki, H., Ericsson, G., & Radeloff, V. C. (2015). Opportunities for the application of advanced remotely-sensed data in ecological studies of terrestrial animal movement. *Movement Ecology*, 3(1), 8.
- Nijland, W., Nielsen, S. E., Coops, N. C., Wulder, M. a., & Stenhouse, G. B. (2014). Fine-spatial scale predictions of understory species using climate- and LiDAR-derived terrain and canopy metrics. *Journal of Applied Remote Sensing*, 8(1), 083572.
- NOAA (2015). What is Lidar? URL: <http://oceanservice.noaa.gov/facts/lidar.html>, accessed 2016-02-16.
- Northrup, J. M., Anderson, C. R., & Wittemyer, G. (2015). Quantifying spatial habitat loss from hydrocarbon development through assessing habitat selection patterns of mule deer. *Global Change Biology*, 21(11), 3961–3970.
- Northrup, J. M., Hooten, M. B., Anderson, C. R. J., & Wittemyer, G. (2013). Practical guidance on characterizing availability in resource selection functions under a use-availability design. *Ecological Society of America*, 94(7), 1456–1463.
- QGIS Development Team (2015). *QGIS Geographic Information System*. Open Source Geospatial Foundation. URL: <http://qgis.osgeo.org>.
- R Core Team (2015). *R: A Language and Environment for Statistical Computing*. R Foundation for Statistical Computing. URL: <https://www.r-project.org/>, Vienna, Austria.
- Radeloff, V. C., Pidgeon, A. M., & Hostert, P. (1999). Habitat and population modelling of roe deer using an interactive geographic information system. *Ecological Modelling*, 114(2-3), 287–304.
- Ryan, P., Petersen, S., Peters, G., & Grémillet, D. (2004). GPS tracking a marine predator: the effects of precision, resolution and sampling rate on foraging tracks of African Penguins. *Marine Biology*, 145(2), 215–223.
- Smart, L. S., Swenson, J. J., Christensen, N. L., & Sexton, J. O. (2012). Three-dimensional characterization of pine forest type and red-cockaded woodpecker habitat by small-footprint, discrete-return lidar. *Forest Ecology and Management*, 281(June), 100–110.
- Stache, A., Heller, E., Hothorn, T., & Heurich, M. (2013). Activity patterns of European Roe Deer (*Capreolus capreolus*) are strongly influenced by individual behavior. *Folia Zoologica*, 62(1), 67–75.
- Stache, A., Löttker, P., & Heurich, M. (2012). Red deer telemetry: Dependency of the position acquisition rate and accuracy of GPS collars on the structure of a temperate forest dominated by European beech. *Silva Gabreta*, 18(1), 35–48.
- Tattoni, C., Rizzolli, F., & Pedrini, P. (2012). Can LiDAR data improve bird habitat suitability models? *Ecological Modelling*, 245, 103–110.
- Thurfjell, H., Ciuti, S., & Boyce, M. S. (2014). Applications of step-selection functions in ecology and conservation. *Movement Ecology*, 2(1), 4.
- Tixier, H. & Duncan, P. (1996). Are European roe deer browsers? A review of variations in the composition of their diets. *Revue d'Ecologie (La Terre et la Vie)*, 51(1), 3–17.
- Tomkiewicz, S. M., Fuller, M. R., Kie, J. G., & Bates, K. K. (2010). Global positioning system and associated technologies in animal behaviour and ecological research. *Philosophical Transactions of the Royal Society of London. Series B, Biological sciences*, 365(1550), 2163–2176.

- Tsui, O. W., Coops, N. C., Wulder, M. A., & Marshall, P. L. (2013). Integrating airborne LiDAR and space-borne radar via multivariate kriging to estimate above-ground biomass. *Remote Sensing of Environment*, 139, 340–352.
- Vierling, K. T., Vierling, L. A., Gould, W. A., Martinuzzi, S., & Clawges, R. M. (2008). Lidar: Shedding new light on habitat characterization and modeling. *Frontiers in Ecology and the Environment*, 6(2), 90–98.
- Weingarth, K., Heibl, C., Knauer, F., Zimmermann, F., Bufka, L., & Heurich, M. (2012). First estimation of Eurasian lynx (*Lynx lynx*) abundance and density using digital cameras and capture-recapture techniques in a German national park. *Animal Biodiversity and Conservation*, 35(2), 197–207.
- Xie, Y., Sha, Z., & Yu, M. (2008). Remote sensing imagery in vegetation mapping: a review. *Journal of Plant Ecology-Uk*, 1(1), 9–23.
- Yao, W., Krzystek, P., & Heurich, M. (2012). Tree species classification and estimation of stem volume and DBH based on single tree extraction by exploiting airborne full-waveform LiDAR data. *Remote Sensing of Environment*, 123, 368–380.

## **Appendix A**

# **Results from a Principle Component Analysis of a LiDAR point cloud**

### A.1 Principle Components of LiDAR point cloud at 5 m resolution

## SUMMARY OF PRINCIPLE COMPONENT ANALYSIS

### **Importance of components:**

	PC1	PC2	PC3	PC4	PC5	PC6	PC7	PC8	PC9	PC10	PC11	PC12	PC13	PC14	PC15	PC16
Standard deviation	0.1522	0.1325	0.09506	0.08304	0.06701	0.05993	0.04947	0.04342	0.03768	0.03378	0.03032	0.02774	0.02543	0.02373	0.02227	0.02114
Proportion of Variance	0.2712	0.2054	0.10582	0.08074	0.05259	0.04205	0.02866	0.02207	0.01663	0.01336	0.01076	0.00901	0.00757	0.00659	0.00581	0.00523
Cumulative Proportion	0.2712	0.4766	0.58241	0.66315	0.71574	0.75779	0.78645	0.80852	0.82515	0.83851	0.84927	0.85828	0.86586	0.87245	0.87826	0.88349
	PC17	PC18	PC19	PC20	PC21	PC22	PC23	PC24	PC25	PC26	PC27	PC28	PC29	PC30	PC31	
Standard deviation	0.02017	0.01941	0.01876	0.01825	0.01783	0.01745	0.01717	0.01688	0.01660	0.01638	0.01618	0.01592	0.01571	0.01546	0.01523	
Proportion of Variance	0.00476	0.00441	0.00412	0.00390	0.00372	0.00357	0.00345	0.00334	0.00323	0.00314	0.00306	0.00297	0.00289	0.00280	0.00271	
Cumulative Proportion	0.88826	0.89267	0.89679	0.90069	0.90441	0.90798	0.91143	0.91477	0.91799	0.92113	0.92420	0.92716	0.93005	0.93285	0.93557	
	PC32	PC33	PC34	PC35	PC36	PC37	PC38	PC39	PC40	PC41	PC42	PC43	PC44	PC45	PC46	
Standard deviation	0.01503	0.01485	0.01462	0.01444	0.01425	0.01404	0.01387	0.01367	0.01351	0.01333	0.01319	0.01303	0.01291	0.01275	0.01265	
Proportion of Variance	0.00265	0.00258	0.00250	0.00244	0.00238	0.00231	0.00225	0.00219	0.00214	0.00208	0.00204	0.00199	0.00195	0.00191	0.00188	
Cumulative Proportion	0.93821	0.94079	0.94330	0.94574	0.94812	0.95042	0.95268	0.95487	0.95700	0.95908	0.96112	0.96311	0.96506	0.96697	0.96884	
	PC47	PC48	PC49	PC50	PC51	PC52	PC53	PC54	PC55	PC56	PC57	PC58	PC59	PC60	PC61	
Standard deviation	0.01255	0.01230	0.01227	0.01207	0.01184	0.01179	0.01153	0.01136	0.01122	0.01093	0.01081	0.01065	0.01039	0.01025	0.01004	
Proportion of Variance	0.00184	0.00177	0.00176	0.00171	0.00164	0.00163	0.00156	0.00151	0.00147	0.00140	0.00137	0.00133	0.00126	0.00123	0.00118	
Cumulative Proportion	0.97068	0.97246	0.97422	0.97592	0.97757	0.97919	0.98075	0.98226	0.98374	0.98513	0.98650	0.98783	0.98910	0.99033	0.99151	
	PC62	PC63	PC64	PC65	PC66	PC67	PC68	PC69	PC70	PC71	PC72	PC73	PC74	PC75		
Standard deviation	0.009689	0.009683	0.009075	0.008512	0.007952	0.007356	0.006796	0.006324	0.005766	0.005253	0.004802	0.004352	0.003943	0.003567		
Proportion of Variance	0.001100	0.001100	0.000960	0.000850	0.000740	0.000630	0.000540	0.000470	0.000390	0.000320	0.000270	0.000220	0.000180	0.000150		
Cumulative Proportion	0.992610	0.993700	0.994670	0.995520	0.996260	0.996890	0.997430	0.997900	0.998290	0.998610	0.998880	0.999100	0.999290	0.999440		
	PC76	PC77	PC78	PC79	PC80	PC81	PC82	PC83	PC84	PC85	PC86	PC87	PC88			
Standard deviation	0.003181	0.002872	0.002561	0.002298	0.002053	0.001826	0.001624	0.001414	0.001237	0.001101	0.000930	0.0008126	0.000688			
Proportion of Variance	0.000120	0.000100	0.000080	0.000060	0.000050	0.000040	0.000030	0.000020	0.000010	0.0000100	0.0000100	0.0000100	0.000010			
Cumulative Proportion	0.999550	0.999650	0.999730	0.999790	0.999840	0.999880	0.999910	0.999930	0.999950	0.999960	0.9999700	0.9999800	0.999990			
	PC89	PC90	PC91	PC92	PC93	PC94	PC95	PC96	PC97	PC98	PC99					
Standard deviation	0.0005812	0.0005139	0.0004084	0.0003635	0.0002945	0.0002189	0.0001926	0.0001507	0.0001257	8.698e-05	6.78e-05					
Proportion of Variance	0.0000000	0.0000000	0.0000000	0.0000000	0.0000000	0.0000000	0.0000000	0.0000000	0.0000000	0.0000000	0.0000000					
Cumulative Proportion	0.9999900	0.9999990	1.0000000	1.0000000	1.0000000	1.0000000	1.0000000	1.0000000	1.0000000	1.0000000	1.0000000					

## A.2 Principle Components of LiDAR point cloud at 10 m resolution

## SUMMARY OF PRINCIPLE COMPONENT ANALYSIS

Importance of components:

## **Appendix B**

### **Sensitivity analysis to estimate random availability**

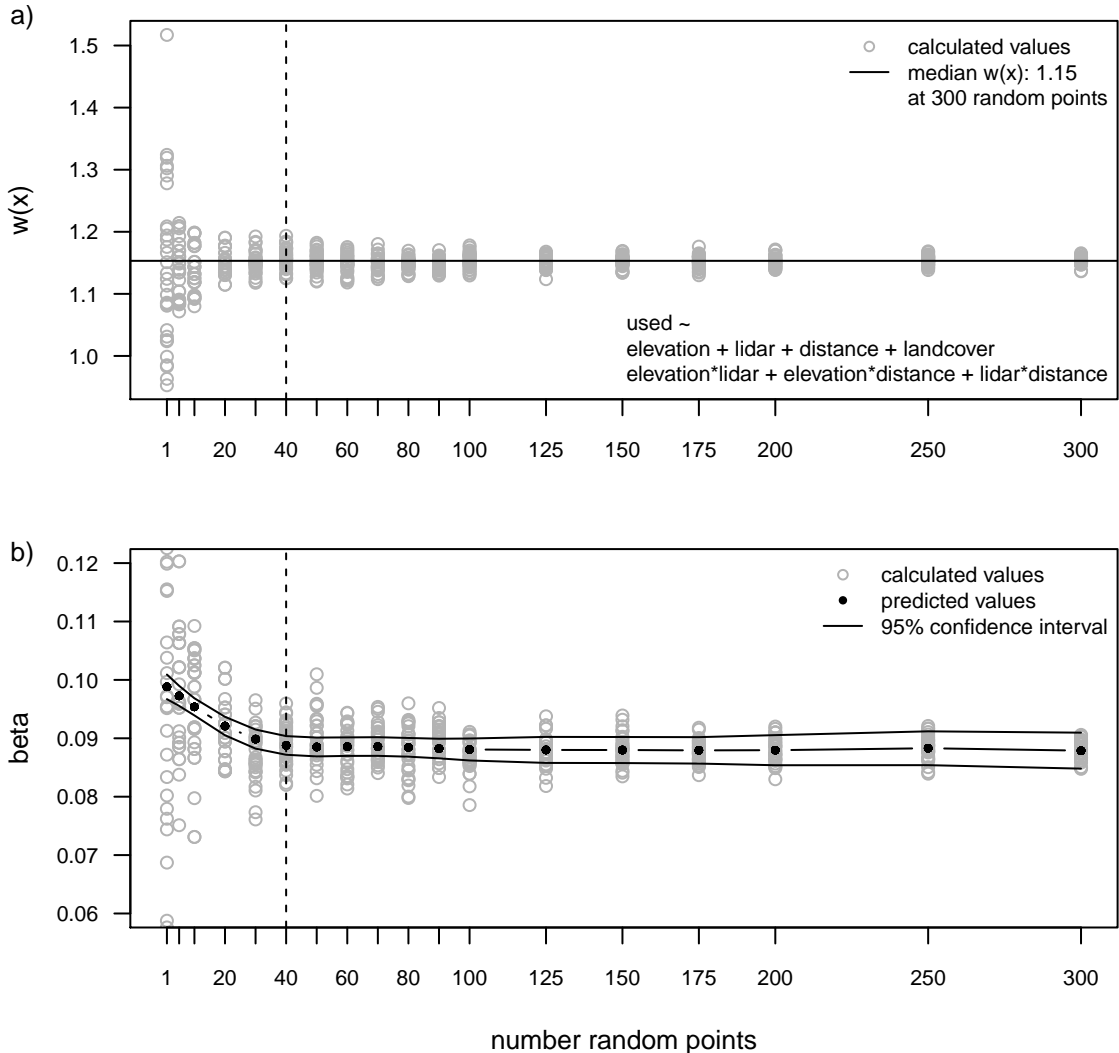


Figure B.1: Sensitivity analysis to estimate availability (random points) in a resource selection function. Generalized linear mixed models were fitted (30 replicates) always with a different sample size of availability (1-300). Results of a) the relative probability of selection ( $w(x)$ ) from the exponential form and b) the covariate estimates ( $\beta$ ; beta) for the predictor lidar are presented. In b) also predictions of covariate estimates from a generalized additive model are shown. The model design is presented in a). The dashed line indicates stabilizing estimates. Notes: elevation (meters a.s.l.) at 1 m resolution; lidar: understory vegetation cover (0.5 m - 2 m) derived from light detection and ranging (LiDAR) data at 1 m resolution; distance: closest distance to the next hiking trail; landcover: land cover classification map, \* indicates interactions of two predictors.

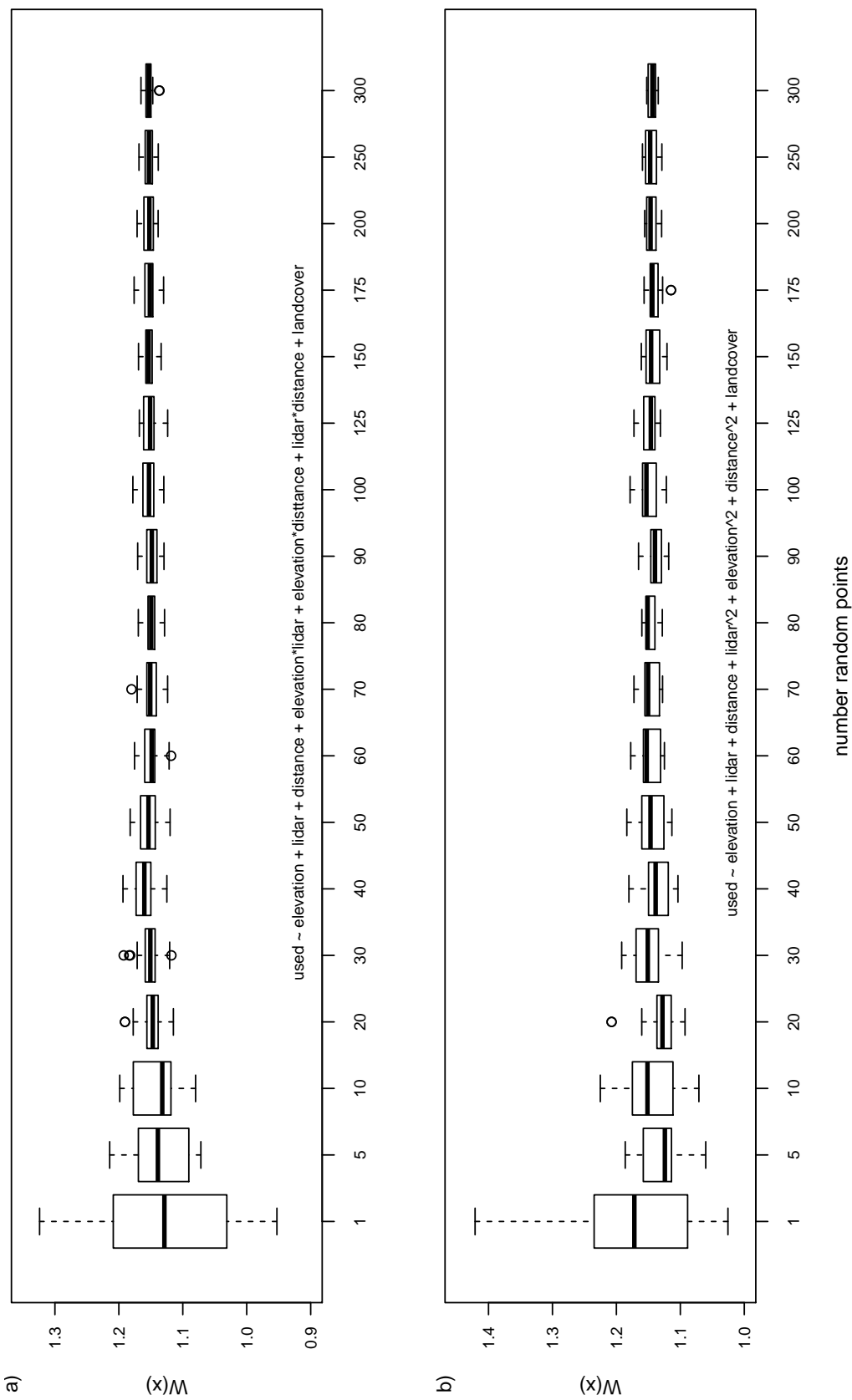


Figure B.2: Variance in predicted relative probability of selection ( $w(x)$ ) in a resource selection function. Generalized linear mixed models were fitted (30 replicates) always with a different sample size of availability (1-300). Two different models where tested including a) interactions (indicated by \*) or b) squared terms (indicated by  $^2$ ).  
 Notes: elevation (meters a.s.l.) at 1 m resolution; lidar: understory vegetation cover (0.5 m - 2 m) derived from light detection and ranging (LiDAR) data at 1 m resolution; distance: closest distance to the next hiking trail; landcover: land cover classification map.

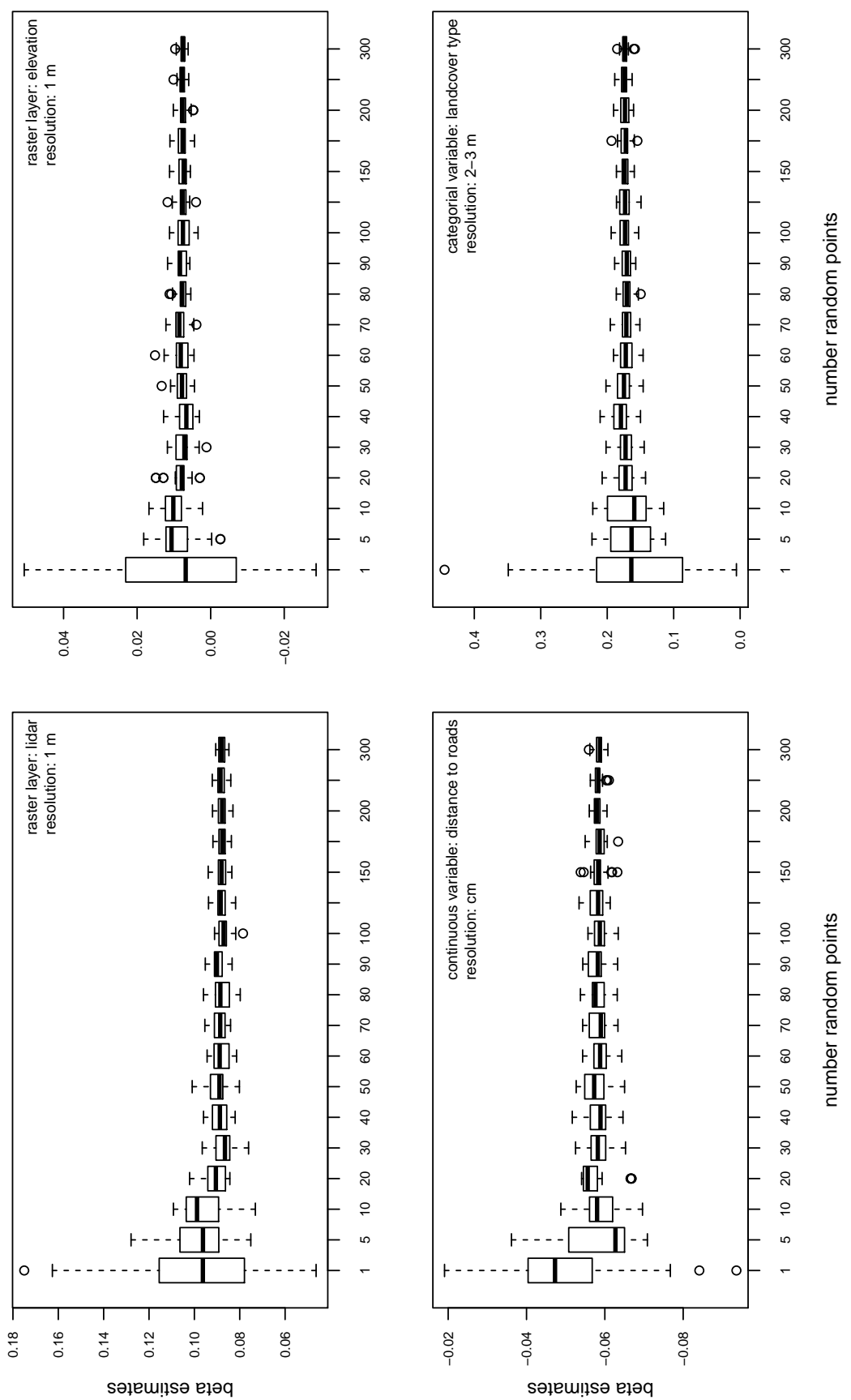


Figure B.3: Variance in covariate estimates ( $\beta$ ; beta) in a resource selection function. Generalized linear mixed models were fitted (30 replicates) always with a different sample size of availability (1-300). This model included interactions of predictors.  
 Notes: elevation (meters a.s.l.) at 1 m resolution; lidar: understory vegetation cover (0.5 m - 2 m) derived from light detection and ranging (LiDAR) data at 1 m resolution; distance: closest distance to the next hiking trail; landcover: land cover classification map.

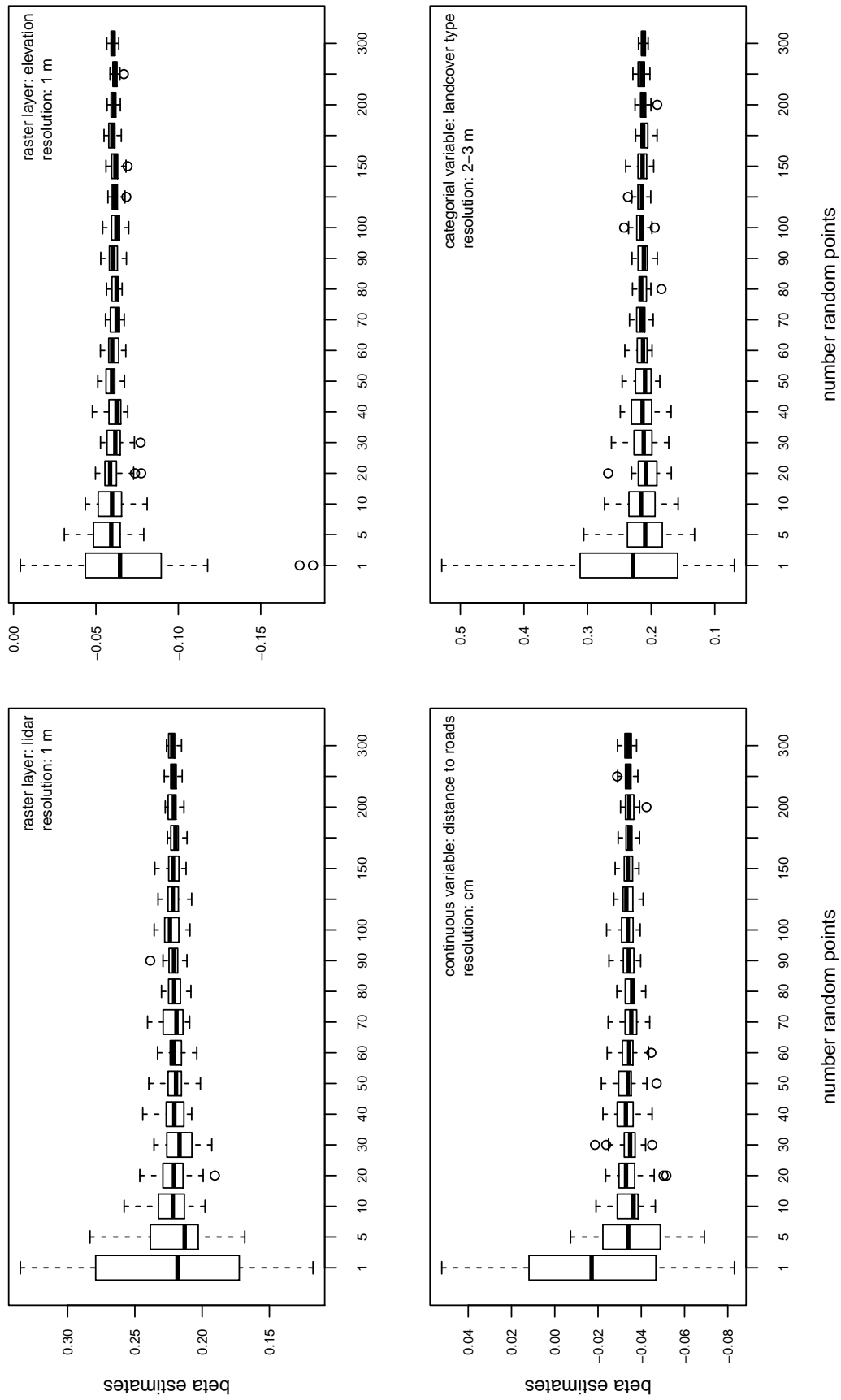


Figure B.4: Variance in covariate estimates ( $\beta$ ; beta) in a resource selection function. Generalized linear mixed models were fitted (30 replicates) always with a different sample size of availability (1-300). This model included squared terms of predictors.  
 Notes: elevation (meters a.s.l.) at 1 m resolution; lidar: understory vegetation cover (0.5 m - 2 m) derived from light detection and ranging (LiDAR) data at 1 m resolution; distance: closest distance to the next hiking trail; landcover: land cover classification map.

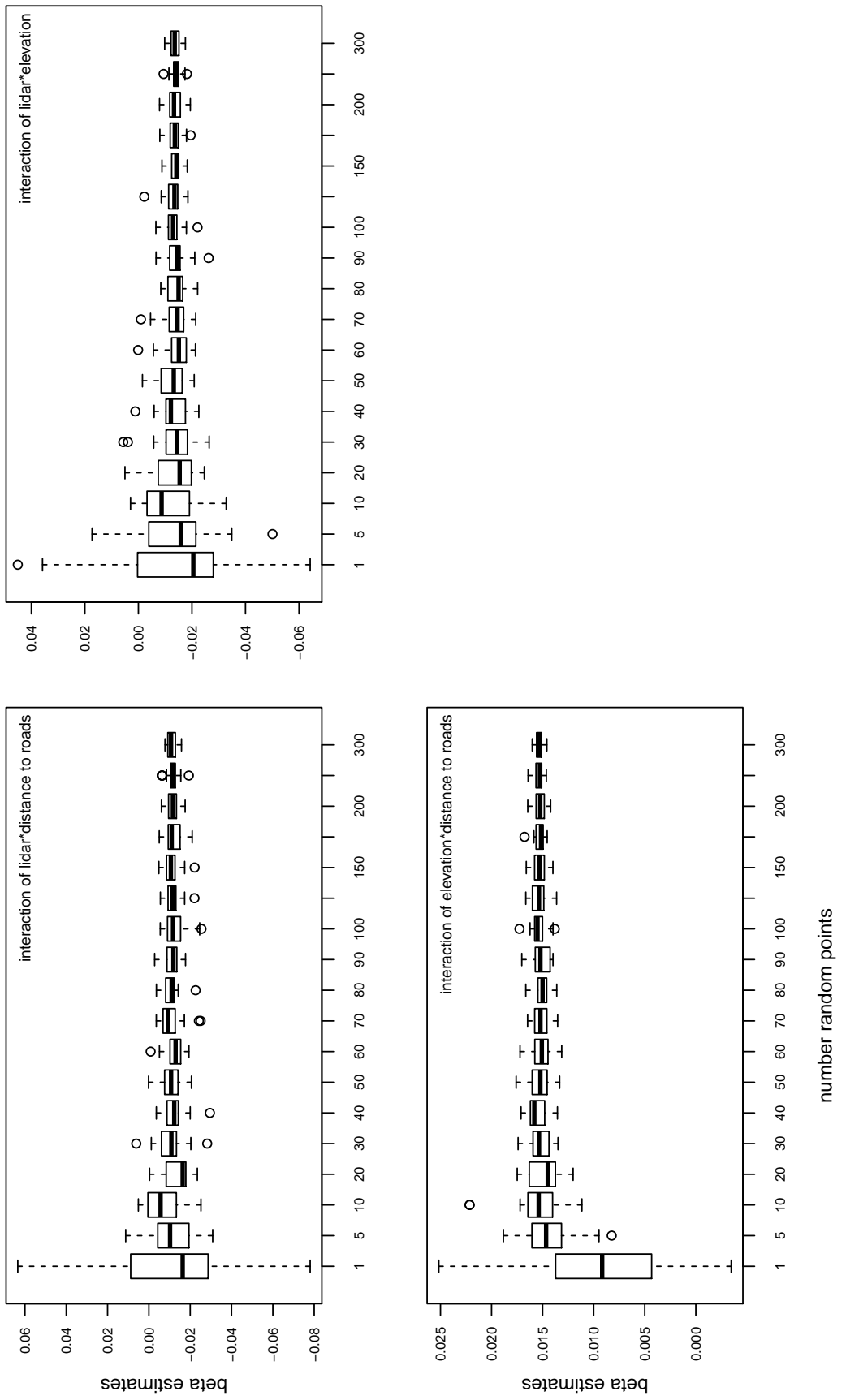


Figure B.5: Variance in covariate estimates ( $\beta$ ; beta) in a resource selection function. Generalized linear mixed models were fitted (30 replicates) always with a different sample size of availability (1-300). This model included interactions of predictors (indicated by \*).  
 Notes: elevation (meters a.s.l.) at 1 m resolution; lidar: understory vegetation cover (0.5 m - 2 m) derived from light detection and ranging (LiDAR) data at 1 m resolution; distance: closest distance to the next hiking trail; landcover: land cover classification map.

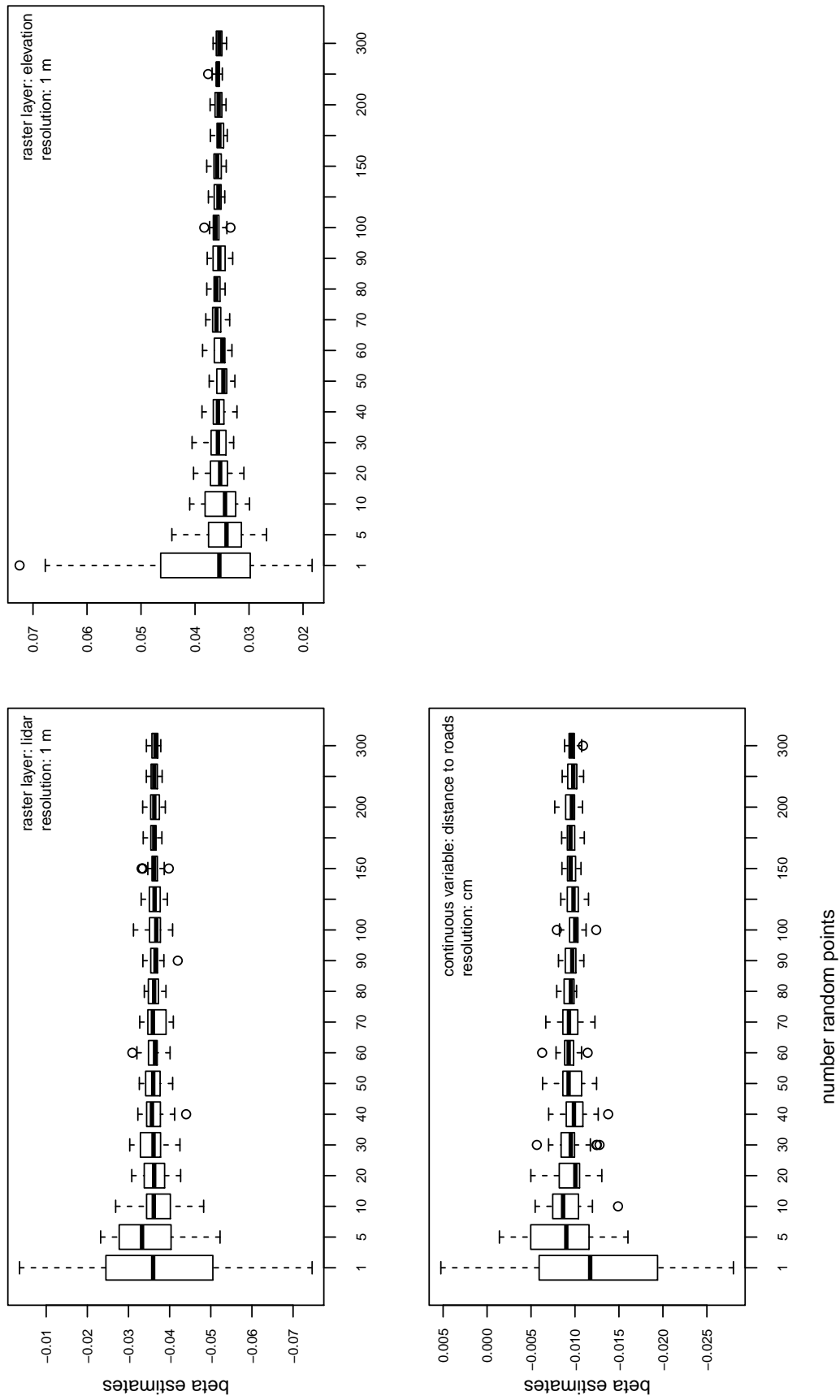


Figure B.6: Variance in covariate estimates ( $\beta$ ; beta) in a resource selection function. Generalized linear mixed models were fitted (30 replicates) always with a different sample size of availability (1-300). Here estimates of the squared terms of predictors are shown.  
 Notes: elevation (meters a.s.l.) at 1 m resolution; lidar: understory vegetation cover (0.5 m - 2 m) derived from light detection and ranging (LiDAR) data at 1 m resolution; distance: closest distance to the next hiking trail; landcover: land cover classification map.

# Appendix C

## Model summaries

This Appendix includes all model summaries of four data sets for red and roe deer. Summaries are given as they are provided in the statistical software R. All models are generalized linear mixed models (GLMMs) fitted by maximum likelihood (Laplace Approximation) with binomial response variable (logit; 1=used, 0=available).

The structure of every model (except the null model) is a following:

```
used ~ scale(sun_elev) + I(scale(sun_elev)^2)      +  FIXED EFFECTS
      scale(rugged_10) + I(scale(rugged_10)^2)      +  "CONFOUNDING FACTORS"
      scale(dist_trails) + I(scale(dist_trails)^2)    +
      solrad_fac          +
      scale(sun_elev) * scale(dist_trails)            +
      scale(sun_elev) * solrad_fac                    +
      scale(sun_elev) * (scale(PREDICTOR FOR VEGETATION) + ... ) +  FIXED EFFECTS
      scale(PREDICTOR FOR VEGETATION) + ...           +  "PREDICTOR FOR VEGETATION"
      I(scale(PREDICTOR FOR VEGETATION)^2)           +
      (1 | id/loc_id)                                NESTED RANDOM EFFECTS
```

Significance code for the p-values is 0 ‘\*\*\*’ 0.001 ‘\*\*’ 0.01 ‘\*’ 0.05 ‘.’ 0.1 ‘ ’ assuming significance if  $p < 0.05$ . Abbreviation descriptions for model predictors are provided below:

abbreviation:	description:
id	id for every individual
loc_id	id for every stratum (available and used locations)
sun_elev	elevation of sun (proxy for daytime)
rugged_10	ruggedness at 10 m resolution
dist_trails	closest distance to hiking trails
solrad_fac	solar radiation as categorial predictor (low, medium and high)
PREDICTOR FOR VEGETATION:	
ndvi_preds	normalized difference vegetation index (NDVI)
MeanHeight	mean height of vegetation
corine	land cover classes (derived from corine)
map	land cover classes (from the Bavarian Forest National Park)
UStory	fractional vegetation cover of strata 0.5 m - 2 m (understory)
MStory	fractional vegetation cover of strata 2 m - 10 m (midstory)
OStory	fractional vegetation cover of strata 10 m - 50 m (overstory)
res5_PC1–PC11	LiDAR data at 5 m resolution (predictors are Principle Components (PCs))
res10_PC1–PC9	LiDAR data at 10 m resolution (predictors are Principle Components (PCs))
st_conif	single tree detection, number of coniferous trees
st_deci	single tree detection, number of deciduous trees
st_dead_all	single tree detection, number of dead trees

## C.1 Red deer telemetry data - 15 minute fix rate MODEL "NO VEGETATION"

MODEL "NULL MODEL"

	AIC	BIC	logLik	deviance	df.resid
	117699.7	117758.1	-58785.9	117571.7	607636
Scaled residuals:					
Min 1Q Median 3Q Max					
-0.1481 -0.1440 -0.1423 -0.1402 10.2718					
Random effects:					
Groups Name Variance Std.Dev.					
loc_id:id (Intercept) 0					
id (Intercept) 0					
Number of obs: 607650, groups: loc_id:id, 11956; id, 10					
Fixed effects:					
(Intercept)					
-3.8534404 0.0235795 -163.42 < 2e-16 ***					
scale (sun_elev)					
-0.0062554 0.0161266 -0.33 0.74451					
I(scale (sun_elev)^2)					
0.0003374 0.0121497 0.03 0.97784					
scale (rugged_10)					
-0.0258405 0.0117739 -2.19 0.02818 *					
I(scale (rugged_10)^2)					
scale (dist_trails)					
0.0367978 0.0142895 2.51 0.01224 *					
I(scale (dist_trails)^2)					
-0.0395202 0.0132614 -2.99 0.00281 **					
solrad_facflow					
0.0022723 0.0226200 0.10 0.91998					
scale (sun_elev):scale(dist_trails)					
0.0014087 0.0226340 0.06 0.95037					
scale (sun_elev):solrad_facflow					
0.0020766 0.0095729 0.22 0.52826					
scale (sun_elev):solrad_facmedium					
0.0095261 0.0230282 0.41 0.67912					
scale (sun_elev):solrad_facmedium					
0.0135538 0.0228973 0.59 0.55389					
Fixed effects:					
(Intercept) 0.0092 0.0092 -224.8 <2e-16 ***					
(Intercept) -3.9085 0.0092 -224.8 <2e-16 ***					

MODEL "NORMALIZED DIFFERENCE VEGETATION INDEX (NDVI)"

MODEL "MEAN VEGETATION HEIGHT"

	AIC	BIC	logLik	deviance	df.resid
117578.8 117771.2 -58772.4 117544.8 607633	117532.8 117725.2 -58749.4 117498.8 60733				
Scaled residuals:					
Min 1Q Median 3Q Max	Min 1Q Median 3Q Max				
-0.1587 -0.1449 -0.1421 -0.1389 9.9806	-0.1487 -0.1455 -0.1436 -0.1402 10.8213				
Random effects:					
Groups Name Variance Std.Dev.	Groups Name Variance Std.Dev.				
loc_id:id (Intercept) 0 0	loc_id:id (Intercept) 0 0				
id (Intercept) 0 0	id (Intercept) 0 0				
Number of obs: 607650, groups: loc_id:id, 11956; id, 10	Number of obs: 607650, groups: loc_id:id, 11956; id, 10				
Fixed effects:					
	Estimate Std. Error z value Pr(> z )				
(Intercept)	-3.843897 0.024535 -156.29 <2e-16 ***				
scale(sun_elev)	0.006596 0.016485 0.40 0.689057				
I(scale(sun_elev)^2)	-0.017428 0.012677 -1.37 0.169227				
scale(rugged_10)	-0.029599 0.011941 -2.48 0.013183 *				
I(scale(rugged_10)^2)	-0.017017 0.006127 -2.78 0.005433 **				
scale(dist_trails)	0.020892 0.019735 1.06 0.289733				
I(scaledist_trails)^2)	-0.033065 0.013413 -2.47 0.013698 *				
solrad_facflow	0.000711 0.022692 0.03 0.975004				
solrad_facmedium	0.01298 0.022684 0.06 0.954372				
scale(ndvi_preds)	-0.029010 0.017626 -1.65 0.089794 .				
I(scale(ndvi_preds)^2)	-0.014371 0.010213 -1.41 0.159339				
scale(sun_elev):scale(dist_trails)	0.049971 0.014347 3.48 0.000496 ***				
scale(sun_elev):solrad_facflow	0.010465 0.023024 0.45 0.659452				
scale(sun_elev):solrad_facmedium	0.014052 0.022898 0.61 0.539435				
scale(sun_elev):scale(ndvi_preds)	0.074292 0.015571 4.77 1.83e-06 ***				
		Estimate Std. Error z value Pr(> z )			
(Intercept)	-3.843897 0.024535 -156.29 <2e-16 ***				
scale(sun_elev)	0.006596 0.016485 0.40 0.689057				
I(scale(sun_elev)^2)	-0.017428 0.012677 -1.37 0.169227				
scale(rugged_10)	-0.029599 0.011941 -2.48 0.013183 *				
I(scale(rugged_10)^2)	-0.017017 0.006127 -2.78 0.005433 **				
scale(dist_trails)	0.020892 0.019735 1.06 0.289733				
I(scaledist_trails)^2)	-0.033065 0.013413 -2.47 0.013698 *				
solrad_facflow	0.000711 0.022692 0.03 0.975004				
solrad_facmedium	0.01298 0.022684 0.06 0.954372				
scale(MeanHeight)	-0.040568 0.022575 -1.80 0.07233 .				
I(scale(MeanHeight)^2)	-0.0220556 0.008665 -2.16 0.03094 *				
scale(sun_elev):scale(dist_trails)	0.010468 0.01048 1.01 0.31019				
scale(sun_elev):solrad_facflow	0.005286 0.023045 0.23 0.81857				
scale(sun_elev):solrad_facmedium	0.009130 0.022903 0.40 0.69017				
scale(sun_elev):scale(MeanHeight)	0.029634 0.010942 2.71 0.00676 **				

MODEL "CORINE LAND COVER CLASSES"

MODEL "HABITAT CLASSIFICATION MAP NPBW"

	AIC	BIC	logLik	deviance	df.resid
	117608.5	117834.8	-58794.2	117568.5	607630
Scaled residuals:					
Min	-1.10	Median	30	Max	
-0.1868	-0.1463	-0.1421	-0.1363	10.5962	
Random effects:					
Groups	Name	Variance	Std.Dev.		
loc_id:id	(Intercept)	0.000e+00	0.000e+00		
id	(Intercept)	4.713e-14	2.171e-07		
Number of obs: 607650, groups: loc_id:id, 11956; id, 10					
Fixed effects:					
	Estimate	Std. Error	z value	Pr(> z )	
(Intercept)	-4.112649	0.058027	-70.88	<2e-16 ***	
scale (sun_elev)	-0.051586	0.060052	-0.86	0.3916	
I(scale (sun_elev)^2)	-0.026135	0.028441	-2.04	0.04183 *	
scale (rugged_10)	-0.024819	0.013092	-1.90	0.05799 *	
I(scale (rugged_10)^2)	-0.012343	0.006369	-1.94	0.05265 *	
scale (dist_trails)	0.025079	0.019186	1.31	0.19115	
I(scale (dist_trails)^2)	-0.036172	0.014382	-2.52	0.01190 *	
solrad_facflow	0.008379	0.022922	0.37	0.7469	
solrad_facmedium	0.004910	0.022952	0.21	0.83062	
mapConiferous stand - medium	0.303963	0.068751	4.42	9.82e-06 ***	
mapConiferous stand - young	0.309856	0.063758	4.63	1.33e-06 ***	
mapdead wood - lying	0.263266	0.056764	4.51	6.34e-06 ***	
mapdead wood - standing	0.129372	0.082271	1.57	0.1583	
mapdeciduous stand - mature	0.186033	0.060202	3.09	0.0200 **	
mapdeciduous stand - medium	0.436474	0.079569	5.49	4.12e-08 ***	
mapdeciduous stand - young	0.266726	0.098067	2.72	0.0653 **	
mapEcotone	0.023033	0.196323	0.12	0.90487	
mapMeadow - cultivated	-0.450758	0.118139	-0.90	0.36840	
mapMeadow - natural	0.366581	0.118372	3.10	0.0196 *	
mapMixed stand - mature	0.057534	0.075734	0.76	0.4466	
mapMixed stand - medium	0.268432	0.070142	3.83	0.00013 ***	
mapMixed stand - young	0.432538	0.068380	6.23	4.54e-10 ***	
mapOthers	0.246844	0.075045	3.29	0.0100 **	
mapresidential area	0.534812	0.271960	1.97	0.04924 *	
scale (sun_elev):scale(dist_trails)	0.013460	0.013058	1.03	0.30265	
scale (sun_elev):solrad_facflow	0.006179	0.028493	0.26	0.79253	
scale (sun_elev):solrad_facmedium	0.019192	0.023312	0.51	0.60848	
scale (sun_elev):mapConiferous stand - medium	0.183895	0.027072	2.55	0.01069 *	
scale (sun_elev):mapConiferous stand - young	0.019451	0.067774	0.29	0.77412	
scale (sun_elev):mapdead wood - lying	0.001520	0.061954	0.02	0.98300	
scale (sun_elev):mapdeciduous stand - mature	-0.202844	0.086582	-2.34	0.01914 *	
scale (sun_elev):mapdeciduous stand - medium	-0.011315	0.084958	-0.13	0.89405	
scale (sun_elev):mapdeciduous stand - young	0.206510	0.095420	2.16	0.3045 *	
scale (sun_elev):mapMeadow - cultivated	-0.266940	0.190250	-1.35	0.17684	
scale (sun_elev):mapMeadow - natural	-0.078029	0.113982	-0.68	0.49361	
scale (sun_elev):mapMixed stand - mature	0.212650	0.07694	2.67	0.0761 **	
scale (sun_elev):mapMixed stand - medium	0.097746	0.074361	1.31	0.8869	
scale (sun_elev):mapMixed stand - young	0.085005	0.072641	1.17	0.24192	
scale (sun_elev):mapOthers	0.099758	0.075295	1.32	0.18821	
scale (sun_elev):mapResidential area	-0.061506	0.263067	-0.23	0.81573	

MODEL "NUMBER OF SINGLE TREES"

MODEL "FRACTIONAL VEGETATION COVER"

	AIC	BIC	logLik	deviance	df.resid	AIC	BIC	logLik	deviance	df.resid
	117453.6	117713.9	-58703.8	117407.6	607627	117246.2	117506.5	-58600.1	117200.2	607627
Scaled residuals:						Scaled residuals:				
Min	-10	Median	30	Max		Min	10	Median	30	Max
-0.2352	-0.1463	-0.1412	-0.1359	10.4310		-0.2171	-0.1483	-0.1422	-0.1329	13.0851
Random effects:						Random effects:				
Groups	Name	Variance	Std.Dev.			Groups	Name	Variance	Std.Dev.	
loc_id:id	(Intercept)	0.0008e+00	0.0008e+00			loc_id:id	(Intercept)	3.947e-17	6.282e-09	
id	(Intercept)	7.448e-14	2.729e-07			id	(Intercept)	0.0008e+00	0.0008e+00	
Number of obs: 607650, groups: loc_id:id, 11956; id, 10						Number of obs: 607650, groups: loc_id:id, 11956; id, 10				
Fixed effects:						Fixed effects:				
	Estimate	Std. Error	z value	Pr(>z)			Estimate	Std. Error	z value	Pr(>z)
(Intercept)	-3.8760051	0.0263311	-147.20	< 2e-16 ***		(Intercept)	-3.839e+00	2.967e-02	-130.06	< 2e-16 ***
scale(sun_elev)	0.0038708	0.0167156	0.23	0.816374		scale(sun_elev)	-1.466e-02	1.70le-02	-0.86	0.383760
I(scale(sun_elev)^2)	-0.0373510	0.0128418	-2.91	0.003631 **		I(scale(sun_elev))	-6.153e-02	1.315e-02	-3.93	8.62e-05 ***
scale(rugged_10)^2	-0.0229167	0.0127028	-3.69	0.000225 ***		scale(rugged_10)	1.785e-03	1.23de-02	0.14	0.88994
I(scale(rugged_10)^2)	-0.0229226	0.0127028	-3.69	0.000225 ***		I(scale(rugged_10)^2)	-1.822e-02	6.152e-03	-2.96	0.03054 *
scaledist_trails	0.0238216	0.0153761	1.56	0.118901		scaledist_trails	2.305e-02	1.556e-02	1.49	0.136955
I(scaledist_trails)^2	-0.0339693	0.01353839	-2.94	0.003266 **		I(scaledist_trails)^2	-4.125e-02	3.44de-02	-3.07	0.02155 **
solrad_facflow	-0.0069865	0.0226794	0.31	0.785752		solrad_facflow	4.255e-03	2.267e-02	0.19	0.851110
solrad_facmedium	0.0052489	0.0226561	0.23	0.816789		solrad_facmedium	-2.283e-03	2.263e-02	-0.10	0.919838
scale(ss_deci)	-0.0403398	0.0210252	-1.92	0.0505030 .		scale(ss_deci)	3.270e-02	1.573e-02	2.08	0.037694 *
scale(st_conif)	0.0005873	0.0134260	0.04	0.965111		scale(st_conif)	1.774e-02	1.617e-02	1.10	0.272636
scale(st_dead_all)	0.0022940	0.0165122	0.14	0.889505		scale(st_dead_all)	-8.668e-02	2.379e-02	-3.64	0.00269 ***
I(scale(st_deci)^2)	0.0009724	0.0062355	0.16	0.876080		I(scale(st_deci)^2)	-7.842e-03	3.665e-03	-0.84	0.402385
I(scale(st_conif)^2)	0.0170714	0.0081198	2.10	0.03514 *		I(scale(st_conif)^2)	2.952e-02	1.105e-02	2.67	0.007523 **
I(scale(st_dead_all)^2)	0.0047915	0.0052096	0.92	0.357713		I(scale(st_dead_all)^2)	-2.416e-02	1.403e-02	-1.72	0.084792 .
scale(sun_elev):scale(dist_trails)	0.0242758	0.0101192	2.40	0.016441 *		scale(sun_elev):scale(dist_trails)	3.678e-02	1.03de-02	3.56	0.003377 ***
scale(sun_elev):solrad_facflow	-0.0001632	0.0230444	-0.01	0.994449		scale(sun_elev):solrad_facflow	-6.712e-04	2.309e-02	-0.02	0.980265
scale(sun_elev):solrad_facmedium	0.0065351	0.0229295	0.29	0.775637		scale(sun_elev):solrad_facmedium	-1.3256e-02	2.298e-02	-0.58	0.563992
scale(sun_elev):scale(st_deci)	0.0265404	0.0109285	5.72	1.05e-08 ***		scale(sun_elev):scale(st_deci)	1.161e-01	1.288e-02	9.01	< 2e-16 ***
scale(sun_elev):scale(st_conif)	0.1021476	0.0112424	9.09	< 2e-16 ***		scale(sun_elev):scale(st_conif)	3.862e-02	1.232e-02	3.13	0.001721 **
scale(sun_elev):scale(st_dead_all)	0.0116422	0.0100655	1.16	0.247418		scale(sun_elev):scale(st_dead_all)	4.7516e-05	1.191e-02	0.00	0.996817

## MODEL "LiDAR PCA RESULTS AT 5 M RESOLUTION"

AIC BIC logLik deviance df.resid

117265.7 117817.6 -58595.8 117191.7 607603

Scaled residuals:		AIC	BIC	logLik	deviance	df.resid
Min 1Q Median 3Q Max		-0.2488	-0.1486	-0.1415	-0.1327	11.3502
Groups	Name	Variance	Std.Dev.			
loc_id:id	(Intercept)	0	0			
id	(Intercept)	0	0			
Number of obs:	607650, groups:	loc_id:id, 11956	id, 10			
Fixed effects:		Estimate	Std. Error	z value	Pr(> z )	
(Intercept)		-3.8533579	0.028650	-133.14	< 2e-16 ***	
scale(sun_elev)		-0.0474847	0.0131119	-3.62	0.000293 ***	
I(scale(sun_elev)^2)		-0.0510708	0.0170077	-0.75	0.454947	
scale(rugged_10)		-0.0177562	0.0061771	-2.87	0.004046 **	
I(scale(rugged_10)^2)		-0.0120116	0.01517852	0.76	0.446466	
scale(dist_trails)		-0.0360077	0.0134699	-2.67	0.007513 **	
I(scale(dist_trails)^2)		-0.0092369	0.0227037	0.41	0.5842120	
solrad_facflow		-0.0913677	0.0227443	0.40	0.687354	
scale_facmedium		-0.0172794	0.0332266	-0.52	0.603266	
scale(res5_PCl)		0.0151379	0.0217245	0.70	0.485220	
scale(res5_Pc2)		-0.0708975	0.0205671	3.45	0.000567 ***	
scale(res5_Pc3)		0.0276881	0.0260146	1.06	0.287179	
scale(res5_Pc4)		-0.0265893	0.0211132	-1.21	0.225510	
scale(res5_Pc5)		-0.0141519	0.0170252	0.83	0.405634	
scale(res5_Pc6)		0.0230040	0.0170754	1.35	0.177916	
scale(res5_Pc7)		-0.0001758	0.0160030	-0.01	0.991236	
scale(res5_Pc8)		0.0336711	0.0155884	2.16	0.030380 *	
scale(res5_Pc9)		-0.0097120	0.01565626	-0.63	0.527264	
scale(res5_Pc10)		-0.0275734	0.0136885	0.20	0.840587	
scale(res5_Pc11)		-0.0216802	0.0138812	-2.28	0.024756 *	
I(scale(res5_Pc1)^2)		-0.0156528	0.0118036	-1.32	0.187341	
I(scale(res5_Pc2)^2)		0.0386056	0.0105351	3.66	0.000248 ***	
I(scale(res5_Pc3)^2)		0.0129561	0.0113321	1.14	0.252908	
I(scale(res5_Pc4)^2)		-0.0106519	0.0120613	-0.88	0.317156	
I(scale(res5_Pc5)^2)		-0.0131390	0.0096015	0.15	0.581556	
I(scale(res5_Pc6)^2)		-0.0197605	0.01283026	-2.38	0.017311 *	
I(scale(res5_Pc7)^2)		0.0156738	0.0073655	2.13	0.033337 *	
I(scale(res5_Pc8)^2)		-0.006122	0.0072205	0.08	0.392331	
I(scale(res5_Pc9)^2)		-0.0008007	0.0070602	-0.11	0.909702	
I(scale(res5_Pc10)^2)		-0.0050528	0.0061984	-0.82	0.414466	
I(scale(res5_Pc11)^2)		-0.0341284	0.0105720	3.23	0.001246 **	
scale(sun_elev);scale(dist_trails)		0.0391927	0.0147706	2.65	0.007068 **	
scale(sun_elev);solrad_facflow		-0.0244249	0.0231476	0.11	0.515949	
scale(sun_elev);solrad_facmedium		-0.0017710	0.0230093	-0.08	0.938647	
scale(sun_elev);scale(res5_Pc1)		0.0072061	0.0121280	0.59	0.552399	
scale(sun_elev);scale(res5_Pc2)		-0.0163626	0.01212192	-1.34	0.180540	
scale(sun_elev);scale(res5_Pc3)		-0.0118777	0.0124673	-0.95	0.340736	
scale(sun_elev);scale(res5_Pc4)		0.0391927	0.0147706	2.65	0.007068 **	
scale(sun_elev);scale(res5_Pc5)		-0.08383808	0.0167024	-6.17	2.32e-07 ***	
scale(sun_elev);scale(res5_Pc6)		-0.0059522	0.0153433	-0.39	0.698063	
scale(sun_elev);scale(res5_Pc7)		-0.0320244	0.0149929	-2.14	0.032682 *	
scale(sun_elev);scale(res5_Pc8)		-0.0018356	0.0145670	-0.13	0.899317	
scale(sun_elev);scale(res5_Pc9)		-0.0045001	0.0146601	-0.31	0.757911	
scale(sun_elev);scale(res5_Pc10)		-0.0038624	0.0149040	-0.26	0.795518	
scale(sun_elev);scale(res5_Pc11)		-0.0193346	0.0128368	-1.51	0.132018	

## MODEL "LiDAR PCA RESULTS AT 10 M RESOLUTION"

AIC BIC logLik deviance df.resid

117244.9 117709.0 -58581.5 117162.9 607609

Scaled residuals:		AIC	BIC	logLik	deviance	df.resid
Min 1Q Median 3Q Max		-0.2103	-0.1489	-0.1412	-0.1324	10.9801
Groups	Name	Variance	Std.Dev.			
loc_id:id	(Intercept)	0	0			
id	(Intercept)	0	0			
Number of obs:	607650, groups:	loc_id:id, 11956	id, 10			
Random effects:		Estimate	Std. Error	z value	Pr(> z )	
Groups	Name	Variance	Std.Dev.			
loc_id:id	(Intercept)	0	0			
id	(Intercept)	0	0			
Number of obs:	607650, groups:	loc_id:id, 11956; id, 10				
Scaled residuals:		Min	1Q	Median	3Q	Max
loc_id:id	(Intercept)	0	0			
id	(Intercept)	0	0			
Random effects:		Estimate	Std. Error	z value	Pr(> z )	
Groups	Name	Variance	Std.Dev.			
loc_id:id	(Intercept)	0	0			
id	(Intercept)	0	0			
Fixed effects:		Estimate	Std. Error	z value	Pr(> z )	
(Intercept)		-3.8533579	0.028650	-133.14	< 2e-16 ***	
I(scale(sun_elev)^2)		-0.0474847	0.0131119	-3.62	0.000293 ***	
scale(rugged_10)		-0.0177562	0.0061771	-2.87	0.004046 **	
I(scale(dist_trails))		-0.0360077	0.0134699	-2.67	0.007513 **	
solrad_facflow		-0.0092369	0.0227037	0.41	0.5842120	
scale_facmedium		-0.0913677	0.0227443	0.40	0.687354	
scale(dist_trails)		-0.0172794	0.0332266	-0.52	0.603266	
solrad_facflow		0.0151379	0.0217245	0.70	0.485220	
solrad_facmedium		-0.0276881	0.0260146	1.06	0.287179	
scale(res5_PCl)		-0.0265893	0.0211132	-1.21	0.225510	
scale(res5_Pc2)		-0.0141519	0.0170252	0.83	0.405634	
scale(res5_Pc3)		0.0230040	0.0170754	1.35	0.177916	
scale(res5_Pc4)		-0.0001758	0.0160030	-0.01	0.991236	
scale(res5_Pc5)		0.0336711	0.0155884	2.16	0.030380 *	
scale(res5_Pc6)		-0.0097120	0.01565626	-0.63	0.527264	
scale(res5_Pc7)		-0.0275734	0.0136885	0.20	0.840587	
scale(res5_Pc8)		-0.0216802	0.0138812	-2.28	0.024756 *	
scale(res5_Pc9)		-0.0156528	0.0118036	-1.32	0.187341	
scale(res5_Pc10)		0.0386056	0.0105351	3.66	0.000248 ***	
scale(res5_Pc11)		-0.0129561	0.0113321	1.14	0.252908	
I(scale(res5_Pc1)^2)		-0.0106519	0.0120613	-0.88	0.317156	
I(scale(res5_Pc2)^2)		-0.0131390	0.0096015	0.15	0.581556	
I(scale(res5_Pc3)^2)		-0.0197605	0.01283026	-2.38	0.017311 *	
I(scale(res5_Pc4)^2)		0.0156738	0.0073655	2.13	0.033337 *	
I(scale(res5_Pc5)^2)		-0.006122	0.0072205	0.08	0.392331	
I(scale(res5_Pc6)^2)		-0.0008007	0.0070602	-0.11	0.909702	
I(scale(res5_Pc7)^2)		-0.0050528	0.0061984	-0.82	0.414466	
I(scale(res5_Pc8)^2)		-0.0341284	0.0105720	3.23	0.001246 **	
I(scale(res5_Pc9)^2)		-0.0244249	0.0231476	0.11	0.515949	
I(scale(res5_Pc10)^2)		-0.0017710	0.0230093	-0.08	0.938647	
I(scale(res5_Pc11)^2)		0.0072061	0.0121280	0.59	0.552399	
scale(sun_elev);scale(res5_Pc1)		-0.0163626	0.01212192	-1.34	0.180540	
scale(sun_elev);scale(res5_Pc2)		-0.0118777	0.0124673	-0.95	0.340736	
scale(sun_elev);scale(res5_Pc3)		-0.0391927	0.0147706	2.65	0.007068 **	
scale(sun_elev);scale(res5_Pc4)		-0.08383808	0.0167024	-6.17	2.32e-07 ***	
scale(sun_elev);scale(res5_Pc5)		-0.0059522	0.0153433	-0.39	0.698063	
scale(sun_elev);scale(res5_Pc6)		-0.0320244	0.0149929	-2.14	0.032682 *	
scale(sun_elev);scale(res5_Pc7)		-0.0018356	0.0145670	-0.13	0.899317	
scale(sun_elev);scale(res5_Pc8)		-0.0045001	0.0146601	-0.31	0.757911	
scale(sun_elev);scale(res5_Pc9)		-0.0038624	0.0149040	-0.26	0.795518	
scale(sun_elev);scale(res5_Pc10)		-0.0193346	0.0128368	-1.51	0.132018	

## C.2 Red deer telemetry data - 1 hour fix rate

MODEL "NO VEGETATION"

MODEL "NULL MODEL"

	AIC	BIC	logLik	deviance	df.resid
	51953.5	52100.5	-259862.7	51925.5	268366
Scaled residuals:					
Min	1Q	Median	3Q	Max	
-0.1695	-0.1479	-0.1429	-0.1363	16.9893	
Random effects:					
Groups	Name	Variance	Std.Dev.		
loc_id:id	(Intercept)	0.000000	0.00000		
id	(Intercept)	0.003248	0.05699		
Number of obs:	268380,	groups:	loc_id:id,	5290;	id, 10
Fixed effects:					
	Estimate	Std. Error	z value	Pr(> z )	
(Intercept)	-3.746011	0.046203	-81.08	< 2e-16 ***	
scale(sun_elev)	-0.018606	0.024901	-0.75	0.454943	
I(scale(sun_elev)^~2)	0.002484	0.018080	0.14	0.890719	
scale(rugged_10)	-0.111326	0.022378	-4.97	6.53e-07 ***	
I(scale(rugged_10)^~2)	-0.020298	0.009992	-2.03	0.042220 *	
scale(dist_trails)	0.107297	0.030056	3.57	0.000357 ***	
I(scale(dist_trails)^~2)	-0.118866	0.023396	-5.08	3.76e-07 ***	
solrad_faclow	0.012312	0.034631	0.36	0.722207	
solrad_facmedium	-0.013074	0.034139	-0.38	0.701754	
scale(sun_elev);scale(dist_trails)	0.008061	0.014744	0.55	0.584584	
scale(sun_elev);solrad_faclow	0.018407	0.034777	0.53	0.596599	
scale(sun_elev);solrad_facmedium	0.003854	0.034488	0.11	0.911028	
Fixed effects:					
(Intercept)	-3.90668	0.01384	-282.2	<2e-16 ***	

MODEL "NORMALIZED DIFFERENCE VEGETATION INDEX (NDVI)"

MODEL "MEAN HEIGHT OF VEGETATION "

	AIC	BIC	logLik	deviance	df.resid		AIC	BIC	logLik	deviance	df.resid
51900.4	52078.9	-25933.2	51866.4	268363	51840.2	52018.7	-25903.1	51806.2	268363		
<b>Scaled residuals:</b>											
Min 1Q Median 3Q Max											
-0.1936 -0.1489 -0.1421 -0.1338 15.3425 -0.1649 -0.1499 -0.1455 -0.1364 17.7266											
<b>Random effects:</b>											
Groups Name Variance Std.Dev.											
loc_id:id (Intercept) 0.00000 0.00000											
(Intercept) 9.131e-13 9.556e-07 id 0.001351 0.036755											
Number of obs: 268380, groups: loc_id:id, 5290; id, 10 Number of obs: 268380, groups: loc_id:id, 5290; id, 10											
<b>Fixed effects:</b>											
Estimate Std. Error z value Pr(> z )											
(Intercept) -3.783592 0.037549 -100.82 < 2e-16 ***											
scale(sun_elev) -0.001857 0.025279 -0.07 0.941433											
I(scale(sun_elev)^2) -0.030156 0.018710 -1.61 0.10702											
scale(rugged,10) -0.102320 0.018758 -5.45 4.90e-08 ***											
I(scale(rugged,10)^2) -0.018966 0.029633 -1.97 0.04836 *											
scale(dist_trails) 0.038877 0.028468 1.26 0.20737											
I(scale(dist_trails)^2) -0.096129 0.022000 -4.37 1.24e-06 ***											
solrad_facflow 0.002225 0.034279 0.06 0.94825											
solrad_facmedium -0.019255 0.034264 -0.56 0.57415											
scale(ndvi_preds) -0.079873 0.027579 -2.90 0.00378 **											
I(scale(ndvi_preds)^2) -0.007724 0.015631 -0.49 0.62120											
scale(sun_elev):scale(dist_trails) 0.126105 0.022886 5.51 3.59e-08 ***											
scale(sun_elev):solrad_facflow 0.034676 0.51 0.60777											
scale(sun_elev):solrad_facmedium 0.034483 0.41 0.68153											
scale(sun_elev):scale(ndvi_preds) 0.166233 0.023786 6.99 2.77e-12 ***											
Estimate Std. Error z value Pr(> z )											
(Intercept) -3.740539 0.051207 -73.06 < 2e-16 ***											
scale(sun_elev) -0.006337 0.028203											
I(scale(sun_elev)^2) -0.001851 0.018102											
scale(rugged,10) -0.063856 0.023895											
I(scale(rugged,10)^2) -0.023563 0.009867											
scale(dist_trails) 0.025178 0.031929											
I(scale(dist_trails)^2) -0.059850 0.023767											
solrad_facflow 0.007385 0.034856											
solrad_facmedium -0.013507 0.034161											
scale(MeanHeight) -0.070884 0.038921											
I(scale(MeanHeight)^2) -0.056372 0.017563											
scale(sun_elev):scale(dist_trails) 0.024866 0.015644											
scale(sun_elev):solrad_facflow 0.012148 0.034892											
scale(sun_elev):solrad_facmedium -0.004056 0.034497											
scale(sun_elev):scale(MeanHeight) 0.059653 0.018816											

## MODEL "CORINE LAND COVER CLASSES"

### MODEL "HABITAT CLASSIFICATION MAP NPBW"

	AIC	BIC	-logLik	deviance	df.resid
	51946.1	52177.1	-26951.0	51902.1	263358
Scaled residuals:					
Min	1Q	Median	3Q	Max	
-0.4575	-0.1481	-0.1430	-0.1361	18.7436	
Random effects:					
Groups	Name	Variance	Std.Dev.		
loc_id:id	(Intercept)	0	0		
id	(Intercept)	0	0		
Number of obs:	268380	groups:	loc_id:id,	5290;	id, 10
Fixed effects:					
	Estimate	Std. Error	z value	Pr(> z )	
(Intercept)	-4.279036	0.088562	-47.90	< 2e-16 ***	
scale (sun_elev)	0.036070	0.087617	0.35	0.72684	
I(scale (sun_elev)^2)	-0.056505	0.019204	-2.94	0.0326 ***	
scale (rugged_10)	-0.078348	0.020480	-3.83	0.00013 ***	
I(scale (rugged_10)^2)	-0.019233	0.010045	-1.91	0.05552 *	
scale (dist_trails)	0.070821	0.027507	2.58	0.00993 ***	
I(scale (dist_trails)^2)	-0.108333	0.023999	-4.53	5.76e-06 ***	
solrad_facflow	0.012741	0.034756	0.37	0.71393	
solrad_facmedium	-0.015933	0.034658	-0.46	0.64571	
map_reclassconiferous_stand - medium	0.576145	0.101568	5.67	1.40e-08 ***	
map_reclassconiferous_stand - young	0.462794	0.096325	4.80	1.55e-06 ***	
map_reclassdead wood - lying	0.480431	0.085515	5.62	1.36e-08 ***	
map_reclassdead wood - standing	0.278148	0.124000	2.24	0.02489 *	
map_reclassdeciduous_stand - mature	0.364399	0.091267	3.99	6.53e-05 ***	
map_reclassdeciduous_stand - medium	0.835360	0.118579	7.04	1.36e-12 ***	
map_reclassdeciduous_stand - young	0.684494	0.227255	0.78	1.71e-06 ***	
map_reclassdecitone	-1.889146	0.768093	-2.46	0.1404 *	
map_reclassdecadow - cultivated	0.591459	0.195395	3.03	0.00247 **	
map_reclassdecadow - natural	-0.001933	0.122903	-0.02	0.95736	
map_reclassdeciduous_stand - mature	0.498875	0.106578	4.68	2.86e-06 ***	
map_reclassdeciduous_stand - medium	0.921723	0.107086	8.61	< 2e-16 ***	
map_reclassdeciduous_stand - young	0.587800	0.117651	5.00	5.85e-07 ***	
map_reclassdeciters	-0.754937	0.930428	-0.81	0.41714	
map_reclassdecidential area	0.036453	0.021192	1.72	0.08541	
scale (sun_elev):scale(df.dist_trails)	0.016571	0.035450	0.47	0.64018	
scale (sun_elev):solrad_facflow	0.016315	0.035168	0.46	0.64271	
scale (sun_elev):solrad_facmedium	0.199950	0.102871	1.94	0.05193	
scale (sun_elev):solrad_facmedium	0.022711	0.034962	0.55	0.58515	
corine_reclassBroad-leaved forest	1.370529	8.462	< 2e-16 ***		
corine_reclassConiferous forest	1.367729	8.454	< 2e-16 ***		
corine_reclassMixed forest	1.363228	8.497	< 2e-16 ***		
corine_reclassTransitional woodland-shrub	1.367961	8.495	< 2e-16 ***		
scale (sun_elev): scale (dist_trails)	-0.034657	0.021709	-1.596	0.1104	
solrad_facflow	0.022711	0.034962	0.650	0.5160	
scale (sun_elev): solrad_facmedium	0.005551	0.034538	0.161	0.8723	
corine_reclassBroad-leaved forest	9.680708	1.066073	8.987	< 2e-16 ***	
scale (sun_elev): corine_reclassBroad-leaved forest	9.357510	1.055203	8.888	< 2e-16 ***	
scale (sun_elev): corine_reclassConiferous forest	9.217182	1.056709	8.723	< 2e-16 ***	
scale (sun_elev): corine_reclassMixed forest	9.452428	1.05595	8.955	< 2e-16 ***	
scale (sun_elev): corine_reclassTransitional woodland-shrub					
scale (sun_elev): map_reclassEccone					
scale (sun_elev): map_reclassDead wood - living					
scale (sun_elev): map_reclassDead wood - standing					
scale (sun_elev): map_reclassDeciduous stand - mature					
scale (sun_elev): map_reclassDeciduous stand - medium					
scale (sun_elev): map_reclassDeciduous stand - young					
scale (sun_elev): map_reclassDecitone					
scale (sun_elev): map_reclassMeadow - cultivated					
scale (sun_elev): map_reclassMeadow - natural					
scale (sun_elev): map_reclassMixed stand - mature					
scale (sun_elev): map_reclassMixed stand - medium					
scale (sun_elev): map_reclassMixed stand - young					
scale (sun_elev): map_reclassOthers					
scale (sun_elev): map_reclassResidential area					

MODEL "NUMBER OF SINGLE TREES"

MODEL "FRACTIONAL VEGETATION HEIGHT"

	AIC	BIC	-logLik	deviance	df.resid	AIC	BIC	-logLik	deviance	df.resid	
51731.2	51972.7	-25842.6	51685.2	268357		51491.5	51733.0	-25722.7	51445.5	268357	
Scaled residuals:											
Min	1Q	Median	3Q	Max		Min	1Q	Median	3Q	Max	
-0.3605	-0.1600	-0.1402	-0.1293	20.0754		-0.2648	-0.1563	-0.1416	-0.1227	19.6195	
Random effects:											
Groups	Name	Variance	Std.Dev.			Groups	Name	Variance	Std.Dev.		
loc_id:id	(Intercept)	0.00000	0.0000			loc_id:id	(Intercept)	0	0		
id	(Intercept)	0.00407	0.0638			id	(Intercept)	0	0		
Number of obs:	268380	groups:	loc_id:id,	5290; id, 10		Number of obs:	268380	groups:	loc_id:id,	5290; id, 10	
Fixed effects:											
	Estimate	Std.	Error	z value	Pr(> z )		Estimate	Std.	Error	z value	Pr(> z )
(Intercept)	-3.800493	0.049805	-76.31	< 2e-16	***	(Intercept)	-3.791324	0.048046	-82.34	< 2e-16	***
scale(sun_elev)	-0.018695	0.025717	-0.73	0.467245		scale(sun_elev)	-0.042366	0.026175	-1.62	0.10554	
I(scale(sun_elev)^~2)	-0.057604	0.019082	-3.02	0.002598	**	I(scale(sun_elev)^~2)	-0.080859	0.019461	-4.15	3.25e-05	***
scale(rugged_10)	-0.069555	0.023470	-2.96	0.003040	**	scale(rugged_10)^~10	-0.036807	0.019439	-1.84	0.06547	.
I(scale(rugged_10)^~2)	-0.026461	0.010188	-2.60	0.009398	**	I(scale(rugged_10)^~2)	-0.026904	0.008732	-2.76	0.00570	**
scale(dist_trails)	0.066945	0.030928	2.21	0.026852	*	scale(dist_trails)	0.0123515	0.022226	0.64	0.52436	
I(scaledist_trails)^~2)	-0.107363	0.023506	-4.57	4.94e-06	***	I(scaledist_trails)^~2)	-0.093814	0.022048	-4.26	2.09e-05	***
solrad_facflow	0.027624	0.034627	0.80	0.425013		solrad_facflow	0.025694	0.031449	0.75	0.45181	
solrad_facmedium	-0.002122	0.034122	-0.06	0.960503		solrad_facmedium	-0.013018	0.034098	-0.38	0.70263	
scale(st_dec1)	-0.114986	0.038310	-3.40	0.000672	***	scale(st_dec1)	0.063050	0.0283805	2.65	0.00808	**
scale(st_conf1)	-0.006849	0.019887	-0.34	0.730568		scale(st_conf1)	0.046324	0.024747	1.88	0.0601	.
scale(st_dead_all)	-0.010542	0.026537	-0.42	0.677373		scale(st_dead_all)	-0.226850	0.038974	-6.14	8.19e-10	***
I(scale(st_dec1)^~2)	0.010566	0.009857	1.10	0.269802		I(scale(st_dec1)^~2)	-0.020800	0.013116	-1.59	0.11278	
I(scale(st_conf1)^~2)	0.034510	0.011434	3.02	0.002543	**	I(scale(st_conf1)^~2)	0.006335	0.016242	0.39	0.69652	
I(scale(st_dead_all)^~2)	-0.020715	0.008540	-0.32	0.750514		I(scale(st_dead_all)^~2)	-0.012795	0.023306	-0.55	0.58300	
scale(sun_elev : scale(dist_trails))	0.050575	0.015696	3.22	0.011273	**	scale(sun_elev : scale(dist_trails))	0.072834	0.016180	4.50	6.74e-06	***
scale(sun_elev : solrad_facflow)	0.015695	0.034861	0.45	0.652559		scale(sun_elev : solrad_facflow)	0.014467	0.034802	0.42	0.67762	
scale(sun_elev : solrad_facmedium)	0.006141	0.034588	0.18	0.868910		scale(sun_elev : solrad_facmedium)	-0.025693	0.034491	-0.75	0.45282	
scale(sun_elev : scale(st_dec1))	0.097353	0.017573	5.54	3.02e-08	***	scale(sun_elev : scale(st_dec1))	0.192822	0.018916	10.18	< 2e-16	***
scale(sun_elev : scale(st_conif))	0.172557	0.016203	10.65	< 2e-16	***	scale(sun_elev : scale(st_conif))	0.057411	0.018488	3.11	0.00190	**
scale(sun_elev : scale(st_dead_all))	0.026158	0.015886	1.65	0.099651	.	scale(sun_elev : scale(st_dead_all))	0.031050	0.019854	1.56	0.11784	

## MODEL "LiDAR PCA RESULTS AT 5 M RESOLUTION"

## MODEL "LiDAR PCA RESULTS AT 10 M RESOLUTION"

	AIC	BIC	logLik	deviance	df.resid		AIC	BIC	logLik	deviance	df.resid	
	51520.8	52014.3	-25713.4	51426.8	268333		51446.4	51876.9	-25682.2	51364.4	268339	
Scaled residuals:												
Min	-1Q	Median	3Q	Max								
-0.2848	-0.1546	-0.1403	-0.1223	22.7526								
Random effects:												
Groups	Name	Variance	Std.Dev.									
loc_id:id	(Intercept)	0	0									
id	(Intercept)	0	0									
Number of obs:	268380	groups:	loc_id:id	5290; id, 10								
Fixed effects:												
(Intercept)		Estimate	Std. Error	z value	Pr(>z)		Estimate	Std. Error	z value	Pr(>z)		
scale(sun_elev)	-3.8567247	0.0451399	-88.42	< 2e-16	***	-1.34	0.179763	-76.42	< 2e-16	***		
I(scale(sun_elev)^2)	-0.0350676	0.0261409	-3.97	7.17	0.05	* **	-0.0372029	0.040252	-86.97	< 2e-16	***	
scale(rugged,10)^2)	-0.0772584	0.0194577	-1.54	0.1228781		-0.0284332	0.040252	-86.97	< 2e-16	***		
scale(dist_trails)	-0.0298453	0.0098076	-2.75	0.006007	**	-0.0924083	0.0179595	-4.67	3.04e-06	***		
I(scale(dist_trails)^2)	-0.0013742	0.0217533	-0.06	0.949928		-0.0152133	0.0188776	-0.77	0.444066			
solrad_fac1on	-0.0288609	0.0341742	0.84	0.398377		-0.0284806	0.008924	-2.88	0.003989	**		
scale(res5,PC1)	0.0023715	0.0341971	0.07	0.944712		-0.0203960	0.0227468	-0.90	0.368904			
scale(res5,PC2)	-0.1812067	0.053684	-3.40	0.000884	***	-0.080094	0.0224418	-3.60	0.000317	***		
scale(res5,PC3)	0.0355089	0.0353999	0.99	0.323399		-0.034767	0.0342444	1.09	0.276354			
scale(res5,PC4)	0.1643490	0.0331668	4.96	7.07e-07	***	0.0085756	0.0342982	0.25	0.802970			
scale(res5,PC5)	-0.0566548	0.0332312	-0.17	0.864380		-0.1206776	0.042991	-2.45	0.014370	*		
scale(res5,PC6)	0.0234239	0.0276269	0.85	0.396512		0.0663786	0.036317	1.83	0.067848	.		
scale(res5,PC7)	0.0286019	0.0280096	1.39	0.166318		0.1702601	0.0322881	5.27	1.34e-07	***		
scale(res5,PC8)	-0.0421924	0.0256830	-1.64	0.100421		0.1061242	0.0434836	2.56	0.10353	*		
scale(res5,PC9)	-0.069973	0.0250064	-0.28	0.779917		0.0656773	0.0324465	0.15	0.877711			
scale(res5,PC10)	-0.0405197	0.0248604	0.89	0.373388		0.00045523	0.0264643	0.02	0.984620			
scale(res5,PC11)	-0.0095159	0.0212359	-0.45	0.654077		-0.0567908	0.0284619	-1.93	0.055905	.		
I(scale(res5,PC1)^2)	-0.0002109	0.0233662	-0.01	0.9829797		-0.0274528	0.030403	-1.57	0.116929			
I(scale(res5,PC2)^2)	-0.0390967	0.0131739	-2.97	0.003000	**	-0.0243897	0.0242017	1.02	0.309954			
I(scale(res5,PC3)^2)	-0.0671515	0.01686072	4.05	5.12e-05	***	-0.0453651	0.0229200	-1.98	0.047784	*		
I(scale(res5,PC4)^2)	-0.0114974	0.0168538	-0.68	0.495122		-0.0131933	0.0174745	-0.07	0.943280			
I(scale(res5,PC5)^2)	-0.0051024	0.0171606	0.36	0.722337		0.0004532	0.0264643	0.39	1.14e-05	***		
I(scale(res5,PC6)^2)	0.00020105	0.0140892	0.14	0.886332		0.0013132	0.0157144	0.08	0.933402			
I(scale(res5,PC7)^2)	-0.0390967	0.0131739	-2.97	0.003000	**	-0.0152332	0.015822	-1.20	0.229054			
I(scale(res5,PC8)^2)	-0.035120	0.0118153	-0.70	0.481058		-0.0243897	0.0242017	1.02	0.309954			
I(scale(res5,PC9)^2)	-0.0671515	0.01686072	4.05	5.12e-05	***	-0.0453651	0.0229200	-1.98	0.047784	*		
I(scale(res5,PC10)^2)	-0.0114974	0.0168538	-0.68	0.495122		-0.0131933	0.0174745	-0.07	0.943280			
I(scale(res5,PC11)^2)	-0.0051024	0.0171606	0.36	0.722337		-0.0004532	0.0264643	0.39	1.14e-05	***		
scale(sun_elev : scale(dist_trails))	0.0727071	0.0166033	4.38	1.19e-05	***	0.0296049	0.017205	5.36	8.23e-08	***		
scale(sun_elev : solrad_fac1ow)	0.0139135	0.0348438	0.40	0.689665		0.0112311	0.0349233	0.32	0.747803			
scale(sun_elev : solrad_facmedium)	-0.0116967	0.0345919	-0.34	0.735263		-0.0127081	0.0346733	-0.37	0.714032			
scale(sun_elev : scale(res5,PC1))	-0.0430209	0.0201376	1.91	0.056099	.	0.0356514	0.0244506	1.68	0.093645	.		
scale(sun_elev : scale(res5,PC2))	-0.0430209	0.0201376	-2.03	0.042371	*	-0.0650047	0.0220336	-2.95	0.003175	*		
scale(sun_elev : scale(res5,PC3))	-0.0153736	0.0212145	-0.72	0.47323		-0.0299116	0.0283688	-0.96	0.338716			
scale(sun_elev : scale(res5,PC4))	-0.0964433	0.0244007	3.95	7.73e-05	***	0.0296049	0.017205	5.36	8.23e-08	***		
scale(sun_elev : scale(res5,PC5))	-0.1128292	0.0274138	-4.20	2.61e-05	***	-0.1128433	0.0307543	-3.67	0.00243	***		
scale(sun_elev : scale(res5,PC6))	-0.0446022	0.0256642	-1.93	0.053268	.	0.0418612	0.0276609	1.51	0.130185			
scale(sun_elev : scale(res5,PC7))	-0.0258380	0.0255310	-1.01	0.311153	.	0.0332145	0.0273124	1.22	0.223948			
scale(sun_elev : scale(res5,PC8))	-0.021836	0.02441574	-0.09	0.927978		-0.0131376	0.0267984	-0.49	0.623967			
scale(sun_elev : scale(res5,PC9))	-0.0068732	0.02428487	-0.28	0.776335		-0.0187813	0.0246777	-0.87	0.386278			
scale(sun_elev : scale(res5,PC10))	0.0062910	0.0249437	0.25	0.800380		-0.0187813	0.0246777	-0.87	0.386278			
scale(sun_elev : scale(res5,PC11))	-0.0484174	0.0201212	-2.41	0.016115	*							

### C.3 Roe deer telemetry data - 1 hour fix rate

MODEL "NO VEGETATION"

MODEL "NULL MODEL"

AIC	BIC	logLik	deviance	df.resid
65671.5	65821.8	-32821.7	65663.5	340151
Scaled residuals:				
Min	1Q	Median	3Q	Max
-0.1604	-0.1457	-0.1437	-0.1398	12.0401
Random effects:				
Groups	Name	Variance	Std.Dev.	
loc_id:id	(Intercept)	0	0	
id	(Intercept)	0	0	
Number of obs:	340165, groups: loc_id:id, 6678; id, 17			
Fixed effects:				
		Estimate	Std. Error	z value Pr(> z )
		(Intercept)	-3.904589	0.02210 -138.41 < 2e-16 ***
		scale (sun_elev)	-0.005648	0.022320 -0.26 0.8002
		I(scale(sun_elev)^~2)	-0.002197	0.018055 -0.14 0.8912
		scale (rugged_10)	-0.076237	0.017672 -4.31 1.6e-05 ***
		I(scale(rugged_10)^~2)	-0.019170	0.008790 -2.18 0.0292 *
		scale (dist_trails)	-0.010111	0.021533 -0.47 0.6387
		I(scale(dist_trails)^~2)	-0.003217	0.005112 -0.63 0.5292
		solrad_facflow	0.004829	0.031461 0.15 0.8780
		solrad_facmiddle	0.023913	0.030246 0.79 0.4292
		scale (sun_elev):scale(dist_trails)	0.032971	0.013372 2.47 0.0137 *
		scale (sun_elev):solrad_facflow	0.011101	0.031765 0.35 0.7267
		scale (sun_elev):solrad_facmiddle	0.015876	0.030353 0.53 0.5987
Fixed effects:				
		(Intercept)	4.31de-12	2.077e-06
		id	0.000e+00	0.000e+00
		(Intercept)	0.000e+00	0.000e+00
		Number of obs:	340165, groups: loc_id:id, 6678; id, 17	

MODEL "NORMALIZED DIFFERENCE VEGETATION INDEX (NDVI)"

MODEL "MEAN VEGETATION HEIGHT"

	AIC	BIC	logLik	deviance	df.resid	AIC	BIC	logLik	deviance	df.resid
6631.1	66813.6	-32798.5	65897.1	340148		65179.0	65361.5	-32672.5	65145.0	34048
<b>Scaled residuals:</b>										
Min	1Q	Median	3Q	Max		Min	1Q	Median	3Q	Max
-0.2532	-0.1445	-0.1415	-0.1383	13.4773		-0.1694	-0.1565	-0.1485	-0.1238	15.2105
<b>Random effects:</b>										
Groups	Name	Variance	Std.Dev.		Groups	Name	Variance	Std.Dev.		
loc_id:id	(Intercept)	0	0		loc_id:id	(Intercept)	0	0.00000	0.0000	
id	(Intercept)	0	0		id	(Intercept)	0.001823	0.0427		
Number of obs:	340165,	groups:	loc_id:id, 6678;	id, 17	Number of obs:	340165,	groups:	loc_id:id, 6678;	id, 17	
<b>Fixed effects:</b>										
	Estimate	Std. Error	z value	Pr(> z )		Estimate	Std. Error	z value	Pr(> z )	
(Intercept)	-3.933271	0.028563	-137.71	< 2e-16 ***	(Intercept)	-3.823732	0.030372	-97.12	< 2e-16 ***	
scale(sun_elev)	-0.001964	0.022339	-0.09	0.929924	scale(sun_elev)	0.051432	0.020310	2.24	0.025408 *	
I(scale(sun_elev)^2)	-0.005051	0.016059	-0.31	0.753131	I(scale(sun_elev)^2)	-0.020642	0.016189	-1.28	0.202282	
scale(rugged_10)	-0.044684	0.018491	2.42	0.015669 *	scale(rugged_10)	0.022265	0.023585	0.94	0.345151	
I(scale(rugged_10)^2)	-0.031352	0.009330	-3.36	0.000778 ***	I(scale(rugged_10)^2)	-0.027186	0.009772	-2.78	0.005404 **	
scaledist(trails)	-0.004151	0.021923	-0.19	0.849811	scaledist(trails)	0.053078	0.022777	2.33	0.019789 *	
I(scaledist(trails)^2)	-0.010714	0.005276	-2.03	0.042288 *	I(scaledist(trails)^2)	-0.020418	0.005498	-3.71	0.00204 ***	
solrad_facflow	0.006740	0.031510	0.21	0.830615	solrad_facflow	0.011800	0.031784	0.37	0.710450	
solrad_facmiddle	0.012994	0.030292	0.43	0.667964	solrad_facmiddle	0.044485	0.030465	1.46	0.144236	
scale(ndvi_preds)	-0.007485	0.013594	-0.55	0.581882	scale(ndvi_preds)	-0.2544821	0.023229	-11.95	< 2e-16 ***	
I(scale(ndvi_preds)^2)	0.007473	0.050877	6.81	9.9e-12 ***	I(scale(ndvi_preds)^2)	-0.098048	0.028428	-4.19	.85e-05 ***	
scale(sun_elev):scale(dist_trails)	0.014142	3.02	0.002500 ***	scale(sun_elev):scale(dist_trails)	0.033459	0.015424	2.49	0.012686 *		
scale(sun_elev):solrad_facflow	0.021436	0.031845	0.67	0.500889	scale(sun_elev):solrad_facflow	-0.008413	0.031884	-0.26	0.791875	
scale(sun_elev):solrad_facmiddle	0.024995	0.030376	0.82	0.410586	scale(sun_elev):solrad_facmiddle	-0.004455	0.030483	-0.15	0.883815	
scale(sun_elev):scale(ndvi_preds)	0.0217140	0.012716	1.71	0.087337 .	scale(sun_elev):scale(ndvi_preds)	0.104483	0.014771	7.07	1.51e-12 ***	

MODEL "CORINE LAND COVER CLASSES"

MODEL "HABITAT CLASSIFICATION MAP NPBW"

	AIC	BIC	logLik	deviance	df.resid	
	65048.8	65521.3	-32480.4	64960.8	340121	
Scaled residuals:						
Min	-1.0	Median	3Q	Max		
-0.2172	-0.1603	-0.1376	-0.1198	18.5765		
Random effects:						
Groups	Name	Variance	Std.Dev.			
loc_id:id	(Intercept)	0.00000	0.00000			
id	(Intercept)	0.01272	0.1128			
Number of obs: 340165, groups: loc_id:id, 6678; id, 17						
Fixed effects:						
(Intercept)						Estimate Std. Error z value Pr(> z )
scale (sun_elev)						-4.109668 0.059715 -68.82 <2e-16 ***
I(scale (sun_elev) ^2)						0.211416 0.048643 4.63 3.62e-06 ***
scale (rugged_10)						-0.045325 0.056540 **
I(scale (rugged_10) ^2)						0.007062 0.024355 0.29 0.771837
scale (dist_trails)						-0.027074 0.009938 -2.72 0.006446 **
I(scale (dist_trails) ^2)						0.046407 0.024696 1.88 0.060226 *
solrad_facflow						-0.021720 0.006148 -3.53 0.004111 ***
solrad_facmiddle						0.049223 0.032376 1.62 0.128420
mapConiferous stand - medium						0.060631 0.030717 1.96 0.050529 .
mapConiferous stand - young						0.066031 0.017123 0.57 0.569423
mapDead wood - lying						0.374287 0.178181 2.10 0.035676 *
mapDead wood - standing						0.551548 0.082590 6.88 2.36e-11 ***
mapDeciduous stand - mature						0.391166 0.093849 4.17 3.07e-05 ***
mapDeciduous stand - medium						-0.046279 0.061293 -0.76 0.462018
mapDeciduous stand - young						-0.356437 0.057643 -1.50 0.133645 **
mapEcotone						0.085917 0.175155 4.86 1.19e-06 ***
mapMeadow - cultivated						0.718774 0.078151 9.20 < 2e-16 ***
mapMeadow - natural						0.468749 0.050171 9.34 < 2e-16 ***
mapMixed stand - mature						0.633094 0.073082 8.66 < 2e-16 ***
mapMixed stand - medium						-0.128503 0.053677 -2.39 0.016665 *
mapMixed stand - young						0.384466 0.049756 4.32 1.43e-06 ***
mapOthers						0.576565 0.060999 8.72 < 2e-16 ***
mapResidential area						0.430054 0.219810 1.96 0.050409 .
scale (sun_elev):scale(dist_trails)						-1.522912 0.281711 -5.41 6.45e-08 ***
scale (sun_elev):solrad_facflow						0.013729 0.015092 0.91 0.362996
scale (sun_elev):solrad_facmiddle						-0.020651 0.032613 -0.63 0.52684
scale (sun_elev):mapConiferous stand - medium						-0.04185 0.030872 -0.46 0.645886
scale (sun_elev):mapConiferous stand - young						0.081709 0.112176 0.73 0.466370
scale (sun_elev):mapDead wood - lying						0.0046530 0.177162 0.03 0.971948
scale (sun_elev):mapDead wood - standing						-0.101487 0.076914 -1.32 0.187006
scale (sun_elev):mapEcotone						-0.196844 0.094880 -2.07 0.038019 *
scale (sun_elev):mapMeadow - natural						0.034968 0.067908 -4.70 2.59e-06 ***
scale (sun_elev):mapMixed stand - mature						-0.036480 0.051237 -0.71 0.476477
scale (sun_elev):mapMixed stand - medium						-0.064217 0.074537 -0.86 0.388834 ***
scale (sun_elev):mapOthers						-4.64 3.42e-06 ***
scale (sun_elev):mapResidential area						-0.350183 0.226407 -1.55 0.121936
scale (sun_elev):mapResidential area						-0.220484 0.296675 -0.74 0.457370

## MODEL "NUMBER OF SINGLE TREES"

## MODEL "FRACTIONAL VEGETATION COVER"

	AIC	BIC	logLik	deviance	df.resid
	65300.9	65547.9	-32627.5	65254.9	340142
Scaled residuals:					
Min	-1Q	Median	3Q	Max	
-0.2310	-0.1551	-0.1410	-0.1269	13.3984	
Number of obs: 340165, groups: loc_id:id, 6678; id, 17					
Random effects:					
Groups	Name	Variance	Std. Dev.		
loc_id:id	(Intercept)	0.000000	0.00000		
id	(Intercept)	0.004257	0.06525		
Number of obs: 340165, groups: loc_id:id, 6678; id, 17					
Fixed effects:					
	Estimate	Std. Error	z value	Pr(> z )	
(Intercept)	-3.919926	0.039471	-99.31	< 2e-16 ***	
scale(sun_elev)	0.077786	0.023231	3.35	0.000813 ***	
I(scale(sun_elev)^2)	-0.045130	0.016518	-2.73	0.006291 **	
scale(rugged_10)	-0.11648	0.023095	-0.50	0.614022	
I(scale(rugged_10)^2)	-0.018774	0.009419	-1.99	0.046254 *	
scale(dist_trails)	0.042442	0.023226	1.83	0.067651 .	
I(scale(dist_trails)^2)	-0.018358	0.005694	-3.22	0.001264 **	
solrad_facflow	0.028152	0.031932	0.79	0.430836	
solrad_facmiddle	0.051098	0.030502	1.68	0.039835 .	
scale(ss_deci)	-0.178319	0.029007	-6.15	7.88e-10 ***	
scale(ss_conif)	-0.178082	0.018374	-9.69	< 2e-16 ***	
scale(st_dead_all)	-0.012646	0.026030	-0.49	0.627096	
I(scale(st_deci)^2)	-0.006371	0.013190	-0.48	0.629101	
I(scale(st_conif)^2)	0.030260	0.011817	2.56	0.010446 *	
I(scale(st_dead_all)^2)	0.002457	0.003430	0.72	0.473776	
scale(sun_elev):scale(dist_trails)	0.028179	0.013475	2.17	0.030356 *	
scale(sun_elev):solrad_facflow	-0.0382207	0.032207	-1.11	0.265981	
scale(sun_elev):solrad_facmiddle	-0.016495	0.030685	-0.54	0.589675	
scale(sun_elev):scale(st_deci)	0.016940	0.015004	4.66	3.14e-06 ***	
scale(sun_elev):scale(st_conif)	0.147027	0.013819	10.64	< 2e-16 ***	
scale(sun_elev):scale(st_dead_all)	0.016408	0.011687	1.40	0.160336	
(Intercept)	-3.883254	0.052443	-72.93	< 2e-16 ***	
scale(sun_elev)	0.076573	0.023301	3.29	0.00102 **	
I(scale(sun_elev)^2)	-0.045224	0.016514	-2.76	0.00584 **	
scale(rugged_10)	-0.021846	0.025956	0.93	0.35451	
I(scale(rugged_10)^2)	-0.030010	0.008750	-3.08	0.00208 **	
scale(dist_trails)	0.074743	0.023751	3.15	0.00165 **	
I(scale(dist_trails)^2)	-0.026524	0.008873	-4.52	6.29e-06 ***	
solrad_facflow	0.018036	0.0302045	0.56	0.57354	
solrad_facmiddle	0.059882	0.030536	1.96	0.04988 *	
scale(ss_trail)	0.028372	0.006691	3.05	0.00227 **	
scale(MStory)	-0.037491	0.028374	-1.48	0.133653	
scale(1Story)	-0.299882	0.020197	-14.85	< 2e-16 ***	
I(scale(1Story)^2)	-0.023455	0.010706	-2.19	0.02846 *	
I(scale(MStory)^2)	0.016363	0.017595	0.90	0.36730	
I(scale(MStory)^2):scale(dist_trails)	-0.015681	0.033663	-0.46	0.64347	
scale(sun_elev):scale(dist_trails)	0.026322	0.016366	1.93	0.05383 .	
scale(sun_elev):solrad_facflow	-0.044662	0.032097	-1.38	0.16789	
scale(sun_elev):solrad_facmiddle	-0.021893	0.030605	-0.72	0.47440	
scale(sun_elev):scale(MStory)	0.055184	0.015299	3.61	0.00031 ***	
scale(sun_elev):scale(MStory)	0.092957	0.016738	4.96	7.19e-07 ***	
scale(sun_elev):scale(MStory)	0.070420	0.015271	4.61	4.00e-06 ***	

## MODEL "LiDAR PCA RESULTS AT 5 M RESOLUTION"

AIC BIC logLik deviance df.resid  
64950.7 65455.4 -32428.4 64856.7 340118

Scaled residuals:		AIC	BIC	logLik	deviance	df.resid
Min	1Q	Median	3Q	Max		
-0.2324	-0.1611	-0.1412	-0.1172	14.5510		
Number of obs:	340165,	groups:	loc_id:id,	6678;	id,	17
Random effects:		Estimate	Std. Error	z value	Pr(> z )	
(Intercept)		-3.892417	0.0459207	-84.83	< 2e-16 ***	
scale(sun_elev)		0.0835386	0.0234807	3.56	0.000374 ***	
I(scale(sun_elev)^2)		-0.0413114	0.0231084	-1.79	0.07320 .	
I(scale(rugged_10))		-0.0362239	0.0098581	-3.57	0.000352 ***	
I(scale(dist_trails))		0.0782445	0.0236754	3.30	0.000360 ***	
I(scale(dist_trails)^2)		-0.0266727	0.0266727	-4.69	2.80e-06 ***	
solrad_facflow		0.0089877	0.0320371	0.28	0.779064	
solrad_facmiddle		0.0368178	0.0305556	1.30	0.194571	
scale(res5_PCl)		-0.2141063	0.0257738	-8.31	< 2e-16 ***	
scale(res5_Pc2)		0.0383111	0.0289747	1.32	0.186092	
scale(res5_Pc3)		0.2457223	0.0212905	11.53	< 2e-16 ***	
scale(res5_Pc4)		0.0777391	0.0321067	2.42	0.015466 *	
scale(res5_Pc5)		0.0241547	0.0208679	1.16	0.247066	
scale(res5_Pc6)		-0.0379191	0.0194017	-1.84	0.065076 .	
scale(res5_Pc7)		0.0749912	0.0176598	4.25	2.17e-05 ***	
scale(res5_Pc8)		0.0047308	0.0190462	0.25	0.803837	
scale(res5_Pc9)		-0.0346658	0.0170301	-0.20	0.838735	
scale(res5_Pc10)		-0.0127387	0.0158614	-0.80	0.421902	
scale(res5_Pc11)		0.0360007	0.0172049	2.03	0.041917 *	
I(scale(res5_Pc12))		0.0247621	0.0285640	-1.21	0.224411	
I(scale(res5_Pc2))		-0.0027544	0.0217417	-0.13	0.899186	
I(scale(res5_Pc3))		0.0727194	0.0202406	3.59	0.000327 ***	
I(scale(res5_Pc4))		0.0080785	0.0163769	0.49	0.621809	
I(scale(res5_Pc5))		-0.0509667	0.0164598	-3.10	0.0019569 **	
I(scale(res5_Pc6))		-0.0633797	0.0122693	-0.52	0.603081	
I(scale(res5_Pc7))		0.0189465	0.0145727	1.65	0.098207 .	
I(scale(res5_Pc8))		-0.0002708	0.0103867	-0.03	0.979199	
I(scale(res5_Pc9))		-0.0132935	0.0104912	-1.27	0.205047	
I(scale(res5_Pc10))		0.0048744	0.0096452	0.51	0.613297	
I(scale(res5_Pc11))		-0.0132481	0.0090708	-1.46	0.144147	
scale(sun_elev):scale(dist_trails)		0.0221505	0.0138160	1.60	0.108379	
scale(sun_elev):solrad_facflow		-0.0573539	0.0322526	-1.78	0.073539 .	
scale(sun_elev):solrad_facmiddle		-0.0327333	0.0307276	-1.10	0.272284	
scale(sun_elev):scale(res5_Pc1)		0.0318888	0.0144110	2.21	0.026315 *	
scale(sun_elev):scale(res5_Pc2)		-0.0613990	0.0150120	-4.09	4.31e-05 ***	
scale(sun_elev):scale(res5_Pc3)		-0.0467335	0.0149762	-3.12	0.001905 **	
scale(sun_elev):scale(res5_Pc4)		0.0449339	0.01456339	3.09	0.002010 **	
scale(sun_elev):scale(res5_Pc5)		-0.1095877	0.0148794	-3.37	1.77e-13 ***	
scale(sun_elev):scale(res5_Pc6)		0.0001633	0.0144902	0.01	0.991012	
scale(sun_elev):scale(res5_Pc7)		-0.0295430	0.0146047	-2.02	0.043089 *	
scale(sun_elev):scale(res5_Pc8)		0.0176509	0.0146290	1.21	0.227800	
scale(sun_elev):scale(res5_Pc9)		0.0086252	0.0149452	0.58	0.563356	
scale(sun_elev):scale(res5_Pc10)		-0.0039076	0.0144943	-0.27	0.787470	
scale(sun_elev):scale(res5_Pc11)		-0.0165467	0.0146606	-1.13	0.259048	

## MODEL "LiDAR PCA RESULTS AT 10 M RESOLUTION"

Scaled residuals:		AIC	BIC	logLik	deviance	df.resid
Min	1Q	Median	3Q	Max		
-0.2324	-0.1611	-0.1412	-0.1172	14.5510		
Number of obs:	340165,	groups:	loc_id:id,	6678;	id,	17
Random effects:		Estimate	Std. Error	z value	Pr(> z )	
(Intercept)		-3.892417	0.0459207	-84.83	< 2e-16 ***	
scale(sun_elev)		0.0835386	0.0234807	3.56	0.000374 ***	
I(scale(sun_elev)^2)		-0.0413114	0.0231084	-1.79	0.07320 .	
I(scale(rugged_10))		-0.0362239	0.0098581	-3.57	0.000352 ***	
I(scale(dist_trails))		0.0782445	0.0236754	3.30	0.000360 ***	
I(scale(dist_trails)^2)		-0.0266727	0.0266727	-4.69	2.80e-06 ***	
solrad_facflow		0.0089877	0.0320371	0.28	0.779064	
solrad_facmiddle		0.0368178	0.0305556	1.30	0.194571	
scale(res5_PCl)		-0.2141063	0.0257738	-8.31	< 2e-16 ***	
scale(res5_Pc2)		0.0383111	0.0289747	1.32	0.186092	
scale(res5_Pc3)		0.2457223	0.0212905	11.53	< 2e-16 ***	
scale(res5_Pc4)		0.0777391	0.0321067	2.42	0.015466 *	
scale(res5_Pc5)		0.0241547	0.0208679	1.16	0.247066	
scale(res5_Pc6)		-0.0379191	0.0194017	-1.84	0.065076 .	
scale(res5_Pc7)		0.0749912	0.0176598	4.25	2.17e-05 ***	
scale(res5_Pc8)		0.0047308	0.0190462	0.25	0.803837	
scale(res5_Pc9)		-0.0346658	0.0170301	-0.20	0.838735	
scale(res5_Pc10)		-0.0127387	0.0158614	-0.80	0.421902	
scale(res5_Pc11)		0.0360007	0.0172049	2.03	0.041917 *	
I(scale(res5_Pc12))		0.0247621	0.0285640	-1.21	0.224411	
I(scale(res5_Pc2))		-0.0027544	0.0217417	-0.13	0.899186	
I(scale(res5_Pc3))		0.0727194	0.0202406	3.59	0.000327 ***	
I(scale(res5_Pc4))		0.0080785	0.0163769	0.49	0.621809	
I(scale(res5_Pc5))		-0.0509667	0.0164598	-3.10	0.0019569 **	
I(scale(res5_Pc6))		-0.0633797	0.0122693	-0.52	0.603081	
I(scale(res5_Pc7))		0.0189465	0.0145727	1.65	0.098207 .	
I(scale(res5_Pc8))		-0.0002708	0.0103867	-0.03	0.979199	
I(scale(res5_Pc9))		-0.0132935	0.0104912	-1.27	0.205047	
I(scale(res5_Pc10))		0.0048744	0.0096452	0.51	0.613297	
I(scale(res5_Pc11))		-0.0132481	0.0090708	-1.46	0.144147	
scale(sun_elev):scale(dist_trails)		0.0221505	0.0138160	1.60	0.108379	
scale(sun_elev):solrad_facflow		-0.0573539	0.0322526	-1.78	0.073539 .	
scale(sun_elev):solrad_facmiddle		-0.0327333	0.0307276	-1.10	0.272284	
scale(sun_elev):scale(res5_Pc1)		0.0318888	0.0144110	2.21	0.026315 *	
scale(sun_elev):scale(res5_Pc2)		-0.0613990	0.0150120	-4.09	4.31e-05 ***	
scale(sun_elev):scale(res5_Pc3)		-0.0467335	0.0149762	-3.12	0.001905 **	
scale(sun_elev):scale(res5_Pc4)		0.0449339	0.01456339	3.09	0.002010 **	
scale(sun_elev):scale(res5_Pc5)		-0.1095877	0.0148794	-3.37	1.77e-13 ***	
scale(sun_elev):scale(res5_Pc6)		0.0001633	0.0144902	0.01	0.991012	
scale(sun_elev):scale(res5_Pc7)		-0.0295430	0.0146047	-2.02	0.043089 *	
scale(sun_elev):scale(res5_Pc8)		0.0176509	0.0146290	1.21	0.227800	
scale(sun_elev):scale(res5_Pc9)		0.0086252	0.0149452	0.58	0.563356	
scale(sun_elev):scale(res5_Pc10)		-0.0039076	0.0144943	-0.27	0.787470	
scale(sun_elev):scale(res5_Pc11)		-0.0165467	0.0146606	-1.13	0.259048	

## C.4 Roe deer telemetry data - 4 hour fix rate

MODEL "NO VEGETATION"

MODEL "NULL MODEL"

	AIC	BIC	logLik	deviance	df.resid		
	13930.3	13957.9	-6962.2	13224.3	72040		
	13881.4	14010.0	-6826.7	13853.4	72029		
Scaled residuals:							
Min	1Q	Median	3Q	Max			
-0.2632	-0.1504	-0.1444	-0.1338	16.6198			
Random effects:							
Groups	Name	Variance	Std.Dev.				
loc_id:id	(Intercept)	0	0				
id	(Intercept)	0	0				
Number of obs:	72043	groups:	loc_id:id, 1415; id, 15				
Fixed effects:							
	Estimate	Std. Error	z value	Pr(> z )			
(Intercept)	-3.904e+00	6.004e-02	< 2e-16	***			
scale(sun_elev)	-3.949e-02	4.980e-02	-0.79	0.427742			
I(scale(sun_elev)^~2)	5.016e-03	3.200e-02	0.16	0.875438			
scale(rugged_10)	-1.377e-01	3.856e-02	-3.57	0.000357	***		
I(scale(rugged_10)^~2)	-3.160e-02	2.167e-02	-1.46	0.144800			
scale(dist_trails)	4.662e-02	4.662e-02	-1.94	0.052659			
I(scale(dist_trails)^~2)	-9.033e-02	1.319e-02	-0.18	0.856557			
solrad_faclow	-2.384e-03	6.752e-05	6.718e-02	0.00	0.999102		
solrad_facmiddle	7.562e-05	6.640e-03	6.579e-02	-0.10	0.919615		
scale(sun_elev);scale(dist_trails)	6.640e-03	6.640e-03	1.392e-01	3.142e-02	4.33	1.46e-05	***
scale(sun_elev);solrad_faclow	4.555e-02	6.935e-02	0.66	0.511263			
scale(sun_elev);solrad_facmiddle	9.264e-02	6.587e-02	1.41	0.159583			
Fixed effects:							
(Intercept)	-3.91030	0.02681	-145.8	<2e-16	***		

MODEL "NORMALIZED DIFFERENCE VEGETATION INDEX (NDVI)"

MODEL "MEAN VEGETATION HEIGHT"

	AIC	BIC	logLik	deviance	df.resid	AIC	BIC	logLik	deviance	df.resid
	13852.4	14008.5	-6909.2	13318.4	72026	13613.5	13769.6	-6789.7	13579.5	72026
Scaled residuals:										
Min 1Q Median 3Q Max										
-0.3431 -0.1486 -0.1410 -0.1327 16.5602										
Random effects:										
Groups Name Variance Std.Dev.										
loc_id:id (Intercept) 0 0+00										
id (Intercept) 0 1e-07										
Number of obs: 72043, groups: loc_id:id, 1415; id, 15										
Fixed effects:										
Estimate Std. Error z value Pr(> z )										
(Intercept) -3.95290 -0.060892 < 2e-16 ***										
scale(sun_elev) -0.040823 0.049820 -0.82 0.41256										
I(scale(sun_elev)^2) 0.013754 0.032054 0.43 0.66787										
scale(rugged_10) -0.075505 0.040094 -1.88 0.05987 .										
I(scale(rugged_10)^2) -0.060385 0.023303 -2.59 0.00956 **										
scale(dist_trails) -0.080499 0.047822 -1.68 0.09331 .										
I(scale(dist_trails)^2) -0.017758 0.013567 -1.31 0.19122										
solrad_facflow 0.002035 0.067208 0.03 0.97534										
solrad_facmiddle -0.029119 0.065958 -0.44 0.65887										
scale(ndvi_preds) -0.038887 0.038471 -1.26 0.20751										
I(scale(ndvi_preds)^2) 0.081205 0.013057 6.22 5.00e-10 ***										
scale(sun_elev):scale(dist_trails) 0.138320 0.033166 4.17 3.04e-05 ***										
scale(sun_elev):solrad_facflow 0.069372 0.066000 1.52 0.12921										
scale(sun_elev):solrad_facmiddle 0.100138 0.098859 0.36 0.72001										
scale(sun_elev):scale(ndvi_preds) 0.027505 0.027505 0.36 0.72001										
Fixed effects:										
Estimate Std. Error z value Pr(> z )										
(Intercept) -3.8457581 -0.0817710 < 2e-16 ***										
scale(sun_elev) 0.03152538 0.0519786 0.60 0.5477										
I(scale(sun_elev)^2) 0.0137921 0.0322651 0.43 0.6690										
scale(rugged_10) 0.0417821 0.0401691 1.04 0.2981										
I(scale(rugged_10)^2) -0.0564137 0.0220295 -2.56 0.0104 *										
scale(dist_trails) -0.0089056 0.0476464 -0.19 0.8517 *										
I(scale(dist_trails)^2) -0.0275325 0.0155832 -2.03 0.0427 *										
solrad_facflow 0.0001645 0.067626 0.00 0.9981										
solrad_facmiddle 0.0012107 0.0660705 0.02 0.9854										
scale(MeanHeight) -0.4715136 0.0407378 < 2e-16 ***										
I(scale(MeanHeight)^2) -0.1432241 0.0572937 -2.50 0.0124 *										
scale(sun_elev):scale(dist_trails) 0.1351601 0.0311056 4.35 1.39e-05 ***										
scale(sun_elev):solrad_facflow 0.0375351 0.0656608 0.54 0.5895										
scale(sun_elev):solrad_facmiddle 0.07993350 0.0605655 1.21 0.2262										
scale(sun_elev):scale(MeanHeight) 0.1829820 0.0333425 5.49 4.07e-08 ***										

MODEL "CORINE LAND COVER CLASSES"

MODEL "HABITAT CLASSIFICATION MAP NPBW"

	AIC	BIC	logLik	deviance	df.resid
13840.5	13907.9	-6730.3	13460.5	72003	
Scaled residuals:					
Min	-1Q	Median	3Q	Max	
-0.2621	-0.1678	-0.1226	-0.1028	24.7723	
Random effects:					
Groups	Name	Variance	Std.Dev.		Estimate Std. Error z value Pr(> z )
loc_id:id	(Intercept)	0.000000	0.00000		-4.191819 0.112484 -37.27 < 2e-16 ***
id	(Intercept)	0.008708	0.09332		0.414572 0.094027 4.41 1.04e-05 ***
Number of obs: 72043, groups: loc_id:id, 1415; id, 15					
Fixed effects:					
(Intercept)					-0.007194 0.033424 -0.22 0.829588
scale(sun_elev)					0.049070 0.052260 0.94 0.347756
I(scale(sun_elev)^2)					-0.056930 0.024002 -2.37 0.017697 *
scale(rugged_10)					0.003528 0.015052 0.07 0.946881
I(scale(rugged_10)^2)					-0.031573 0.014362 -2.21 0.027041 *
scale(dist_trails)					0.042521 0.068638 0.62 0.536548
I(scale(dist_trails)^2)					0.019388 0.066911 0.29 0.770003
solrad_facmiddle					-0.153771 0.307026 -5.50 0.616483 ***
mapConiferous_stand - medium					0.857557 0.170088 5.04 4.62e-07 ***
mapDead_wood - lying					0.708884 0.190494 3.72 0.00199 ***
mapDead_wood - standing					-0.143871 0.135471 -1.06 0.288415
mapPreciduous_stand - mature					-0.982400 0.587794 -1.67 0.094856 .
mapPreciduous_stand - medium					0.966110 0.168780 5.72 1.04e-08 ***
mapEcorone					0.799647 0.107094 7.47 8.22e-14 ***
mapMeadow - cultivated					0.773993 0.158038 4.90 9.71e-07 ***
mapMeadow - natural					-0.022726 0.070906 -1.93 0.053731 .
mapMixed_stand - mature					0.472077 0.171183 2.76 0.005820 *
mapMixed_stand - medium					0.797240 0.141200 5.66 1.64e-08 ***
mapMixed_stand - young					0.790728 0.243122 3.26 0.01144 **
mapOthers					-2.102599 0.715004 -2.94 0.003275 **
mapDiscontinuous_area					0.075555 0.034668 2.18 0.029302 *
scale(sun_elev):scale(dist_trails)					-0.032726 0.070906 0.46 0.644421
scale(sun_elev):solrad_facflow					0.032376 0.066917 0.48 0.628624
scale(sun_elev):solrad_facmiddle					0.296523 0.264383 1.12 0.262047
scale(sun_elev):mapOniferous_stand - medium					-0.257733 0.162337 -1.59 0.112367
scale(sun_elev):mapDead_wood - lying					0.032385 0.182000 -1.78 0.075654 .
scale(sun_elev):mapDead_wood - standing					-0.323895 0.182000 -1.73 0.083334 .
scale(sun_elev):mapEciduous_stand - mature					-0.387119 0.598208 -0.65 0.517547
scale(sun_elev):mapPreciduous_stand - medium					0.150576 -1.14 0.254028
scale(sun_elev):mapEcorone					-0.171750 0.098296 -7.66 1.89e-14 ***
scale(sun_elev):mapMeadow - natural					-0.764067 0.158278 -4.83 1.38e-06 ***
scale(sun_elev):mapMixed_stand - mature					-0.251659 0.105492 -2.39 0.017039 *
scale(sun_elev):mapMixed_stand - medium					-0.228734 0.163658 -1.40 0.162223 ***
scale(sun_elev):mapMixed_stand - young					-0.499854 0.135289 -3.69 0.000220 ***
scale(sun_elev):mapOthers					-0.317544 0.248022 -1.28 0.200013
scale(sun_elev):mapResidential_area					-0.404288 0.166393 -0.53 0.597832

MODEL "FRACTIONAL VEGETATION COVER"

MODEL "NUMBER OF SINGLE TREES"

	AIC	BIC	logLik	deviance	df.resid	AIC	BIC	logLik	deviance	df.resid
	13565.4	13776.7	-6759.7	13519.4	72020	13615.2	13826.4	-6784.6	13569.2	72020
Scaled residuals:										
Min	1Q	Median	3Q	Max		Min	1Q	Median	3Q	Max
-0.2778	-0.1659	-0.1313	-0.1020	22.1493		-0.3044	-0.1589	-0.1351	-0.1097	19.5095
Random effects:										
Groups	Name	Variance	Std.Dev.			Groups	Name	Variance	Std.Dev.	
loc_id:id	(Intercept)	0.000e+00	0.00e+00			loc_id:id	(Intercept)	0	0	
id	(Intercept)	6.55de-14	2.56e-07			id	(Intercept)	0	0	
Number of obs: 72043, groups: loc_id:id, 1415; id, 15						Number of obs: 72043, groups: loc_id:id, 1415; id, 15				
Fixed effects:										
	Estimate	Std. Error	z value	Pr(> z )		Estimate	Std. Error	z value	Pr(> z )	
(Intercept)	-3.894402	0.098398	-39.57	< 2e-16 ***		(Intercept)	-3.983109	0.071604	-55.63	< 2e-16 ***
scale(sun_elev)	0.053122	0.051977	1.02	0.306774		scale(sun_elev)	0.064658	0.050268	1.24	0.214221
I(scale(sun_elev)^2)	0.005177	0.032722	0.16	0.874283		I(scale(sun_elev)^2)	-0.018684	0.032995	-0.56	0.573264
scale(rugged_10)	0.073348	0.041055	1.79	0.074020	.	scale(rugged_10)	0.010852	0.040967	0.26	0.791035
I(scale(rugged_10)^2)	-0.065890	0.022373	-2.95	0.003229 ***		I(scale(rugged_10)^2)	-0.038009	0.021670	-1.75	0.079434
scale(dist_trails)	0.029600	0.048990	0.60	0.545717		scale(dist_trails)	0.005886	0.049406	0.12	0.903217
I(scale(dist_trails)^2)	-0.036043	0.013670	-2.64	0.008371 **		I(scale(dist_trails)^2)	-0.026361	0.015304	-1.96	0.050918
solrad_facflow	0.016156	0.068023	0.24	0.812285		solrad_facflow	0.028975	0.067861	0.43	0.669404
solrad_facmiddle	0.029427	0.066169	0.44	0.656521		solrad_facmiddle	0.066072	0.42	0.675042	
scale(USStory)	0.086664	0.059857	1.36	0.175608		scale(st_deci)	-0.306082	0.063922	-4.79	1.68e-06 ***
scale(MStory)	-0.100519	0.051971	-1.93	0.053099	.	scale(st_comif)	-0.313301	0.037427	-8.37	< 2e-16 ***
scale(OSStory)	-0.453422	0.038564	-11.76	< 2e-16 ***		scale(st_dead_all)	-0.033256	0.050767	0.26	0.792568
I(scale(OSStory)^2)	-0.032171	0.023407	-1.37	0.169301		I(scale(st_deci)^2)	-0.036326	0.035979	-1.02	0.306053
I(scale(MStory)^2)	0.056656	0.038341	1.56	0.119723		I(scale(st_comif)^2)	0.031679	0.020204	1.17	0.241098
I(scale(OSStory)^2)	-0.112712	0.074205	-1.54	0.128778		I(scale(st_dead_all)^2)	0.002889	0.005510	0.37	0.713633
scale(sun_elev : scale(dist_trails))	0.109883	0.031290	3.42	0.000628 ***		scale(sun_elev : scaledist_trails)	0.120047	0.031127	3.86	0.000115 ***
scale(sun_elev : solrad_facflow)	-0.004333	0.069730	-0.06	0.980340		scale(sun_elev : solrad_facflow)	-0.008125	0.069899	-0.12	0.907580
scale(sun_elev : solrad_facmiddle)	0.066204	0.066189	1.00	0.317201		scale(sun_elev : solrad_facmiddle)	0.061938	0.061660	0.94	0.349181
scale(sun_elev : scale(OSStory))	0.112130	0.033131	3.38	0.000713 ***		scale(sun_elev : scale(st_deci))	0.106223	0.031444	2.96	0.003179 **
scale(sun_elev : scale(MStory))	0.083277	0.034717	2.54	0.010987 *		scale(sun_elev : scale(st_comif))	0.0289674	0.030399	9.53	< 2e-16 ***
scale(sun_elev : scale(OSStory))	0.158848	0.032922	4.73	2.2e-06 ***		scale(sun_elev : scale(st_dead_all))	0.005131	0.022789	0.23	0.821862

## MODEL "LiDAR PCA RESULTS AT 5 M RESOLUTION"

### MODEL "LiDAR PCA RESULTS AT 10 M RESOLUTION"

	AIC	BIC	logLik	deviance	df.resid	AIC	BIC	logLik	deviance	df.resid			
	13518.4	13950.1	-6712.2	13424.4	71996	13485.4	13862.0	-6701.7	13403.4	72002			
Scaled residuals:													
Min	-1Q	Median	3Q	Max		Min	-1Q	Median	3Q	Max			
-0.3265	-0.1665	-0.1316	-0.1008	25.5890		-0.3075	-0.1657	-0.1313	-0.0985	26.9759			
Number of obs:	72043	groups:	loc_id:id,	1415; id,	15	Number of obs:	72043	groups:	loc_id:id,	1415; id,	15		
Random effects:						Random effects:							
Groups	Name	Variance	Std.Dev.			Groups	Name	Variance	Std.Dev.				
loc_id:id	(Intercept)	0	0			loc_id:id	(Intercept)	0	0				
id	(Intercept)	0	0			id	(Intercept)	0	0				
Number of obs:	72043	groups:	loc_id:id,	1415; id,	15	Number of obs:	72043	groups:	loc_id:id,	1415; id,	15		
Fixed effects:						Fixed effects:							
	Estimate	Std.	Error	z	value	Pr(> z )		Estimate	Std.	Error	z	value	Pr(> z )
(Intercept)	-3.9441977	0.0914624	-43.12	< 2e-16	***	(Intercept)	-3.9441977	0.0867170	-45.95	< 2e-16	***		
scale(sun_elev)	0.0735176	0.0530384	1.39	0.165710		scale(sun_elev)	0.086721	0.0531148	1.52	0.128807			
I(scale(sun_elev)^2)	-0.0117346	0.0530079	-0.05	0.958088		I(sun_elev)	0.0014288	0.030358	0.04	0.965602			
scale(rugged_10)	0.0778960	0.0410225	1.90	0.057586	*	scale(rugged_10)	0.0955547	0.043329	2.31	0.021056	*		
I(scale(rugged_10)^2)	-0.0729393	0.0224414	-3.26	0.001443	**	I(scale(rugged_10)^2)	-0.0802099	0.025656	-3.56	0.000376	***		
scale(dist_trails)	0.0988140	0.0491689	0.20	0.841795		scale(dist_trails)	0.0275973	0.0487053	0.56	0.578746			
I(scale(dist_trails)^2)	-0.036190	0.0136745	-2.46	0.094082	*	I(scale(dist_trails)^2)	-0.0376891	0.0183204	-2.73	0.006376	**		
solrad_fac10	0.0005057	0.0681769	0.01	0.954082		solrad_fac10	0.0000396	0.0683435	0.01	0.989030			
solrad_facmiddle	-0.0395924	0.0663203	-0.06	0.952478		solrad_facmiddle	-0.0000337	0.0664252	-0.01	0.993549			
scale(res5_PC1)	-0.3349292	0.0470916	-7.11	1.14e-12	***	scale(res10_PC1)	-0.3955503	0.041446	-6.73	< 2e-16	***		
scale(res5_PC2)	0.0744603	0.0676397	1.17	0.240091		scale(res10_PC2)	0.0673418	0.0677270	0.79	0.427483			
scale(res5_PC3)	0.3662233	0.0456422	8.02	1.3e-15	***	scale(res10_PC3)	0.3415316	0.0442510	7.72	1.18e-14	***		
scale(res5_PC4)	0.1259280	0.0717337	1.76	0.079182	*	scale(res10_PC4)	0.1297596	0.0683888	1.87	0.064147	*		
scale(res5_PC5)	0.0634722	0.0446775	1.42	0.155412		scale(res10_PC5)	0.0599023	0.0489239	1.30	0.192103			
scale(res5_PC6)	-0.1527014	0.0457541	-3.34	0.000464	***	scale(res10_PC6)	0.01008042	0.0449191	2.24	0.024824	*		
scale(res5_PC7)	0.1532767	0.0429487	3.57	0.000359	***	scale(res10_PC7)	-0.1450110	0.0441714	-3.28	0.01027	**		
scale(res5_PC8)	-0.0342235	0.0437235	-0.78	0.434266		scale(res10_PC8)	-0.127318	0.0446038	-0.29	0.772657			
scale(res5_PC9)	-0.0855670	0.0400112	-0.21	0.830587		scale(res10_PC9)	0.0265029	0.0409720	0.66	0.512213			
scale(res5_PC10)	-0.1051617	0.0465676	-0.04	0.965676		I(scale(res10_PC1)^2)	-0.0872842	0.0644261	-1.35	0.175483			
scale(res5_PC11)	0.0783488	0.0396678	1.96	0.049614	*	I(scale(res10_PC2)^2)	-0.046414	0.0511718	-0.09	0.927729			
I(scale(res5_PC1)^2)	-0.0845759	0.0654211	-1.29	0.196083		I(scale(res10_PC3)^2)	0.1642188	0.04837388	3.39	0.006388	***		
I(scale(res5_PC2)^2)	-0.022919	0.0297037	-0.82	0.414498		I(scale(res10_PC4)^2)	-0.0056651	0.0331154	-0.17	0.864167			
I(scale(res5_PC3)^2)	-0.0183316	0.0475983	3.82	0.000134	***	I(scale(res10_PC5)^2)	-0.0598270	0.0397270	-1.76	0.077659			
I(scale(res5_PC4)^2)	-0.0131453	0.03626288	0.36	0.717723		I(scale(res10_PC6)^2)	0.0199897	0.0269214	0.73	0.464321			
I(scale(res5_PC5)^2)	-0.0342614	0.0310435	-2.83	0.004826	**	I(scale(res10_PC7)^2)	-0.0392736	0.0275683	-1.42	0.154276			
I(scale(res5_PC6)^2)	-0.0242124	0.0297037	-0.82	0.414498		I(scale(res10_PC8)^2)	-0.0200179	0.0245440	0.82	0.414732			
I(scale(res5_PC7)^2)	-0.0066643	0.0261620	-0.25	0.798300		I(scale(res10_PC9)^2)	-0.0303842	0.0232412	-1.31	0.191098			
I(scale(res5_PC8)^2)	-0.0031091	0.0265496	-0.12	0.906778		I(scale(res10_PC10)^2)	-0.0317824	0.0319833	2.78	0.005375	**		
I(scale(res5_PC9)^2)	-0.0049465	0.0245729	0.20	0.840465		I(scale(res10_PC1)^2)	-0.0450589	0.0307340	-0.64	0.521827			
I(scale(res5_PC10)^2)	-0.0230238	0.0230238	-0.33	0.741709		I(scale(res10_PC2)^2)	-0.0392736	0.0275683	-1.42	0.154276			
scale(sun_elev : scale(dist_trails))	0.0975209	0.0315374	3.06	0.002191	**	I(scale(res10_PC3)^2)	-0.0751882	0.0331967	-2.26	0.023517	*		
scale(sun_elev : solrad_facmiddle)	-0.0310942	0.0701214	-0.44	0.657452		I(scale(res10_PC4)^2)	-0.0926434	0.0334122	-2.77	0.005559	**		
scale(sun_elev : scale(facmiddle))	0.0432636	0.0665972	0.65	0.515304		I(scale(res10_PC5)^2)	-0.0984123	0.0317824	3.10	0.011959	**		
scale(sun_elev : scale(res5_PC1))	0.0876049	0.0315914	2.76	0.005704	**	I(scale(res10_PC6)^2)	-0.1602437	0.0342705	-4.68	2.93e-06	***		
scale(sun_elev : scale(res5_PC2))	-0.0649088	0.0327910	-1.98	0.047763	*	I(scale(res10_PC7)^2)	-0.227954	0.035220	0.70	0.483352			
scale(sun_elev : scale(res5_PC3))	-0.0507404	0.0328917	-1.54	0.122915		I(scale(res10_PC8)^2)	-0.1607734	0.0349868	0.46	0.645939			
scale(sun_elev : scale(res5_PC4))	0.0911220	0.0317268	2.87	0.004078	**	I(scale(res10_PC9)^2)	-0.098036	0.0331321	0.30	0.767311			
scale(sun_elev : scale(res5_PC5))	-0.1988958	0.0331298	-5.94	2.80e-09	***	I(scale(res10_PC10)^2)	-0.0567548	0.0333117	-1.12	0.263165			
scale(sun_elev : scale(res5_PC6))	0.0069962	0.0331431	0.21	0.832817		I(scale(res10_PC11)^2)	-0.0391487	0.0349873	-0.50	0.613918			
scale(sun_elev : scale(res5_PCP8))	0.0066317	0.0332814	0.29	0.772274									
scale(sun_elev : scale(res5_PCP9))	0.0096939	0.0339966	0.27	0.789337									
scale(sun_elev : scale(res5_PCP10))	-0.00565325	0.0332988	-0.17	0.868040									
scale(sun_elev : scale(res5_PCP11))	-0.05667548	0.0333117	-1.70	0.088428									

## **Appendix D**

### **Predictions for resource selection in deer**

## D.1 Predictions from five different models for red deer

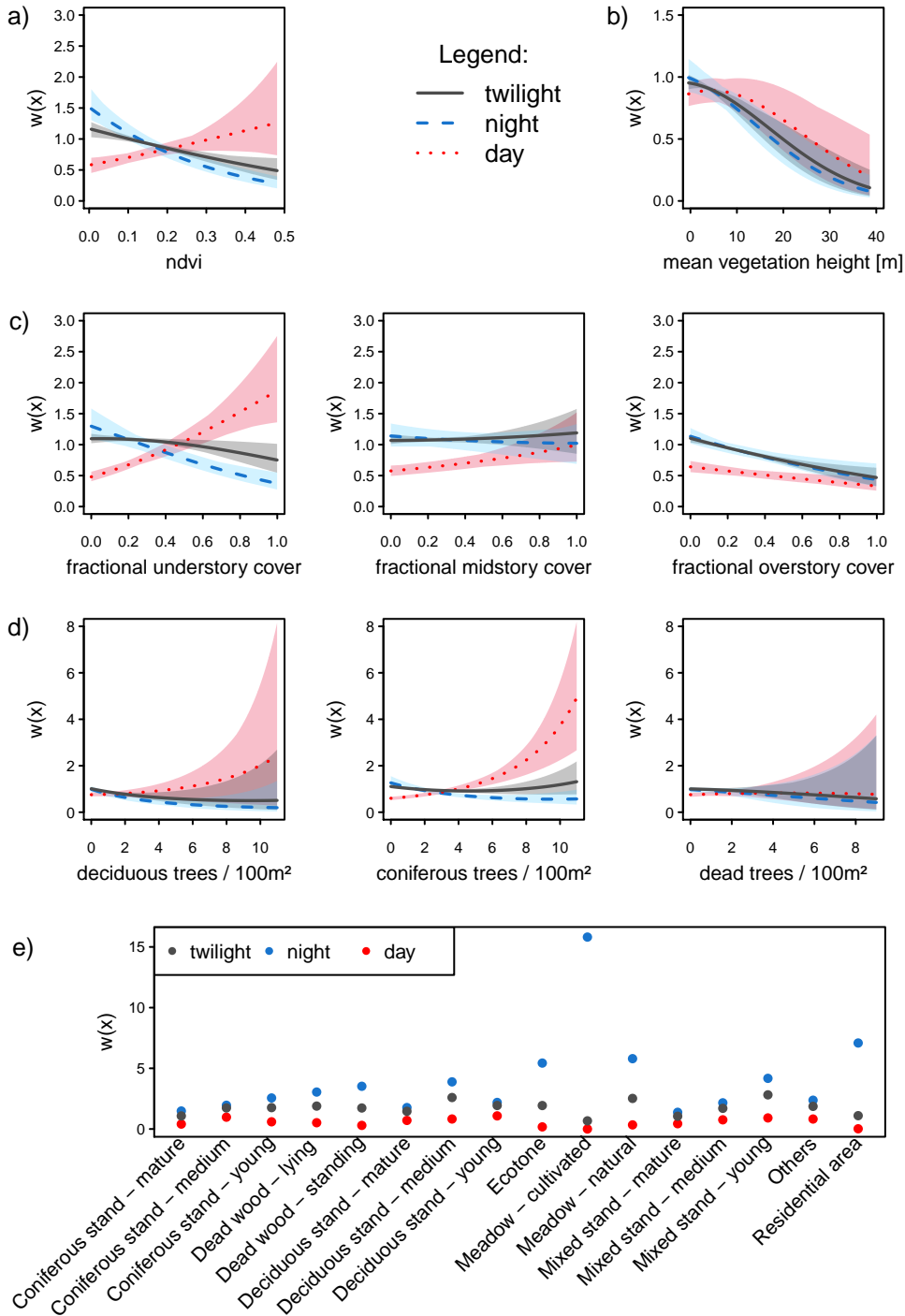


Figure D.1: Predicted relative probability of selection  $w(x)$  for red deer at 1 hour fix rate. Predictions are from models always incorporating the same confounding factors as well as nested random effects. Only the predictors to describe habitat characteristics were changing among a) normalized difference vegetation index, b) mean vegetation height, c) fractional vegetation cover, d) number of single trees and e) habitat classification map of the Bavarian Forest National Park. Variables were interacted with the time of the day (twilight, night, day).

## D.2 Predictions from five different models for roe deer

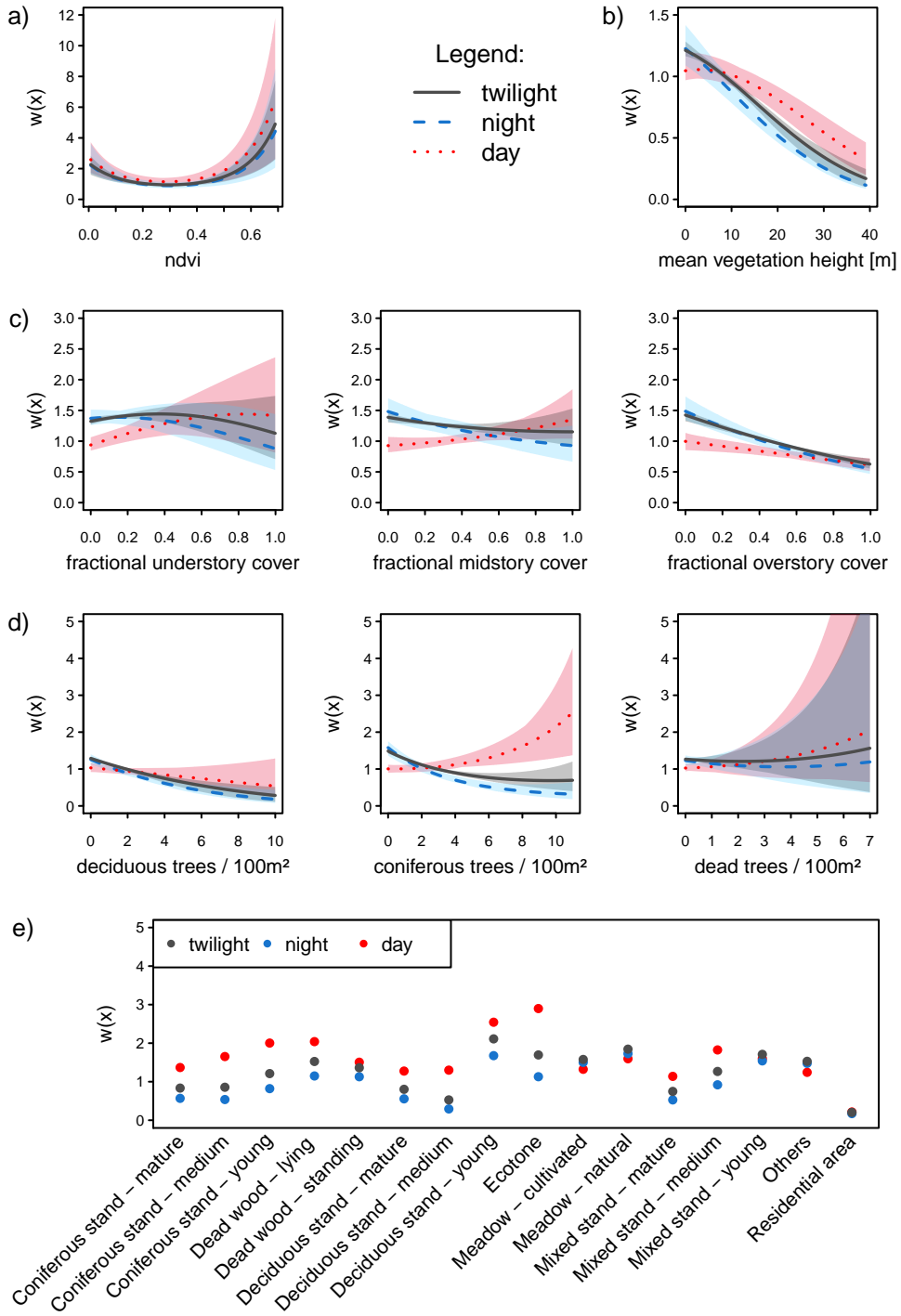


Figure D.2: Predicted relative probability of selection  $w(x)$  for roe deer at 1 hour fix rate. Predictions are from models always incorporating the same confounding factors as well as nested random effects. Only the predictors to describe habitat characteristics were changing among a) normalized difference vegetation index, b) mean vegetation height, c) fractional vegetation cover, d) number of single trees and e) habitat classification map of the Bavarian Forest National Park. Variables were interacted with the time of the day (twilight, night, day).

# Selbstständigkeitserklärung

## Erklärung

Ich versichere hiermit, dass ich die vorliegende Arbeit ohne fremde Hilfe selbstständig verfasst und nur die angegebenen Quellen und Hilfsmittel benutzt habe. Wörtlich oder dem Sinn nach aus anderen Werken entnommene Stellen habe ich unter Angabe der Quellen kenntlich gemacht.

(I hereby declare that I have composed this document unassistedly and that I only used the sources and devices I declared. Passages taken verbatim or in meaning from other sources are identified as such and the sources are acknowledged and cited.)

Freiburg, 1st of April 2016